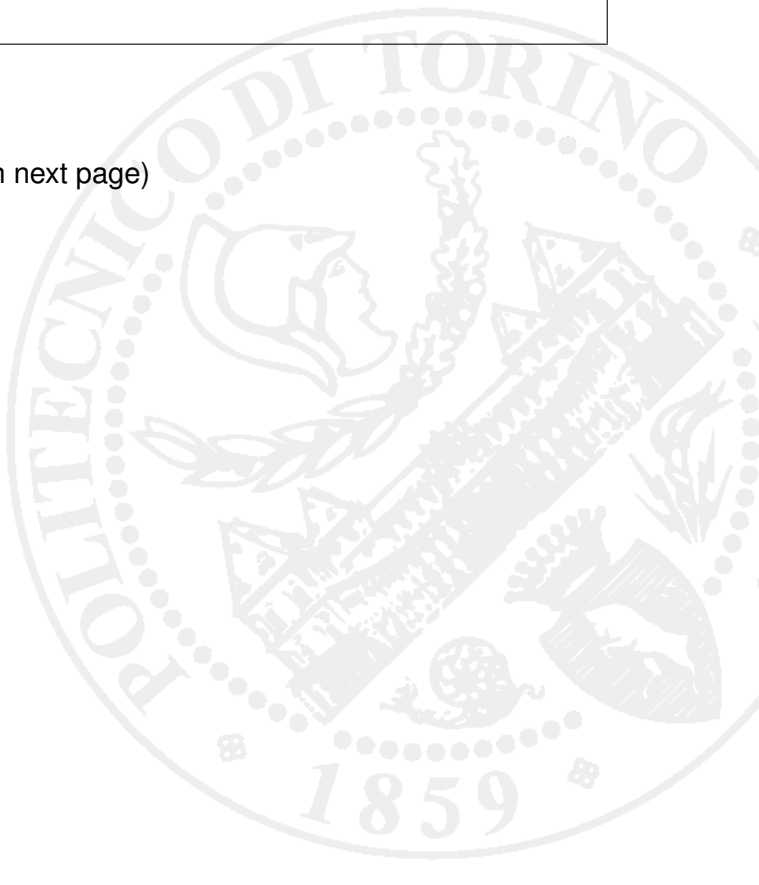

POLITECNICO DI TORINO

DOCTORATE SCHOOL

Ph.D in Mechanics

(XXVII Ph.D Course cycle)

PH.D THESIS

LIGHTWEIGHT DESIGN OF VEHICLE SIDE DOOR

JINDONG JI

ID: 189899

PhD Supervisor:

Prof. Giovanni Belingardi

PhD Coordinator:

Prof. Luigi Garibaldi

February 2015

Introduction

Due to increasing environmental concern about emission of Green House Gas and government regulations on vehicle safety, vehicle manufacturers, and their suppliers, must turn to new technologies. This is the main way to help them to achieve the goals of making vehicles lighter and safer. These two targets seem to be in deep contrast one with the other as increasing expectations from car consumers and the crashworthiness requirements.

Nowadays a lot of innovative vehicle technologies are being considered in order to reduce emissions of GHG, such as engine with increased efficiency, less drag losses, regenerative braking systems, lower weight and so on. Lightweight design is becoming an effective way to get higher fuel efficiency and less vehicle emissions in recent years. Some vehicle weight reduction techniques such as vehicle redesign and vehicle downsizing are playing a negative role on both customer comfort and vehicle safety, since vehicle size and safety are linked together. Consequently, research work and car makers design departments are willing to find advanced materials with excellent performances to substitute traditional materials, such as high strength steel, aluminum, magnesium, composite and so on. Composite have many advantages comparing to traditional materials, such as their relatively higher strength and lower weight, better corrosion resistance, better energy absorption in case of impact and so on. But many difficulties are encountered on the way of successful incorporation of huge quantities of composites, which could be divided into some categories: production cost, production volume, design methodologies, joining technology, repair and recycling issues. Also vehicle safety should be discussed when lighter materials are adopted into automobiles.

The research activity in this PhD thesis is motivated and drawn from the above stated problems. Vehicle lateral door substructure is the focus point of this study. Vehicle side door is not a simple panel but rather a substructure system which satisfies many different functions. This structure is traditionally built with steel material traditionally. Basically, the door is composed by an outer panel supported by an inner panel where different additional components are placed. Furthermore, nowadays car doors usually have a reinforcing element (side impact beam) placed longitudinally

between outer and inner panels which protects the driver and passengers in case of a side impact event.

This thesis has developed several composite side door structures for vehicle model Toyota Yaris 2010, considering static design requirements, NVH design criteria and crashworthiness. All the composite models are simulated with numerical tools ABAQUS and LS-DYNA. The original Yaris steel door structure is considered as reference solution in this study and its performance compared with all composite solutions.

The first chapter is dedicated to vehicle fuel consumption and emissions in Europe during recent years. Then the chapter discusses the CO_2 emission limitations from Euro 1 to Euro 6 for gasoline and diesel passenger cars.

The second chapter covers technological strategies adopted by car manufacturers in order to reach vehicle noxious gas emissions and fuel consumption reduction. Lightweight design is the main way considered in this thesis and then advanced materials used to substitute traditional material are summarized. Both advantages and disadvantages of composite materials are discussed in detail; also safety of lighter vehicles is covered briefly in the end.

The third chapter introduces the particular application of the vehicle lateral door in the past. In this activity, the differences between finite element model of Yaris and real car are investigated. Active safety and passive safety of vehicle is discussed, usually the passive safety includes frontal crash, side crash and rear crash. Every vehicle fleet must pass not only legislation safety tests before they are permitted to be sold in market but also “New car Assessment Program”, all the NCAP established in different countries are summarized. The Federal Motor Vehicle Safety Standard 214 is the reference normative in the study, which is discussed in deepth. Biomechanical response of instrumented dummy is used to assess injury risk of body part, including Head Injury Criteria (HIC), thorax, abdomen and pelvis. At the end, three composite door solutions developed in this study are briefly described.

The fourth chapter covers composite characterization; types of fiber and matrix common in use are summarized at first. The selection of composite for vehicle side door should consider bending stiffness, strength and capacity to absorb energy. As a response, several composite materials are

considered because of their own advantages, they are carbon fiber reinforced plastic (CFRP), E-Glass/epoxy composite (GFRP), glass mat thermoplastic (GMT), GMT-UD, GMT-TEX and semi impregnated micro sandwich material (SIMS).

The fifth chapter introduces composite door solutions in detail, such as sizes of models, types of element and so on. The first composite door solution is framed by composite thin-walled beams based on the size of Yaris door. The composite beams are connected by aluminum joint through epoxy adhesives. In this case, outer panel and inner panel of door structure are not considered, so it is not possible to integrate this solution into Yaris vehicle directly. The second solution is to substitute traditional materials using composite, interesting parts are outer panel, inner panel and impact beam. In third solution, one innovative side door reinforcing structure is presented, the proposal is that traditional impact beam and some particular reinforcements are replaced by an innovative composite reinforcing panel, and this innovative panel could be bonded with outer surface panel and inner surface panel together.

The sixth chapter is covering numerical simulation results for first and second solutions under static loading cases, including vertical, horizontal, lateral stiffness, sagging and quasi static intrusion simulation test. At the end the modal analysis is done for second solution. All the numerical results of composite solutions are compared with Yaris reference solution.

The crashworthiness evaluation is in chapter seven, including intrusion displacements of compartment and biomechanical response of instrumented dummy which is placed at driver's seat. Acceleration of head, rib deflection, abdominal force and pubic symphysis force are used to assess the injury risk of body parts. All the biomechanical response of composite solutions is compared with steel reference solution and limitation value required in regulation FMVSS214. Finally in chapter eight the main conclusions of this research activity are briefly summarized.

Acknowledgement

First and foremost I want to thank my supervisor, Professor Giovanni Belingard. It has been an honor to be his Ph. D student. His support, encouragement, supervision and inspiration from the preliminary to the concluding level enabled me to develop an understanding of the subject. I appreciate all his contributions of time, ideas, and funding to make my Ph.D experience productive and stimulating.

I would like to thank the professors, colleagues, members of mechanical department for supporting me in different ways during my study.

My special thanks go to my family members for their continuous encouragement.

Lastly, I offer my regards to all of those who supported me in any respect during the completion of the thesis.

TABLE OF CONTENTS

LIST OF FIGURES

LIST OF TABLES

1 Chapter 1 Vehicle fuel consumption and emissions

1.1 Introduction

As stated in the report of European Vehicle Market Statistics in 2013 [1], the number of new passenger car registrations continued on the generally descending path started in 2007 (as shown in Figure 1.1-1), since that year the number of new registration cars has decreased from 15.6 million to 12.0 million by 23% reduction. The trend shows the close relationship between vehicle sales and the economic depression. Therefore it is reported that in southern Europe, where vehicle sale numbers have decreased by 60% in Spain and 45% in Italy since 2007. But in Germany, the number of vehicles sold in 2012 was about the same as in 2007. One obvious sales peak in 2009 did interrupt the general descending trend of the past five years, but this is attributed to economic stimulus programs created by many national governments at that time, which encouraged people to buy new cars, not any constructive change in the market.

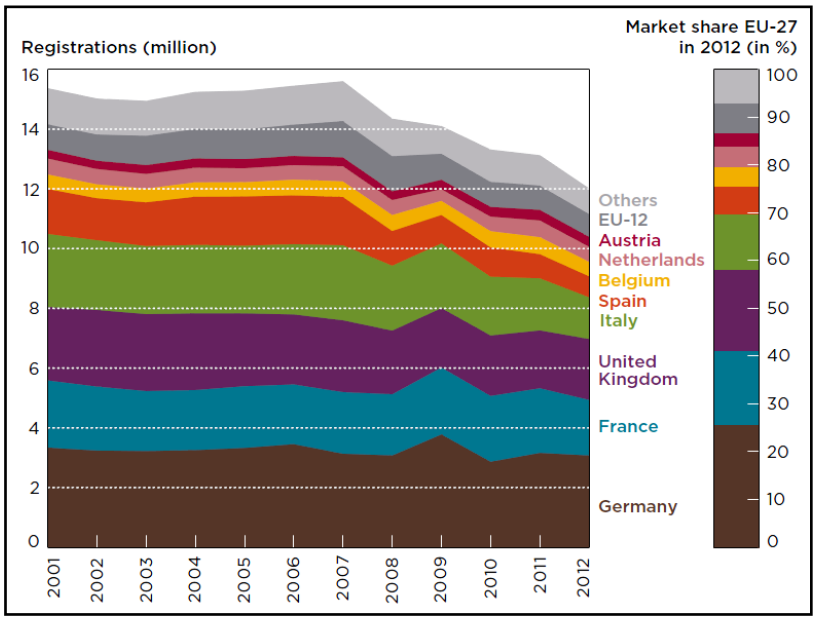

Figure 1.1-1 Passenger cars registrations by member state [1]

The European market is dominated by a few countries; Figure 1.1-1 is showing that 75% of all new passenger car registrations occur in the five largest markets, which are Germany, France, United Kingdom, Italy, and Spain. However from the point view of car manufacturers, the vehicle market is

much more different: the top seven brands shared only about 50% of the market, which is shown in Figure 1.1-2.

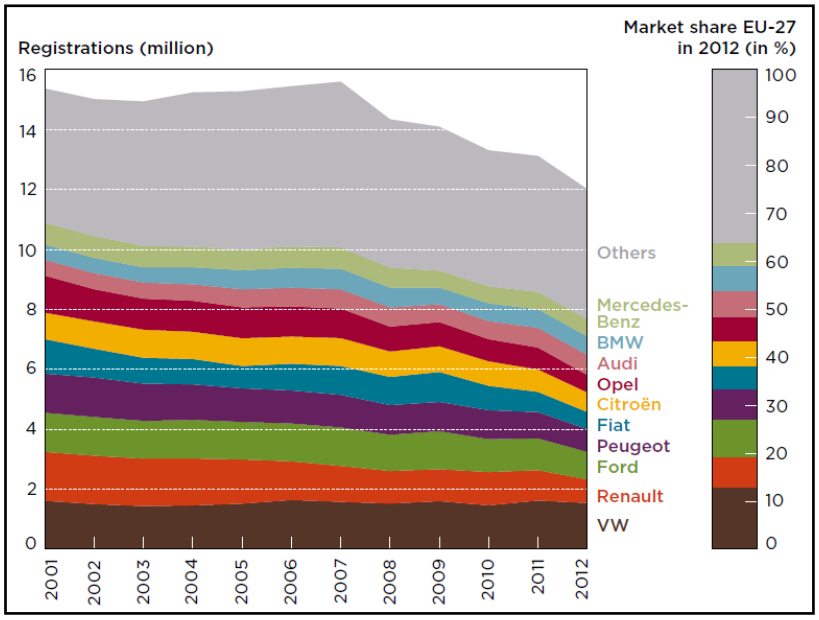

Figure 1.1-2 Passenger cars registrations by vehicle brand [1]

Globally, the total number of vehicle sold in EU market was about 77 million in 2012, with a 6% increase compared to year 2011, around 50 million cars and 27 million commercial vehicles were included in that number. The three biggest markets are China (19 million vehicles sold in 2012), the U.S. (15 million), and the EU (14 million), the fastest increasing markets in 2012 were Thailand (+80%), Japan (+28%), Indonesia (+25%), and the U.S. (+13%). Since 2007, vehicle sales have doubled in China, India, Thailand, and Indonesia. During this period, vehicle markets in the EU, North America, and Japan remained steady or decreased a little [1].

1.2 Vehicle consumption and CO_2 emissions

Scientific research revealed that the earth's average temperature is growing slowly because of increased global emissions of greenhouse gases (carbon dioxide, methane, hydrocarbons and nitrogen oxide). As predicted by Intergovernmental Panel on Climate Change (IPCC), there will be a rise in global temperatures of between 1° and 2° Celsius by 2020 and between 2° and 5° Celsius by 2070 [2]. Increased international awareness of this climate change phenomena has led to considerable international effort, such as the United Nations Framework Convention on Climate

Change (UNFCCC) and the Kyoto Protocol agreed several years ago, both of them are established in order to prevent climate change by trying to reduce emissions.

According to the latest report of European Environment Agency (EEA) [3], carbon dioxide (CO_2) emissions from road transport have increased by 21% from year 1990 to year 2011, and they contributed around 23% of the EU's total CO_2 emissions. To make sure EU could satisfy its greenhouse gas emission targets established in the Kyoto Protocol, a strict standard to reduce CO_2 emissions from new cars and vans sold in the European Union was executed since 2009, officially regulation (EC) No 443/2009 aiming at reducing the average CO_2 emissions of new passenger cars was established. A short-term target of $130g\ CO_2/km$ by 2015 and a long term target of $95g\ CO_2/km$ by 2020 are established in the regulation. The average $CO2$ emission level of year 2012 was $132\ g/km$ [1], which is very close to the 130 g/km target set for 2015. It is obviously that CO_2 emissions and fuel consumption are directly related together, so emission level could be translated into fuel consumption, it is about $5.2\ liters/100km$ for year 2015 target and $3.8\ liters/100km$ for 2020 target. Also European Commission document agreed a 2025 target range of $68-78\ g/km$ of $CO2$ emissions.

Under EU regulation, CO_2 emission targets for every car manufacturer are adjusted for the average weight of their specific vehicles, so manufacturers of heavier vehicles have a less strict target to meet (shown in Figure 1.2-1). The reduction in CO_2 emissions (equal to fuel consumption) required between 2015 and 2020 is 27 percent reduction for all car manufacturers. But absolute reduction value required for different manufacturers are different because their initial emission values are different. Some manufacturers (in particular PSA and Toyota) have already satisfied their 2015 targets and they are trying to obtain further improvements in order to meet the 2020 target. Figure 1.2-2 is showing that Germany's average emissions are the highest one while France's are among the lowest, though they both have about the same domestic production. The most important characteristic of passenger cars sold in two countries is that cars sold in Germany are about 11% heavier and 25% more powerful. Also we can see that the emission trend in the Netherlands is

remarkable: average CO_2 emissions have decreased by 28% since 2007, about nearly 6% per year (see Figure 1.2-2).

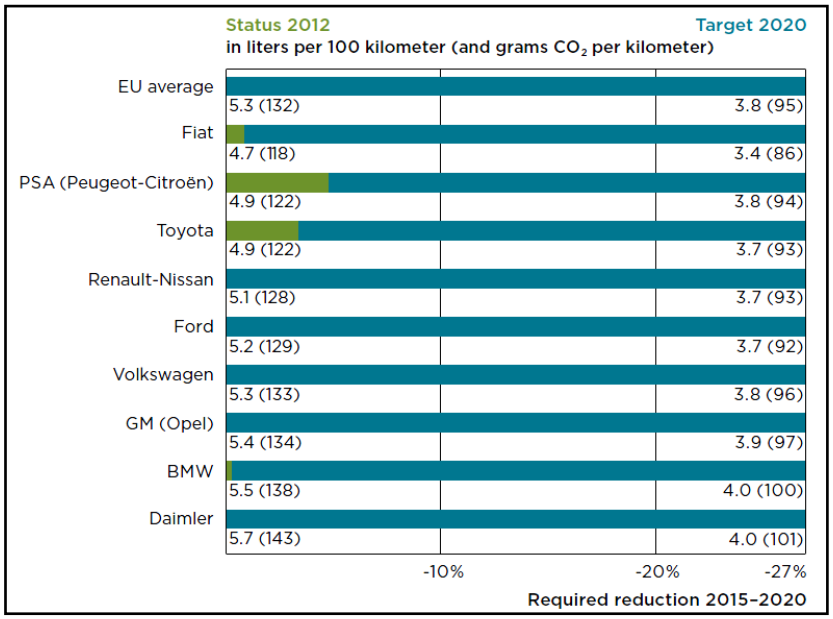

Figure 1.2-1 Average fuel consumption in the EU by vehicle manufacture [1]

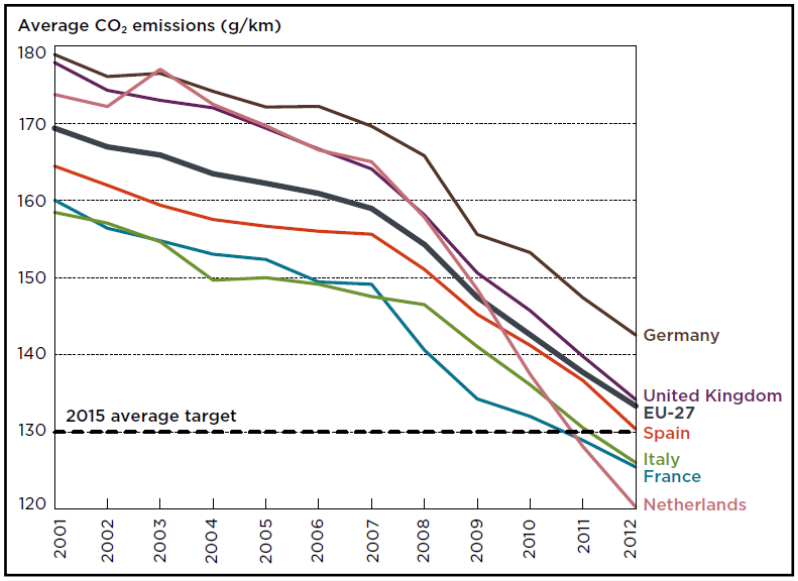

Figure 1.2-2 Passenger cars CO_2 emissions by member state [1]

Also average CO_2 emissions of different vehicle brand and different vehicle segment are shown in Figure 1.2-3. The emissions of luxury and sport cars are the highest ones because they have larger exhaust volume in order to get excellent performances.

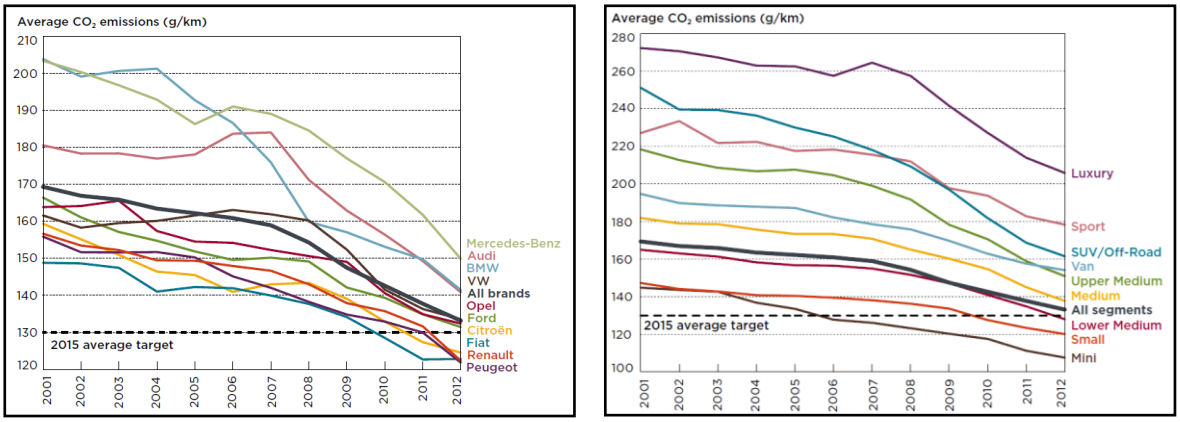

Figure 1.2-3 Passenger cars CO_2 emissions by vehicle segment [1]

1.3 Other emissions

The Euro 6 emission standard was put into effect in year 2014, limitations that range from 68% (gasoline carbon monoxide) to 96% (diesel particulates), that is lower than those determined under Euro 1 in 1992. At the moment less than 1% of new registration vehicles already satisfied the Euro 6 standard, at same time 91% of all cars sold complied with the Euro 5 standard. Real world emissions, that is emissions are measured outside a vehicle laboratory, have not yet decreased to the target suggested by the Euro standards. This is particularly true especially for NO_x emissions from diesel cars and the limitation for these emissions has decreased by 64% from Euro 3 in year 2000 to Euro 5 in year 2009. According to available information real world emissions during this period have reduced by only 18% [4], so there is a huge gap between 64% and 18%. The most important cause is air quality problems, especially in urban areas.

Table 1.3-1EU emission limits for gasoline passenger cars, g/km [1]

	Date	CO	HC	$NMHC$	NOx	$HC + NOx$	PM	PN
Euro 3	Jan 2000	2.30	0.20	-	0.15	-	-	-
Euro 4	Jan 2005	1.00	0.10	-	0.08	-	-	-
Euro 5	Sep 2009	1.00	0.10	0.068	0.06	-	0.0050	-
Euro 6	Sep 2014	1.00	0.10	0.068	0.06	-	0.0045	6.0×10^{11}

Table 1.3-2 EU emission limits for diesel passenger cars, g/km [1]

	Date	CO	HC	$NMHC$	NOx	$HC + NOx$	PM	PN

Euro 3	Jan 2000	0.64	-	-	0.50	0.56	-	-
Euro 4	Jan 2005	0.50	-	-	0.25	0.30	-	-
Euro 5	Sep 2009	0.50	-	-	0.18	0.23	0.0050	-
Euro 6	Sep 2014	0.50	-	-	0.08	0.17	0.0045	6.0×10^{11}

The EU emission limitations form Euro 1 to Euro 6 for gasoline and diesel passenger cars are summarized in Table 1.3-1 and Table 1.3-2 respectively.

Specific meanings of emission symbols listed in tables are:

- $\boldsymbol{CO}$: Carbon Oxide, product of incomplete combustion;
- $\boldsymbol{HC}$: Hydrocarbons, result when fuel molecules in the engine do not burn or burn only partially.
- $\boldsymbol{NMHC}$: Non-Methane Hydrocarbon, NMHC emissions from vehicles include refueling losses (controlled by onboard refueling vapor recovery systems in newer vehicles and at the pump in certain areas), starting emissions, evaporative losses, and tailpipe emissions.
- $\boldsymbol{NOx}$: Nitrogen Oxide, a generic term which is used to describe various nitrogen oxides produced during combustion.
- $\boldsymbol{PM}$: Particular Matter, which is the general term for the mixture of solid particles and liquid droplets found in the air. Particulate matter includes dust, dirt, soot, smoke and liquid droplets. It can be emitted into the air from natural or man-made sources, such as windblown dust, motor vehicles, construction sites, factories and fires. Particles are also formed in the atmosphere by condensation or through the transformation of emitted gases such as nitrogen oxides, and volatile organic compounds.
- $\boldsymbol{PN}$**:** the number of solid particles, which could cause health issues.

1.4 Solutions for reducing vehicle emissions

A number of technical and non-technical measures are adopted in terms of their potential contribution to CO_2 reduction in passenger cars, but at same time cost of these strategies is considerable. These measures have been identified by the European Commission and can be

regarded as complementary options, including the following technical and non-technical measures [5]:

Technical measures:

- Technical improvements to reduce fuel consumption at the vehicle level;
- Adoption of fuel efficient air conditioning systems;
- Options to reduce vehicle and engine resistance factors;
- Strategies for application of alternative fuels based on fossil energy;
- Biofuels research;
- Possibilities to include N_1 vehicles into the commitments (N_1 vehicles are vehicles designed and constructed for the carriage of goods and having a maximum mass not exceeding 3.5 ton).

Non-technical measures:

- Fuel efficient driving;
- CO_2 based taxation schemes for passenger cars;
- Strategies for improved energy or CO_2 labeling;
- Public proposals;

Car manufacturers are adopting many technological strategies to reduce the fuel consumption and CO_2 emissions, such as improvement of the engine efficiency, reduction of transmission loss, decrement of vehicle drag coefficient, reduction weight and so on, these technical improvements will be discussed in next section.

1.5 Conclusion

In this chapter, vehicle fuel consumption and emissions have been discussed. As the number of cars on the road has grown, consequently, carbon dioxide (CO_2) emissions from road transport have increased by $21\ \%$ between 1990 and 2011, and they account for about 23% of the EU's total CO_2 emissions, which is responsible for global temperature increasing and climate change at the moment. In order to ensure that the EU meets its greenhouse gas emission targets under the Kyoto Protocol, a comprehensive strategy to reduce CO_2 emissions from new cars and vans sold in

the European Union was adopted in 2009. The Regulation sets a short-term target of $130\ g\ CO_2\ /\ km$ by 2015, to be phased in from 2012, and a long term target of $95 g\ CO_2\ /km$ by 2020.

In order to satisfy $CO2$ emission limits in regulations, different technological and non-technological strategies are adopted at the moment and for sure, many more innovative strategies will be explored in future.

1.6 Reference

[1]. The International Council on Clean Transportation, “European Vehicle Market Statics, Pocketbook 2013”.

[2]. The Organization for Economic Co-operation and Development (OECD), “Strategies to Reduce Greenhouse Gas Emissions from Road Transport: Analytical Methods”, 2002.

[3]. European Environment Agency, “Monitoring CO_2 emissions from new passenger cars in the EU: summary of data for 2012”.

[4]. David C., Sean B., Emily W. and Martin W., “Trends in NOx and NO_2 emissions and ambient measurements in the UK”, 2011.

[5]. TNO Science and Industry, “Review and analysis of the reduction potential and cost of technological and other measures to reduce CO_2-emisssions from passenger cars”, 2006.

2 Chapter 2 Technological strategies to reduce vehicle emissions

2.1 Introduction

Improvement of traditional vehicle efficiency has been considered as an effective means to reduce fuel consumption and emissions. Vehicles consume different quantity fuel because of different contributions of their sizes, weight and technologies. However, both car designers and consumers consider fuel economy very carefully before they make decisions, which is one of the most important operating performances of vehicle. Figure 2.1-1 is showing vehicle energy flows in a 2.5L Camry in an urban driving cycle [1].

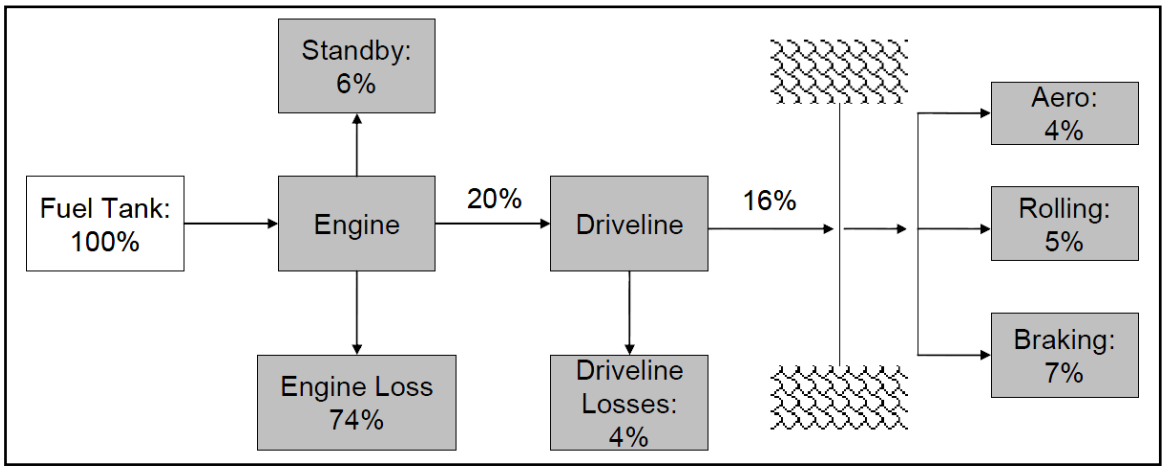

Figure 2.1-1 Representative vehicle energy flows in an urban driving cycle [1]

Nowadays a number of innovative vehicle technologies are being considered in order to reduce emissions of greenhouse gas, but feasible and commercialized degree of the technology should be assessed first because it is related to industrial application. During the past years many options have been verified to improve fuel economy for traditional internal combustion engine (ICE) vehicle, Figure 2.1-2 shows some key corresponding technologies which are already existing and used in automotive systems in order to reduce vehicle emissions [2].

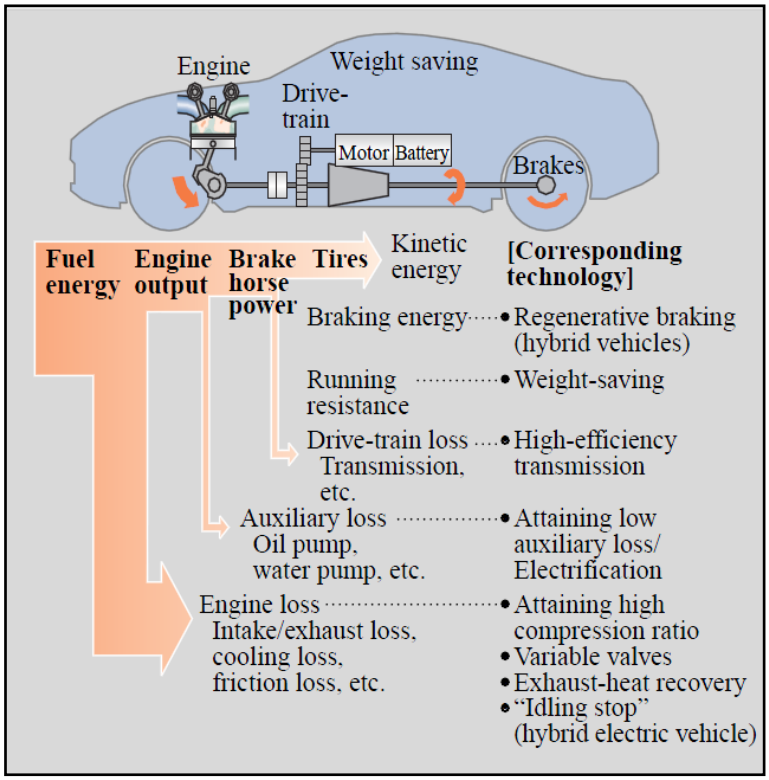

Figure 2.1-2 Energy flow within an automotive vehicle [2]

Figure 2.1-1 and Figure 2.1-2 are showing that most of the input energy is dissipated through different losses and anti-resistances, effective options which could result in less fuel consumption are: engine with increased efficiency, less drag losses (improved aerodynamic behavior) , regenerative braking systems, lower weight and so on. These important technological improvements being considered and adopted in vehicle industry during recent years are discussed in the following sections:

2.1.1 Engine technologies

Innovative engine technologies are developed to improve engine efficiency in order to reduce fuel consumption, some of them could increase the efficiency of all types of engines, which are: boosting (turbocharger and supercharger), idle off, direct-injection engine systems, variable-valve systems. Also different types of engines are adopted. Furthermore, because of high engine control possibility, some improvements applied to engine system properties such as engine-knock resistance, electronic lean burn and large-scale EGR (exhaust recirculation) results beneficial also for reduction of fuel consumption.

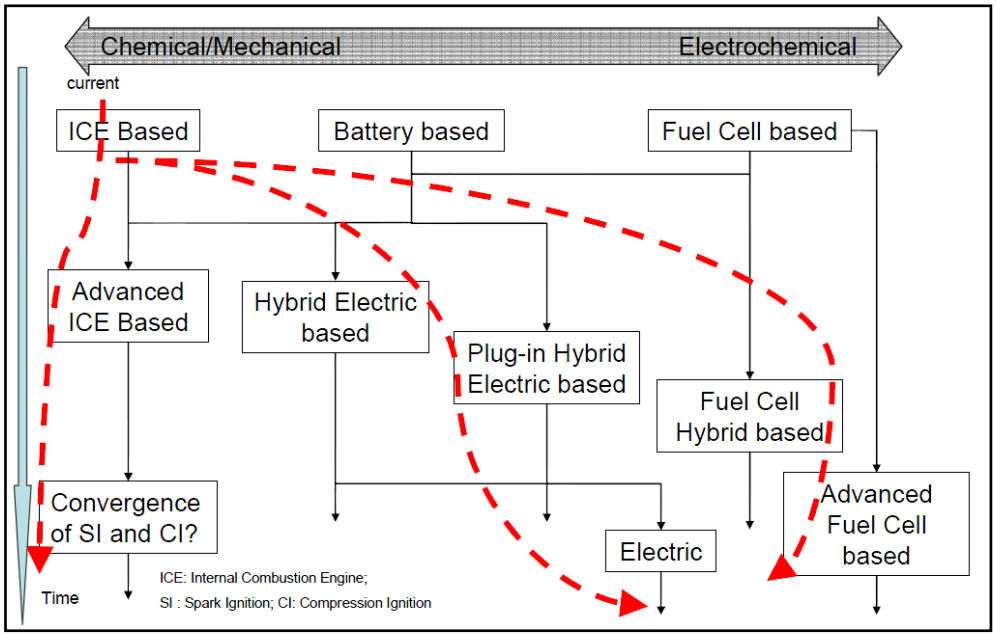

Figure 2.1-3 Future propulsion system pathways [1]

Figure 2.1-3 [1] is showing the possible evolution of vehicle propulsion systems which could be adopted over the next decades. The most conventional vehicle propulsion system at the moment in automotive industry is internal combustion engine (ICE) that release the chemical energy of fuels by combustion and convert it to mechanical energy. The U.S light-duty market is dominated by gasoline-powered spark-ignition (SI) engines, while diesel powered compression ignition (CI) engines are dominating the European light-duty vehicle market and the global heavy-duty vehicle market. Also battery based and fuel cell based systems already exist in market, such as Tesla Model S and BMW 1 series.

2.1.2 Transmissions efficiency

Transmission system is one of the most important subsystems in vehicle engineering because it impacts much on the performances of vehicles, especially related to the comfort degree of driver and passengers. Many different transmission systems are already developed in automotive industry, such as manual transmissions, torque-converter transmissions, dual-clutch transmissions, CVTs and so on, which are working with different class vehicle in order to get the best performance. The best options to make engine run with better fuel efficiency with less power loss is to increase the number of gears and the

transmission-ratio spread. Many options could be considered to improve the transmission efficiency: fuel efficient transmission oil using, more efficient lubrication systems and pumps, improvements of shifting strategies, better gearings, optimized bearings and seals/gaskets. When a component made with traditional iron-based material is substituted by a new designed one made with lightweight materials, this result in higher specific workload, the torque-to-weight ratio of the transmission could be remarkably increased.

In this transmission area, further improvements will be developed in future through the use of new lubricants, advanced materials, redesigned components and innovative manufacturing technologies.

2.1.3 Regenerative braking system

Regenerative braking system is allowing vehicle to recapture energy that would otherwise be dissipated as heat when vehicle is going to slow down or park, the system is usually assembled in electrical vehicles (energy is recaptured by battery system). Usually regenerative braking systems recover as much kinetic energy as possible and store it as electrical energy. Then stored energy would be used to drive the vehicle when vehicle is started again.

2.1.4 Aerodynamic drag reducing

Drag is a force that acts in the same direction as the airflow when vehicle is running, the drag coefficient C_d is a common measure in automotive design as it is related to dynamic behaviors. Usually the average modern automobile achieves a drag coefficient of between 0.30 and 0.35, SUVs could achieves a C_d=0.35-0.45 with their typically boxy shapes. For a perfect car body configuration the lowest possible aerodynamic drag coefficient is 0.16. Drag coefficient of Tesla Model S is about 0.24 as reported officially, which is an exceptionally good design [3].

Reducing the drag coefficient in an automobile could improve the performance of the vehicle as it is linked directly to fuel consumption. Many various approaches of structural devices are adopted to reduce vehicle drag: front screens, rear screens, structural

elements that localize the area of flow detachment (edging), vortex air flow generators, deflectors located over the rear part of vehicle's roof, four element rear fairing and its components and front fairing. From previous research work done by Upendra S.R in 2012 [4], the use of rear screen resulted a reduction in aerodynamic drag by up to 6.5% and rearing fairing as part of flow separation area behind the vehicle can reduce aerodynamic drag of the vehicle with particular configuration by up to 26%. There are other passive strategies that have potential to reduce dragging force, front structural elements result in decrement of the drag coefficient up to 2.24% and vortex generator shows a decrement up to 1.24% . There is much space to achieve further improvement of aerodynamic performance with the understanding of fluid field and optimization of vehicle configuration design.

2.1.5 Vehicle weight reduction

Fuel economy can be improved by reducing aerodynamic drag and increasing the thermodynamic efficiency of the engine, however remarkable gains can also be achieved by reducing vehicle weight. Some advanced materials with high specific stiffness and strength properties are adopted into the automotive applications. From the research study [1], every 10% of weight reduced from the average new car or light truck can decrease fuel consumption by 6.9%, as shown in Figure 2.1-4 [1].

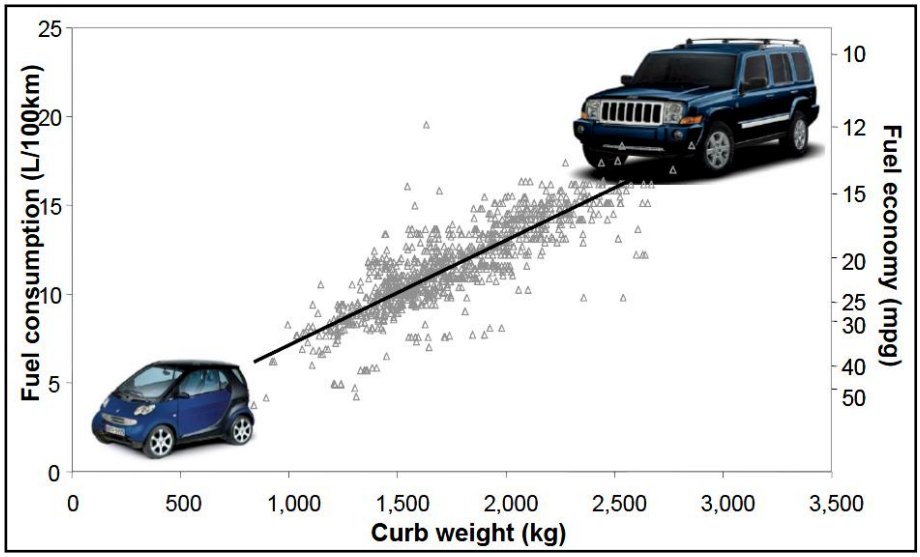

Figure 2.1-4 Curb weight and fuel consumption of U.S. model year 2005 [1]

In past years, many technological improvements have been developed in order to increase fuel economy; they are listed in Table 2.1-1 where also how much potential fuel economy could be obtained is summarized [4].

Table 2.1-1Fuel Economy Improvement Potential of Conventional Vehicle Technologies [4]

Technology	Fuel economy improvement potential
2-stroke engines	15% to 20% (compared to 4-stroke engines of similar power output)
4-stroke direct injection stratified charge engines	18% to 23%
Direct-injection diesel engines	25% to 40% (compared to similar displacement gasoline engines)
Continuously variable transmissions (CVTs)	3% to 10%
Lightweight materials: aluminum, magnesium, plastics, composites, powdered metals	10% to 20% (assuming weight reduction of 30% without compromising safety, comfort, or performance)
Reduced rolling resistance	5% to 8% (assuming 30% reduction in rolling resistance)
Improved aerodynamics	5% to 15% (based on reduction in wind resistance of up to 30% without radically changing vehicle shape or restricting comfort)

Table 2.1-1 is telling us that fuel economy could increase 10% to 20% if weight reduction is about 30%, so this reduction space is considerable and more technological improvements would be discussed now and in future. The next section is dedicated to lightweight design of vehicle.

2.2 Lightweight design of vehicle

2.2.1 Introduction

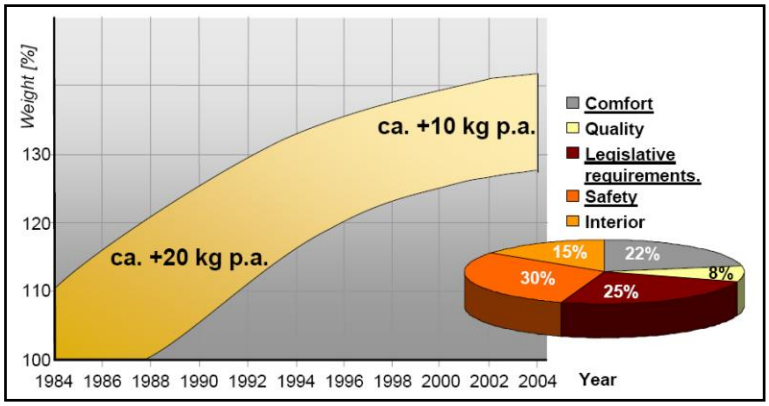

Figure 2.2-1 Trend total vehicle weight [5]

Since vehicle was born, people have had more and more demands to vehicles, which are including safety, comfort, quality, interior, speed and so on. These requirements could be obtained by using of heavier engines, improved chassis, higher stiffness in Body in White (BiW) and more accessory parts. Vehicle weight history during past 30 years is shown in Figure 2.2-1 and Figure 2.2-2 [5, 6]. Factors related to vehicle safety, national legislative requirements and comfort degree, are the most important three factors impacting vehicle history development.

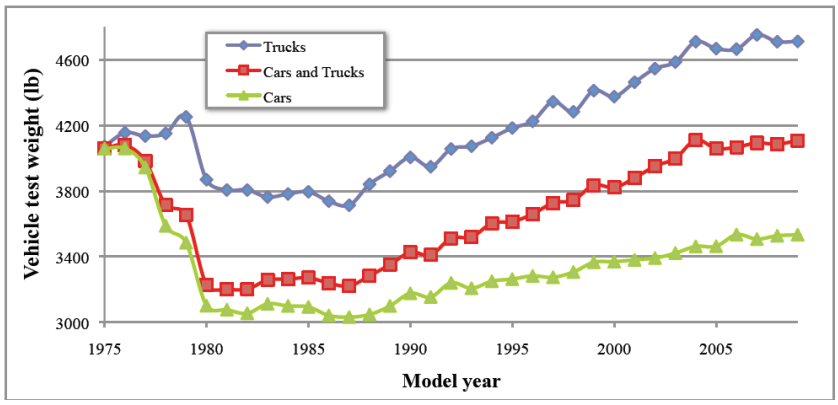

Figure 2.2-2 Different segment vehicle mass change [6]

Figure 2.2-2 is showing the weight trend for light-duty vehicles in past 30 years in U.S market, with two major categories contained in light duty family (based on data available from report of U.S. EPA, 2009a [6]). Both phases of decreasing and increasing weight are visible in U.S market during this period. The first time period is from 1975-1980, 21% decrease in average new light duty vehicle weight (with a 25% decrease for cars and 9% for light trucks) was exhibited because of fuel economy standard established by federal government as a consequence of the first big energetic

crisis that leaded also to a large increment in the fuel price. The second time period is from 1987 to 2009, the trend has been toward progressively heavier vehicles, with a 28% weight increase for new light duty vehicles (27% weight increase for cars, 17% for trucks). This increasing trend happened because of the stable environmental constraints, including clear federal standards and stable resource prices.

As shown by Figure 2.2-3, the average mass of new registration cars in EU in 2012 was $1400\ kg$; vehicle weight was always increasing slowly with a small decrement around year 2009 when the EU emission standard was established. From figure we could see that both German and Swedish new cars were in average much heavier than the EU average level in 2012, around 1489 and $1580\ kg$ respectively. On the other hand, French, Italian, and Netherland people preferred significantly lighter cars ($1342\ kg$, $1313\ kg$, and $1252\ kg$ respectively) [7].

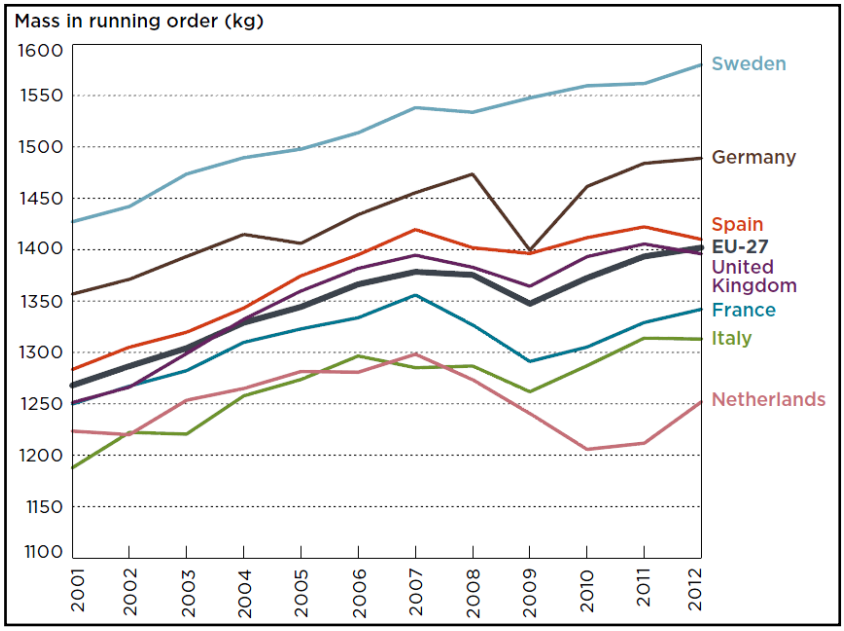

Figure 2.2-3 Vehicle weight change by member state in EU [7]

2.2.2 Options to achieve weight reduction

Many options are explored to reduce weight of vehicle sold in the market in order to improve fuel economy, which from a general perspective could be summarized in three ways:

- Redesigning the vehicle substructure:

On a component level, some amount of weight savings could be obtained from new architectures design without compromising key performance of the component. Some other advantages could be obtained by a proper extensive use of structural optimization procedures.

- Reducing vehicle size:

  It is clear that vehicle weight could be reduced by downsizing vehicle. As predicted by published studies [1] weight savings of $9\% - 12\%$ could be achieved by changing large vehicle to midsize and changing midsize to small size, size classes were identified by U.S EPA. At the same time higher weight savings, of the order of magnitude of 26%, could be obtained if SUVs, minivans and pickups are downsized.

- Lightweight material substitution:

  More and more alternative lightweight materials are available and can be used in automotive industry at the moment, such as high strength steel (HSS), aluminum, magnesium, composites and so on. Usually advanced materials have higher specific stiffness/strength than traditional material. Research studies revealed that traditional steel is usually used to build vehicle body panel and in this case $1\ kg$ of aluminum can replace $3-4\ kg$ of steel. For some concept vehicles, the weight savings could research $20\% - 45\%$ if advanced lightweight materials are used, which was demonstrated in research work [1].

Advanced material substitutions in automotive industry are discussed in next paragraph.

2.2.3 Vehicle weight reduction by lightweight material substitution

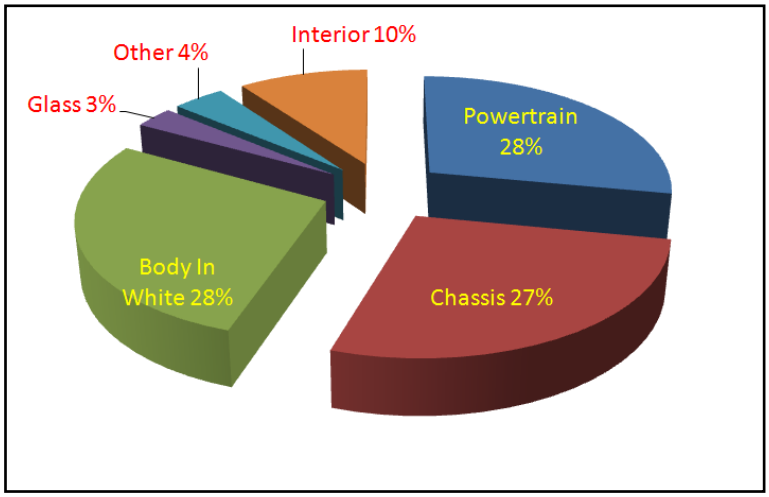

Figure 2.2-4 Vehicle weight composition by mass ratio [8]

Generally 75% of total vehicle weight is occupied by Body in White, power train and chassis (see Figure 2.2-4) [8], which are built with steel normally. The rest 25% of weight is given by aluminum, plastic composites, glass and other materials. Figure 2.2-5 [9] is showing the compositions change of vehicle weight by mass percent from year 1975 to year 2007, the mass ratio of mild steel has been decreasing remarkably from 56% to 43%, at the same time applications of other materials were increasing a lot, such as other types of steels, aluminum, magnesium and plastics. Plastics composites used in automotive structure are increased from 4% to 8% during past 40 years, i.e. percentage is doubled.

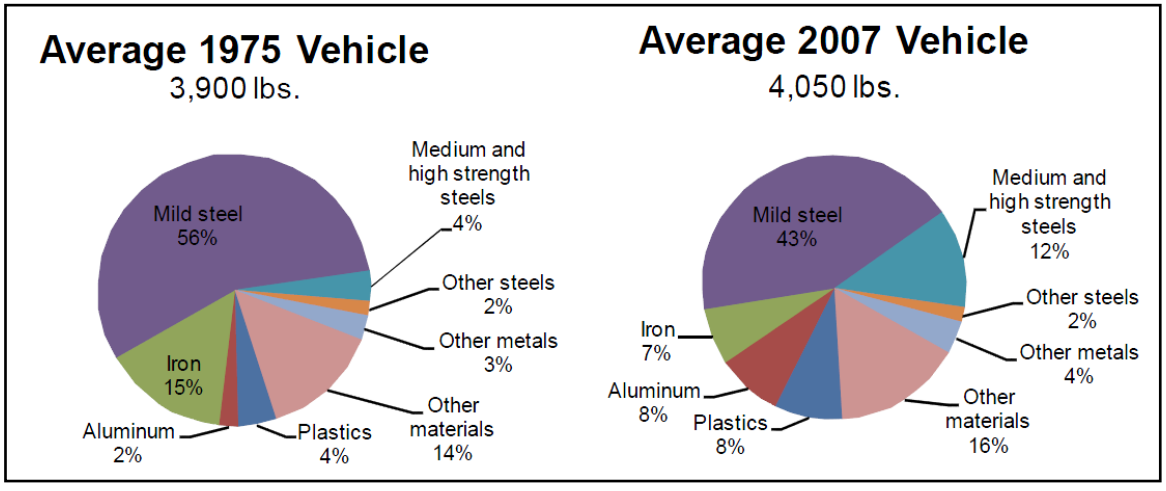

Figure 2.2-5 1975 and 2007 average vehicle mass breakdown by material [9]

The materials used in the automotive industry, including traditional and advanced materials, relevant mechanical properties and relative cost are summarized in Table 2.2-1 below, which will be discussed separately in detail.

Table 2.2-1Properties and prices of alternative lightweight automotive materials [1]

Material	**Density, $g/cm3$ (relative)**	**Yield strength, MPa**	**Tensile strength MPa**	**Elastic modulus GPa**	**Relative cost per part [Powers 2000]**
Mild steel	7.86 (1.0)	200	300	200	1.0
High strength steel (A606)	7.87 (1.0)	345	483	205	1.0-1.5
Iron (D4018)	7.10 (0.9)	276	414	166	-
Aluminum (AA6111)	2.71 (0.34)	275	295	70	1.3-2.5
Magnesium (AM50)	1.77 (0.23)	124	228	45	1.5-2.5
Composites • ***Carbon fiber*** • ***Glass fiber***	1.57 (0.20)	Flexural 200	810	190	2.0-10.0

We can see that advanced materials have better mechanical properties comparing to traditional material with much weight reduction, but at same time higher cost factor is presented.

2.2.3.1 High-Strength Steels (HSS)

Early in the 1970's, high strength steels (HSS) was introduced into automotive industry with development of low carbon steels, and in 1980 dual phase steels (DP) and bake hardening steels (BH) were also adopted. Then transformation induced plasticity steel (TRIP) application was beginning in the 1990's. In recent years, ultra high strength steels (UHSS) have been brought into automotive engineering.

HSS are classified as steels with yield strength from 210 to $550\ MPa$. Ultra high strength steels (UHSS) reach yield strengths above $550\ MPa$. The HSS grades include interstitial free steel (IF), bake hardening steel (BH), carbon-manganese (C-Mn) and high strength low alloy (HSLA) steels. Advanced high strength steel (AHSS) family contains dual phase steel (DP), complex phase steel (CP) and transformation induced plasticity steel (TRIP). These materials are applied in different

automotive components because of their different characteristics; specific applications are shown in Figure 2.2-6 [10].

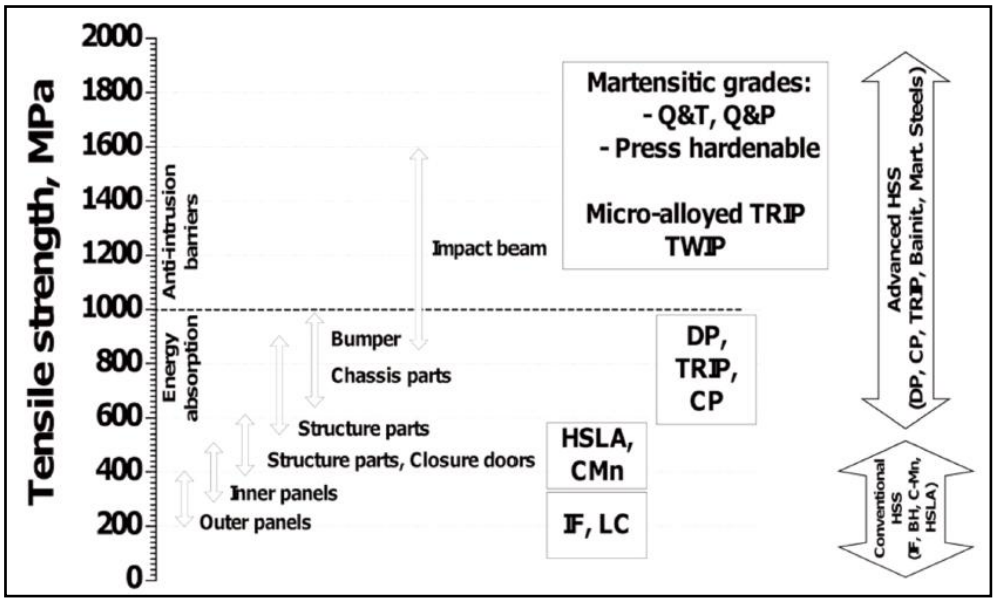

Figure 2.2-6 Tensile strength requirements of different components of passenger cars and range of application of HSS [10]

Symbols meanings in Figure 2.2-6:

HSS: high strength steel;

Q&T: quenching and tempering steel;

Q&P: quenching and partitioning steel;

TRIP: transformation induced plasticity steel;

TWIP: twinning-induced plasticity steel;

DP: dual phase steel;

CP: complex phase steel;

HSLA: high strength low alloy steel;

CMN: carbon manganese steel;

IF: interstitial free steel;

LC: low carbon steel.

In automotive industry, these high strength steels can provide the required mechanical properties at low cost and with low vehicle emissions. TRIP steel is the first choice material for crash impact design, thanks to its higher capacity of energy absorption [10].

2.2.3.2 Aluminum

The intensive use of aluminum could be found easily in European automotive industry, the European automotive industry has more than doubled the average amount of aluminum used in passenger cars during the last decade (see Figure 2.2-5) , and for sure much more aluminum applications will be adopted in coming years.

Figure 2.2-7 is showing that an average of $102\ kg$ aluminum was used in automotive parts in Western Europe in year 2000 while, according to data published in [11], it is expected that the amount of aluminum will become $230\ kg$ rapidly in 2015.

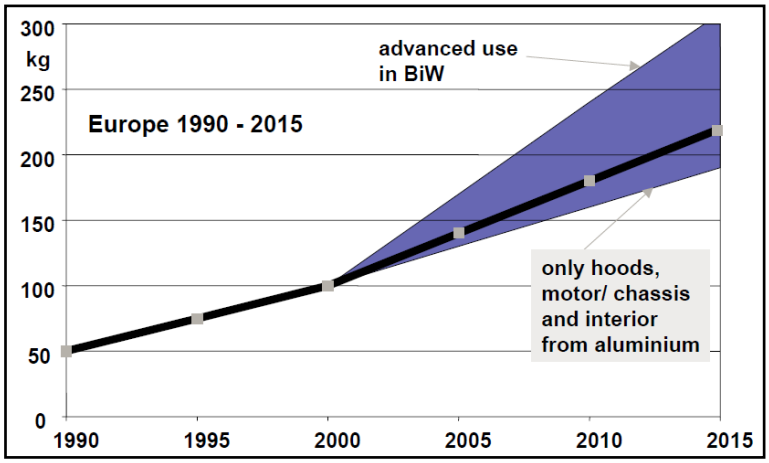

Figure 2.2-7 Average use of aluminum per car in Western Europe [11]

Real industrial applications of aluminum are shown in Figure 2.2-8, up to $300\ kg$ are used in AUDI A2 body and $500\ kg$ in AUDI A8 [11]. However, aluminum is heavier than other lighter weight materials, such as magnesium and fiber reinforced composites. But better manufacture characteristics could be found in aluminum: complex configuration availability, good recyclability and lower cost.

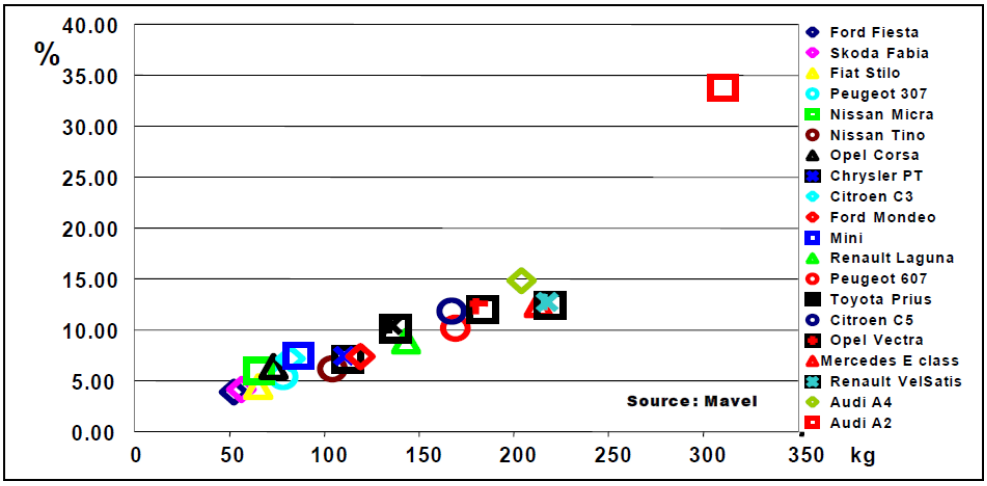

Figure 2.2-8 Relative and absolute use of Aluminum in European cars [11]

Furthermore, one important factor of aluminum application is that it is available for a lot of semi-finished product forms such as extrusions, shape castings and sheets. Many semi finished products could be easily adopted for high volume production and innovative solutions, with a higher integrated level that have a better structural integrity and higher structural stiffness. In this case, many traditional parts which are connected together through additional bonding strategy could be replaced by only one aluminum part. This means that the number of parts in whole vehicle structure will be reduced considerably, and it result in less manufacture cost and better structural performances.

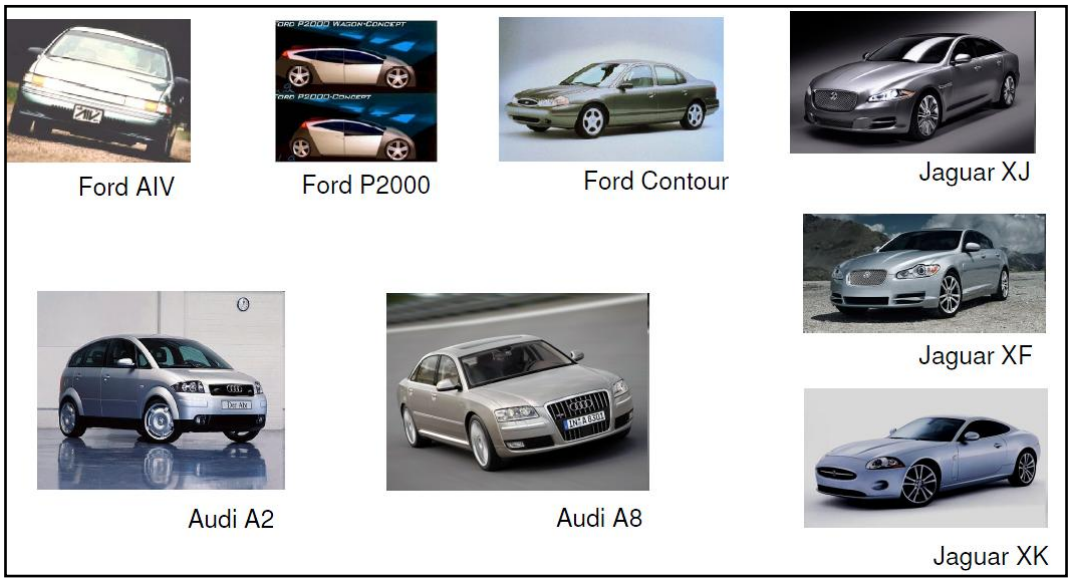

Figure 2.2-9 Aluminum intensive vehicles

Disadvantages of aluminum application in automotive industry are joining techniques and surface treatment strategies for many semi-products which are used in different parts in vehicle structure. Many aluminum intensive applications are shown in Figure 2.2-9, that are usually in engine blocks, power train parts and space frames (Audi A2, BMW Z8, Lotus Elise), sheet structures (Honda NSX, Jaguar) or as closures and hang-on parts (e.g. DC-E-class, Renault , Peugeot) and other structural components [11].

2.2.3.3 Magnesium

Comparing to steel and aluminum material, magnesium alloy is 30% and 50% lighter respectively. Also it is much easier to manufacture and machine as different shapes, with a lower latent heat because it becomes solid phase faster. But magnesium has a lower ultimate tensile strength, smaller modulus and hardness than aluminum (see Table 2.2-1), also it has a worse fatigue resistance. Finally it generally has poor corrosion resistance.

At the moment magnesium alloy is usually manufactured as instrument panels and cross car beams through casting process. Other applications could be found in seat frames, knee bolsters, valve covers and intake manifolds. Content of magnesium part in vehicle structure is around $10\ kg$ [12]. The U.S. Automotive Materials Partnership (USAMP) has predicted a significant trend that magnesium alloys mass will reach almost $160\ kg$ by 2020.

However, shortcomings of magnesium applications in automotive industry are bad creep properties under high temperature, corrosion phenomena, die casting quality and so on.

2.2.3.4 Composite

Figure 2.2-10 Composite applications in different areas

Recently the use of composite materials has increased considerably in automotive industry. According to the report [13], the global consumption of lightweight materials used in transportation system is increasing at a compound annual growth rate (CAGR) of 9.9% in mass point view between 2006 and 2011 [14]. Usually composite could be found in automotive parts such as bumpers, fuel tanks, chassis parts, drive shafts, brake discs (in this case Metallic Matrix Composite are considered) and so on. Figure 2.2-11 is showing the trend of different materials use in automotive engineering during past 35 years; result reveals that plastics and composites are growing slowly according to the mass perspective point view.

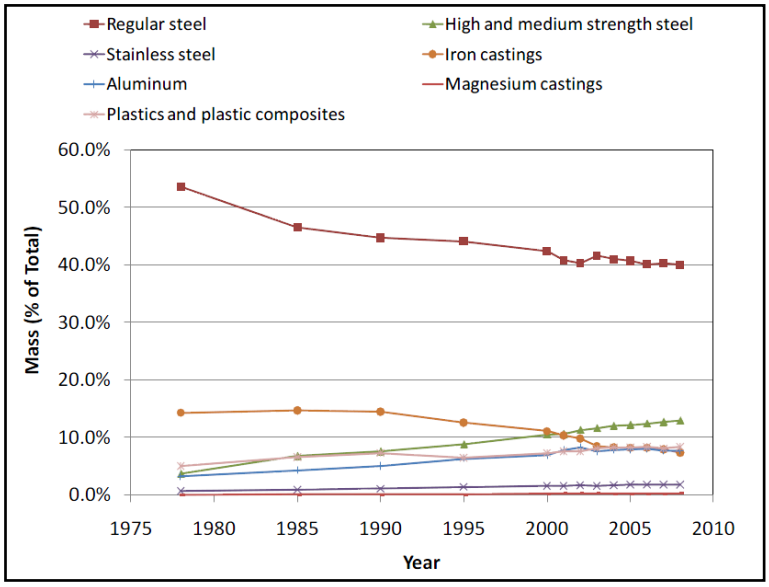

Figure 2.2-11 Vehicle material compositions by percent mass [15]

Based on a history point of view, the first car body made from glass fiber reinforced polymer composites was the Chevrolet Corvette, which was shown to people at New York in 1953 [16]. Since that time, the Corvette industry was always using composite materials in its own design. In 1981 racing car McLaren MP4 also adopted carbon fiber reinforced composite materials, consequently, overall vehicle performances were improved significantly, and particularly the force of tires to grip ground increased a lot because of a better weight distribution. At the moment, almost every racing car is using composites in huge amount, especially Formula 1 cars.

Composites have many advantages comparing to traditional materials as mentioned before, such as their relatively higher strength and lower weight (see Figure 2.2-12), better corrosion resistance, better energy absorption in case of impact and so on.

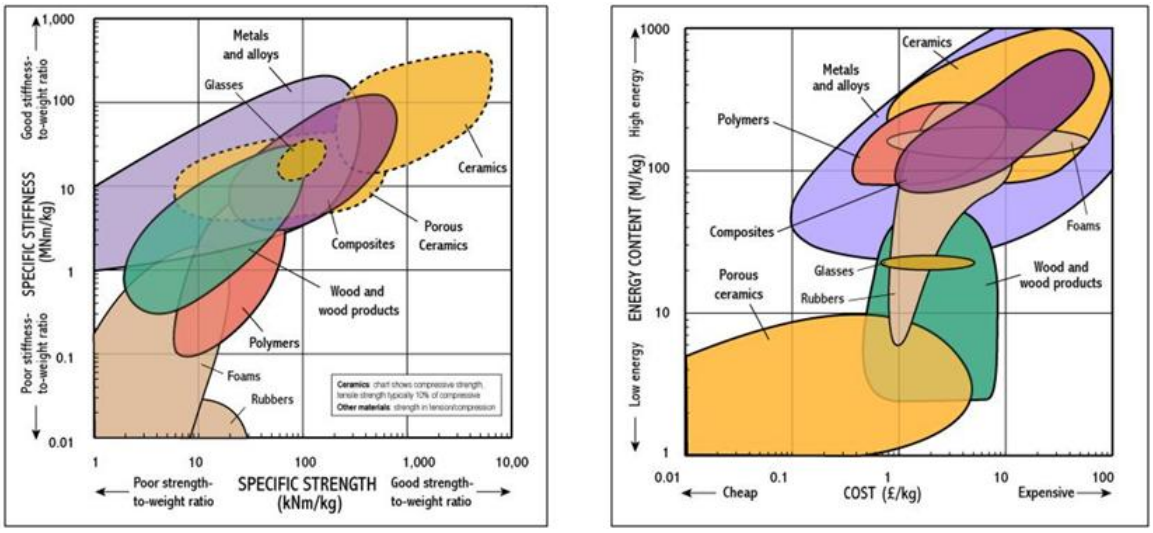

Figure 2.2-12 Ashby maps for comparison of mechanical performance of materials

Usually we can get a higher horsepower/weight ratio and a better weight distribution in vehicle structure if composite materials are adopted in vehicle industry, also lighter vehicles lead to a decrement of fuel consumption, which could reduce the environmental pressure remarkably. As predicted in some studies [13, 14], fuel economy could be improved by 7% for every 10% of weight reduction from a vehicle's total weight.

Research work said that using carbon fiber composites instead of traditional steel material in vehicle pats could obtain 50% weight reduction [13, 14] if structural component are designed properly, which is a significant way to reduce vehicle emissions. Many composite materials application could be found in many vehicles (see Figure 2.2-14). For example, in the electric

vehicle BMW i3 (see Figure 2.2-15), most of internal part and body structure are made with carbon fiber reinforced plastic (CFRP), the passenger compartment is totally made with CFRP , which comprises around 150 CFRP parts with a weight reduction 30% [19].

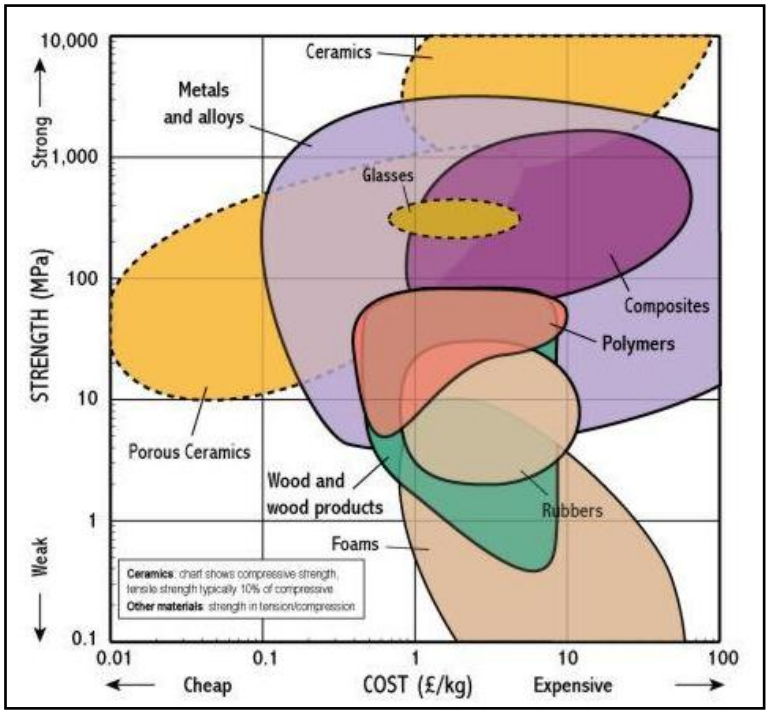

Figure 2.2-13 Ashby maps for comparison of strength and cost of materials

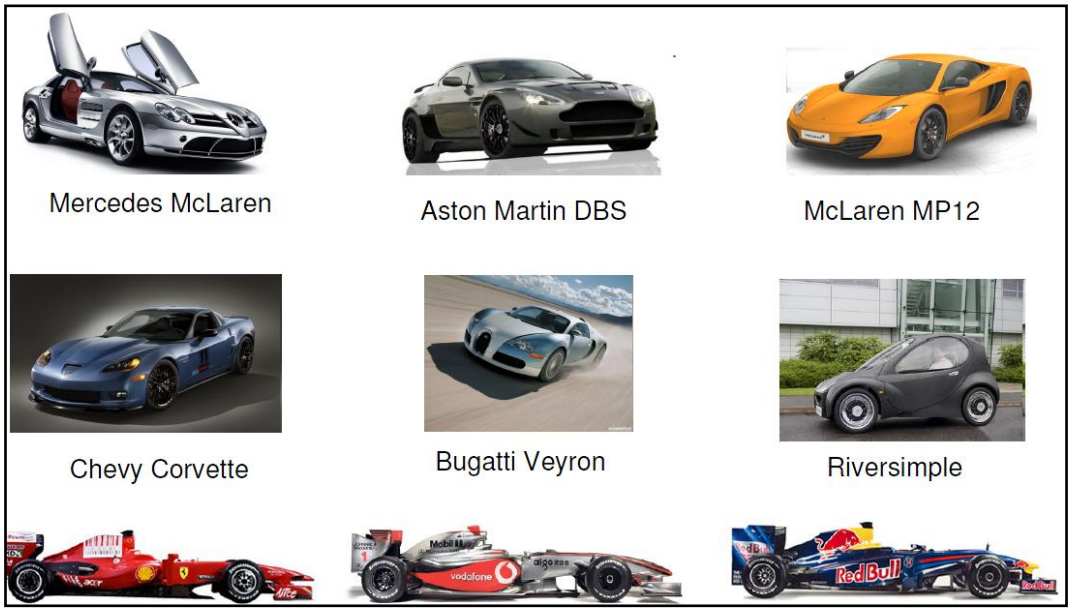

Figure 2.2-14 Vehicles with reinforced carbon fibers

Figure 2.2-15 Configure of BMW i3 [19]

Many difficulties are encountered on the way of successful incorporation of huge quantities of carbon fiber into car structures of the future. The high cost of the fiber is the largest difficulty to produce carbon fiber composites as a structural component. The primary technical challenges are significant and are generally divided into five broad categories:

- Cost —raw materials and manufacturing (see Figure 2.2-13);
- Manufacture speed — high volume production with low cost;
- Design/test methodologies— how to design and test components and subsystems to assure long term performances;
- Joining technology— especially to dissimilar materials ;
- Recycling and repair— how to repair without replacing and recycle at the end of life.

2.3 Requirements about safety

Vehicle safety should be discussed when lightweight materials are adopted in automotive industry. Usually people think that lighter vehicles are at a greater risk during crash events than heavier vehicles. The overall safety of transportation system should include safety of the driver and the other passengers on board, vulnerable road users and specific accident environment. But this can be questionable, in fact if we, for example, consider two different weighted vehicles crash with same speed, it may result that the lighter vehicle is safer because the heavier vehicle need to absorb higher kinetic energy.

It is reasonable that there will be little decrement in crashworthiness when reducing the weight and size of the vehicle if safety strategies are considered in proper way. It is possible to design quality small vehicles with similar crashworthiness as heavier ones by using new materials, such as

aluminum or composites, which could offer better cash energy absorption. Further adjunctive passive safety strategies could be adopted, such as seat and side airbags. Manufacturers are already making smaller cars that can protect their occupants better. For example, the MINI Cooper scored 4 out of 5 stars in the U.S. National Highway Traffic Safety Administration frontal and side crash ratings [1] and FIAT 500 got the best five stars in the EURO-NCAP adult occupant test in 2007 [20].

Apart from the crashworthiness of the vehicle safety, also rollover risk, aggressiveness of vehicles to other vehicles and other road users (compatibility), should be considered. On the overall road safety point of view, large heavy SUVs and pickups actually create great risks for their drivers or other road users [17]. Hence, there is little drawback in safety if vehicle weight is reduced, and overall road safety could be improved if the heaviest vehicles could be replaced by lighter ones.

2.4 Conclusion

This chapter has discussed the strategies adopted by car manufacturers in order to reach vehicle noxious gas emissions and fuel consumption reduction. One of the possible concurrent strategy is weight reduction. Every 10% of weight reduced from the average new car or light truck can decrease fuel consumption by around 7%. Three conventional strategies are: (1) vehicle redesign, (2) vehicle downsizing, and (3) lightweight material substitution.

Vehicle weight savings can be obtained by redesigning or reconfiguring the vehicle and/or downsizing the vehicle. If people are willing to choose a small car instead of a midsize, or a midsize instead of a large car, the vehicle's weight could be reduced by 9% to 12%. For SUVs, minivans and pickups, the weight savings even can reach 26%.

Alternative materials are used to substitute the traditional materials to reach the lightweight design target, such as high strength steels, aluminum, magnesium and composites. These materials have many advantages comparing to traditional material and could easily satisfy structural requirement, such as high strength and high capacity to absorb energy during crash impact; however other problems must be considered before they are brought into automotive industry with a huge amount

of produced parts, problems such as high cost and low production speed. Anyway, alternative material substitutions in automotive engineering have a promising future.

Also safety of lighter vehicles is discussed briefly in the end. Lightweight design of vehicle could improve overall safety of transportation system, including the safety of other drivers, other passengers, pedestrian and other vulnerable road users.

2.5 Reference

[1]. Anup B., Kristian B., Lynette C., Christopher E., Tiffany G., John H., Emmanuel K., Matthew K. and Malcolm W., " Reducing Transportation's Petroleum Consumption and GHG Emissions", Report No. LFEE 2008-05 RP, MIT, 2008.

[2]. Junichi I., Minoru O., Takashi O., Hideki Miyazaki, Mitsuru K. and Koichiro T., "Reduction of CO_2 Emissions for Automotive Systems", Hitachi Review Vol. 57 (2008), No. 5.

[3]. Sherman D, "Drag Queens: Aerodynamics Compared-Comparison Test", Car and Driver, June 2014.

[4]. Volodynyr S., Roman P. and Upendra S. R., "Methods of Reducing Vehicle Aerodynamic Drag", proc. of Heat Transfer Conference of ASME, 2012.

[5]. Interlaboratory Working Group on Energy-Efficient and Low-Carbon Technologies, "Scenarios of US Carbon Reductions: Potential Impacts of Energy Technologies by 2010 and Beyond", 1997.

[6]. www.autosteel.org.

[7]. Nicholas L., "Review of technical literature and trends related to automobile mass-reduction technology", report for California Air Resources Board, May 2010.

[8]. The International Council on Clean Transportation, "European Vehicle Market Statics, Pocketbook 2013".

[9]. Stodolsky F., A. Vyas, et al. (1995), "Life-Cycle Energy Savings Potential from Aluminum-Intensive Vehicles", Conference Paper, 1995 Total Life Cycle Conference&Exposition. October 16-19, 1995, Vienna, Austria.

[10]. Abraham, A. Ducker Worldwide. (2011, May). “Future Growth of AHSS [PowerPoint presentation at Great Designs in Steel Seminar]”.

[11]. J. Galan, L. Samek, P. Verleysen, K. Verbeken and Y.Houbaert, “Advanced high strength steels for automotive industry”, Revista de Metalurgia, 48 (2), ISSN: 0034-8570.

[12]. J.Hirsch, “Automotive Trends in Aluminum- The European Perspective”, Materials Forum Volume 28, 2004.

[13]. Ducker Worldwide, “The Past, Present and Future of Aluminum in North American Light Vehicles”, October 16, 2012.

[14]. McWilliams A., “Advanced Materials, Lightweight Materials in Transportation”, report, Report Code: AVM056A, 2007.

[15]. Ghassemieh E., “Materials in Automotive Application, State of the Art and Prospects, New Trends and Developments in Automotive Industry”, InTech, Marcello Chiaberge, ISBN: 978-953-307-999-8, 2011.

[16]. http://wardsauto.com/subscriptions/facts-figures.

[17]. Taub A., Krajewski P., Luo A. and Owens J., “The Evolution of Technology for Materials Processing over the Last 50 Years: The Automotive Example ”, JOM, February.

[18]. Marc R., Deena P. and Tom W., “Vehicle Design and the Physics of Traffic Safety”, Physics Today, January 2006.

[19]. http://www.bmw.com/

[20]. http://www.euroncap.com/tests/fiat_500_2007/298.aspx.

3 Chapter 3 Frontal lateral side door structure in vehicles

3.1 Introduction

Side doors of vehicles allow people to enter and exit the vehicle, usually they can be opened manually, sometimes they are electrically powered. A conventional car side door is hinged at its front edge, allowing the door to rotate outward from the car body. Characteristic of this type of door is that if it is opened when vehicle is going forward, the wind dynamics will work against the opening door surface, and will forces its closure immediately (see Figure 3.1-1).

Figure 3.1-1 Conventional car side door

Depending on the type of car, there are also other door constructions in use (see Figure3.1-2):

- Rear-hinged doors (Figure3.1-2a);
- Scissor doors (Figure3.1-2b);
- Butterfly doors (Figure3.1-2c);
- Sliding doors (Figure3.1-2d);

The car door structure is not a simple panel but rather a substructure system which satisfies many different functions. Basically, the door is composed by an outer panel supported by an inner panel where different additional components are placed. Furthermore, nowadays car doors usually have a reinforcing element (side impact beam) placed longitudinally between outer and inner panels which protects the driver and passengers in case of a side impact event.

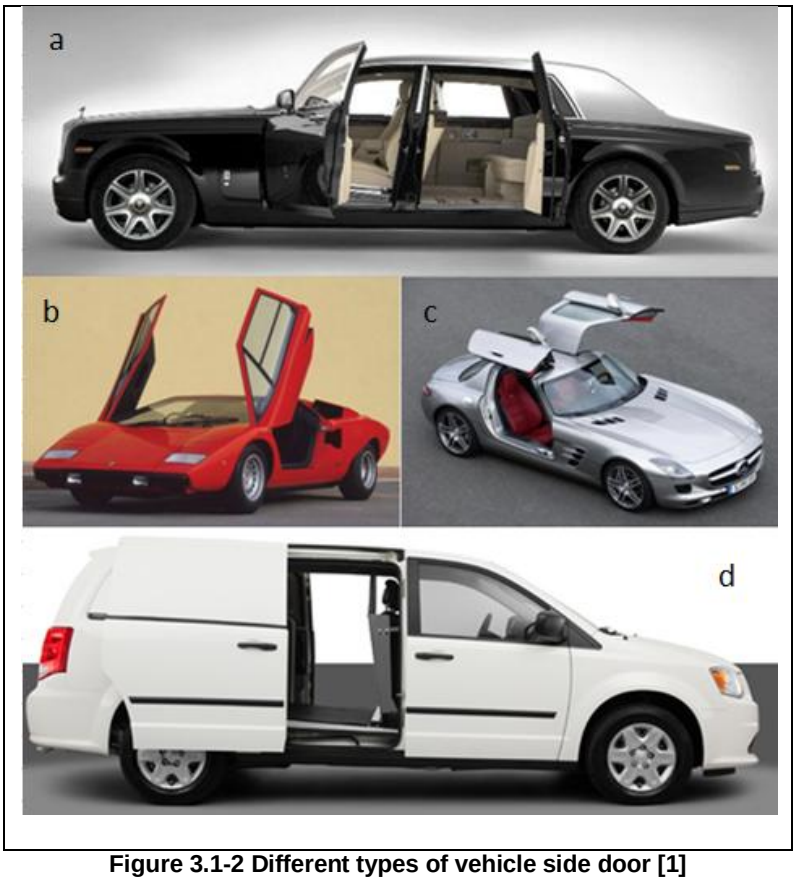

Figure 3.1-2 Different types of vehicle side door [1]

The door panels are holding many small parts together, some most important additional parts integrated into the door body are:

- ***Hinges***: the hinges connect the door to the car body structure and allow opening and closing of the door.
- ***Door handle and lock***: these parts allow the door to open/close by hand easily and prevent it from opening by itself. Many lock systems are adopted in automotive structures and newer cars are equipped with a power lock that allows drivers to remotely open/lock all doors. The door handles are placed both on the inside and outside of the car door.
- ***Windows and window regulator***: Usually car door window glasses could move downward into the space created by two panels and window regulator is placed inside door body, which could raise and lower window glasses. Generally car door windows are opened either with a manual crank or small electrical motor.

Another important part of door body is interior panel, which is not only an esthetic part but also offers much functionality and improves the ergonomics of the car body. Many elements are

attached on the interior panel: door handle, switches of windows, storage tray and so on. There are several different constructions of side door in automotive engineering, as shown in Figure 3.1-3 [2].

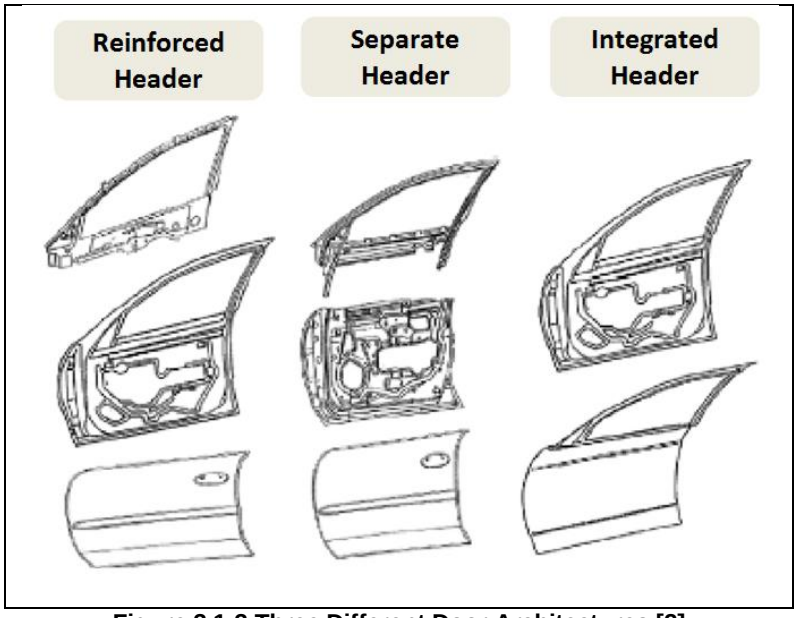

Figure 3.1-3 Three Different Door Architectures [2]

Beside the three important parts mentioned above, other elements are also included inside door body: electronic control system of windows, locking system, loudspeakers and possibly airbags, which can protect driver or passenger during a side crash event (see Figure 3.1-4).

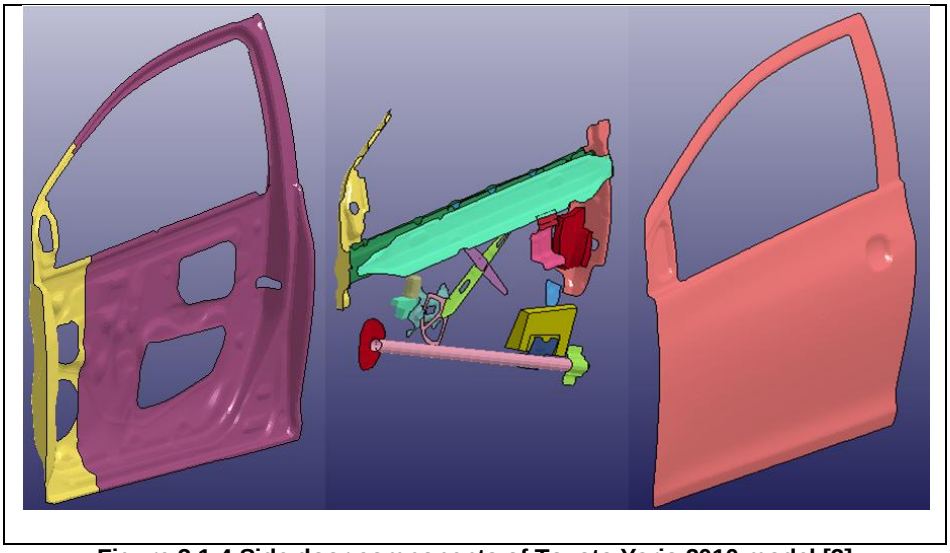

Figure 3.1-4 Side door components of Toyota Yaris 2010 model [3]

The target car chosen to develop the research study of this PhD thesis is the 2010 Toyota Yaris Passenger Sedan (see Figure 3.1-5).

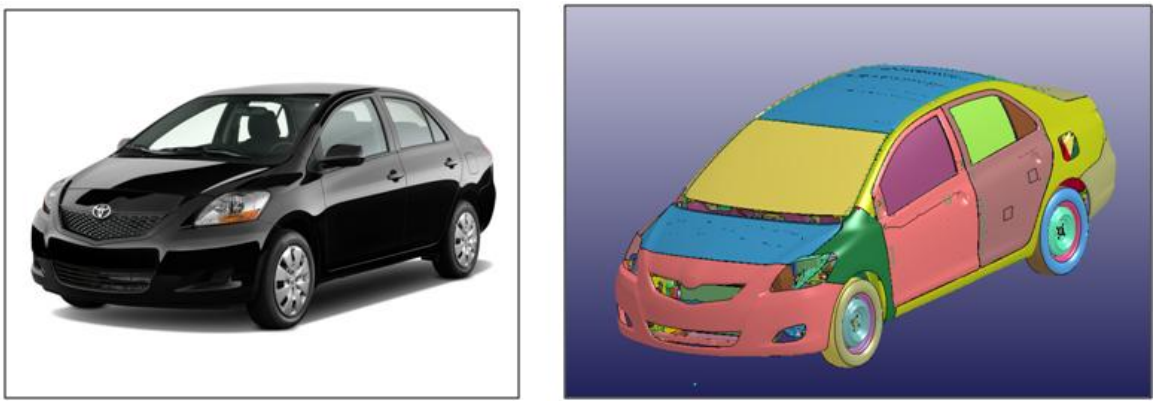

Figure 3.1-5 2010 Actual Toyota Yaris passenger sedan and FE model

A finite element (FE) model (see Figure 3.1-5) [3] based on a 2010 Toyota Yaris passenger sedan was developed through the process of reverse engineering at the National Crash Analysis Center (NCAC) of the George Washington University (GWU) in 2011. This model became part of the array of FE models developed to support crash simulation and the model was validated against the National Highway Traffic Safety Administration (NHTSA) frontal New Car Assessment Program (NCAP) test for the corresponding vehicle. The comparison between actual vehicle and FE model is summarized in Table 3.1-1 [9], which are related to vehicle mass, inertia and CG positions.

Table 3.1-1 Comparison between actual vehicle and FE model of Toyota Yaris 2010 [3]

	Weight (kg)	**Pitch inertia** $(kg * m^2)$	**Yaw inertia** $(kg * m^2)$	**Roll inertia** $(kg * m^2)$	**Vehicle CG** X (mm)	**Vehicle CG** Y (mm)	**Vehicle CG** Z (mm)
Actual vehicle	1078	1498	1647	388	1022	-8.3	558
FE model	1100	1566	1739	395	1004	-4.4	569

As we mentioned above, the door subsystem structure is also designed to absorb energy during the side crash event in order to reduce the risk of injuries of the driver and passengers. New registered vehicles must pass the national mandatory side impact test before they are sold on market, such as FMVSS. The safety of vehicle would be discussed in the following section.

3.2 Passive safety of vehicle

3.2.1 Introduction

According to the report of Health Organization (WHO), there were 1.24 million deaths because of road accidents in 2010, almost same number as in 2007 while the number of new registrations vehicles has increased by 15% [10]. About 31,000 road traffic fatalities were found in EU27 countries in 2010[11], which had a decrement of 11% compared to year 2009. Figure 3.3-2 shows that there is a 60% reduction of road traffic fatalities from year 1991 to year 2010 in EU countries thanks to the attention paid to the safety problem by automotive industries, public authorities and consumer organizations.

However, much more efforts are necessary to continue this reduction of road fatalities in future.

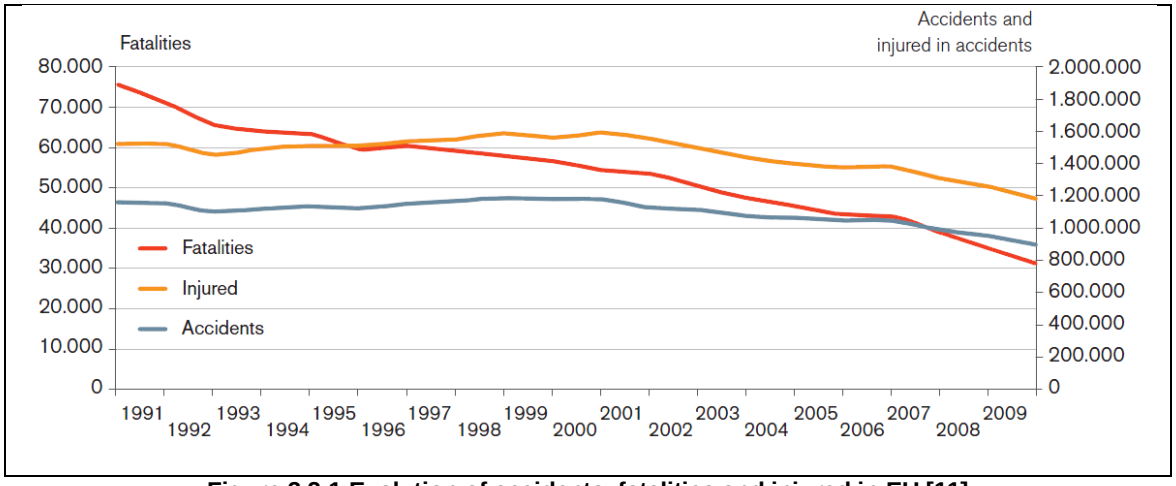

Figure 3.2-1 Evolution of accidents, fatalities and injured in EU [11]

The restraint system is adopted into automotive engineering in order to protect driver and passenger better during car crash accident, which is divided into active safety and passive safety , as shown in Figure 3.2-2 [12].

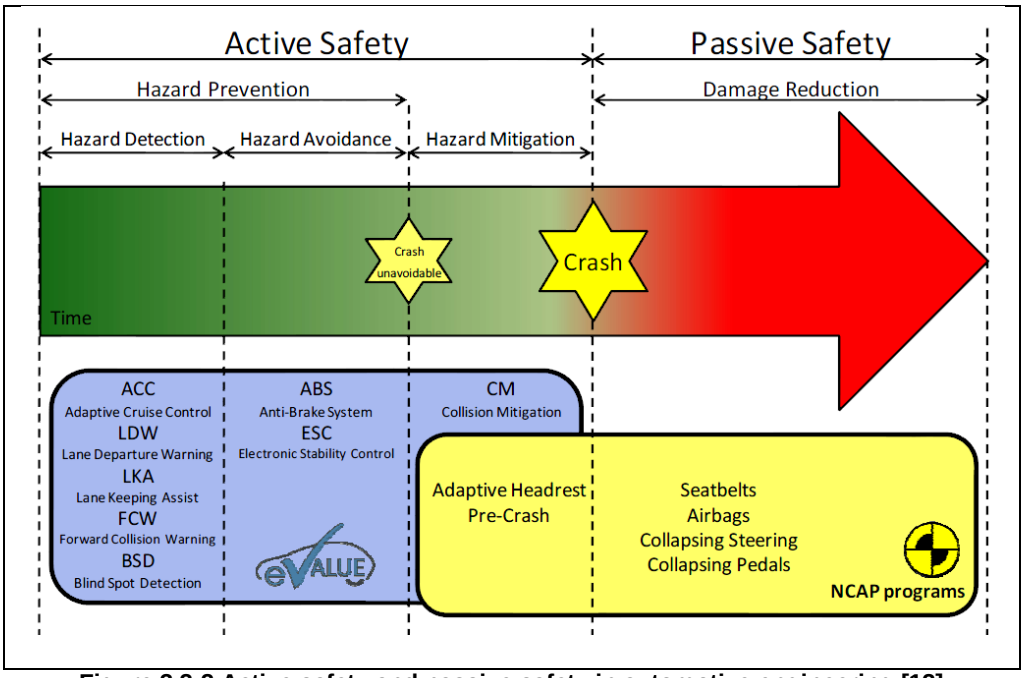

Figure 3.2-2 Active safety and passive safety in automotive engineering [12]

Active safety is intending to prevent accident in advance, such as ABS, ESC, ACC systems and so on, as we can find in Figure 3.2-2; passive safety is designed to reduce the injury risk transferred to occupant as much as possible while crash impact is happening, such as use of seatbelts and airbags. However, passive safety is not restricted only to the protection of vehicle passengers but also includes the protection of other traffic participants like pedestrians and cyclists.

Regarding to passive safety, additional key points are the inner and outer compatibility. While the inner compatibility means the protection of passengers by sufficient deformation zones, design of interior and restraint systems. The outer compatibility regards to energy absorption distributions to all participants of the accident, such as energy absorption distribution between one frontal zone and another side impact zone. All the biomechanical response measured by means of instrumented dummy should be under the limit value in order to make sure that human subjected to crash are safe enough. The most important points to achieve this result come from all passive safety strategies, such as the cooperation of physical structure and airbags. The timing of airbags start to work is critical, which is usually different from car to car because cars have different physical structures. All protection strategies are supposed to work together effectively.

The structural components of vehicles are usually designed based on some rules according to passive safety:

- Sufficient strength of passenger compartment;
- Adequate energy absorption in order to make sure that biomechanical response is under limit value;
- Compatibility with other traffic participants.

Different zones of vehicle structure evolved in crash impact are shown in Figure 3.2-3.

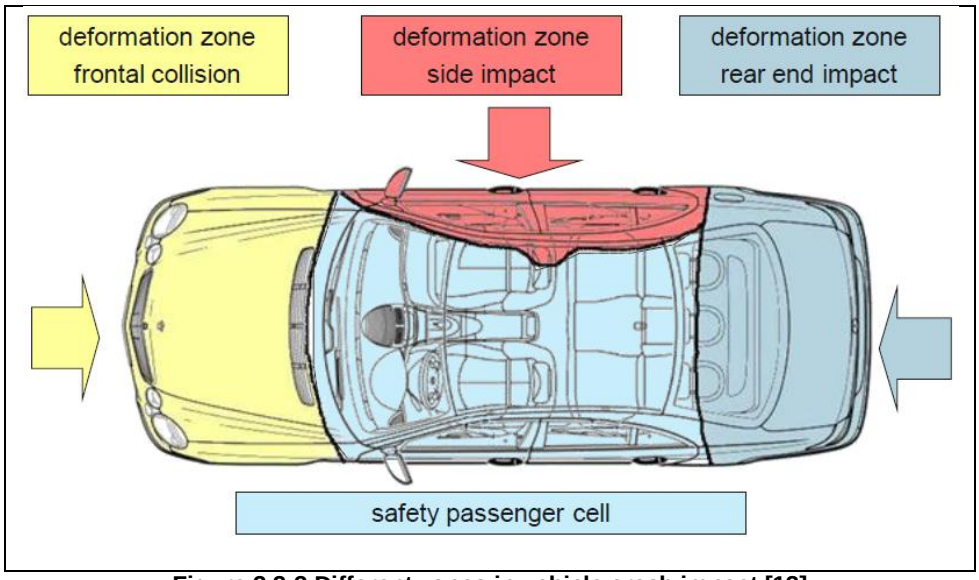

Figure 3.2-3 Different zones in vehicle crash impact [13]

Frontal crash, side impact crash and rear impact crash are three common scenarios in accidents, consequently, there are crash tests related to these three crash impacts. We could see that side impact event is happening in vehicle side door zones and design of vehicle side door is the focusing point of this paper.

3.2.2 Vehicle crash standards

Vehicle crash standard can be subdivided into two groups according to their intentions: legislation standard and consumer protection laws, Figure 3.2-4 gives an overview of the categorization of crash standards according to the named subdivisions. Usually both these two types of standard could be found in each market of the world.

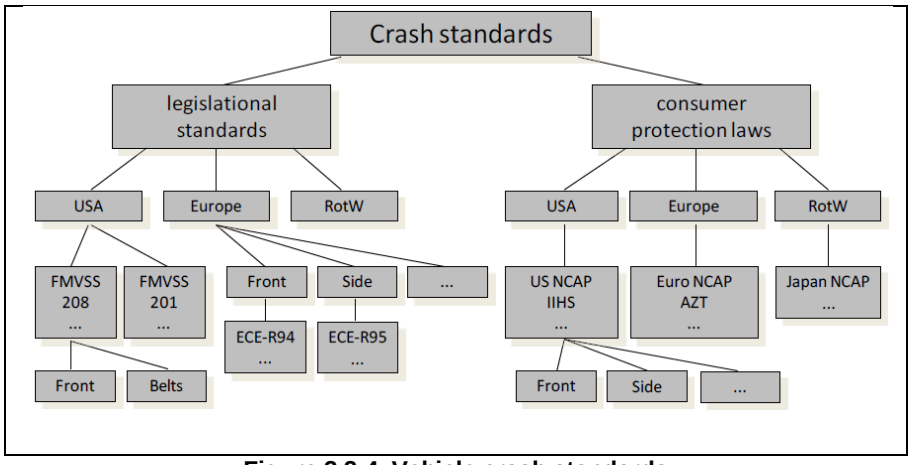

Figure 3.2-4 Vehicle crash standards

Every vehicle fleet must pass legislation safety tests before they are permitted to be sold in market, which is the lowest threshold of safety standard. Furthermore, consumer protection laws give an overall assessment of new vehicle safety including active safety and passive safety, which is called “New Car Assessment Program”, such as Euro-NCAP, US-NCAP, J-NCAP, C-NCAP and so on. Based on the result rankings of all vehicles from NCAP, consumers could get a clear idea about the safety of the vehicle they want to buy. Usually the NCAP has higher standards than legislation standards.

A summary of each test protocol is presented in the following table 3.2-1, it is obvious that vehicle side door is linked to side tests directly, which includes Movable Deformable Barrier (MDB) test and Rigid Pole test. MDB test is to simulate car to car impact in real side accident and rigid pole test is designed to simulate the target-stable crash impact, such as tree-crash accident.

Table 3.2-1 Crash test set-up, angle and velocity from different countries

NCAPs	Frontal and side crash test protocol in different countries	Others
U.S **NCAP**	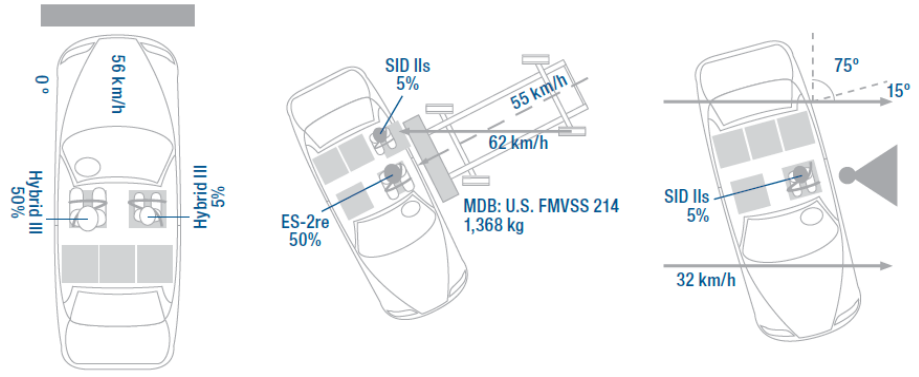	• Rollover resistance; • Assistance systems: SBR, SAS, ESC...

EURO- **NCAP**	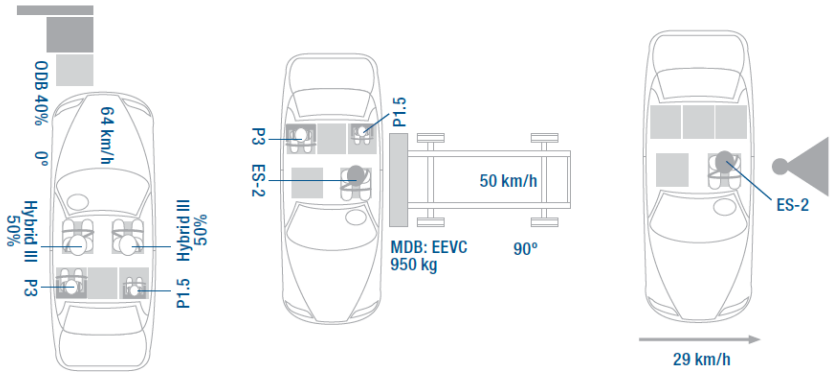	• Pedestrian test; • Child test; • Whiplash mitigation tests; • Assistance systems.
J- **NCAP**	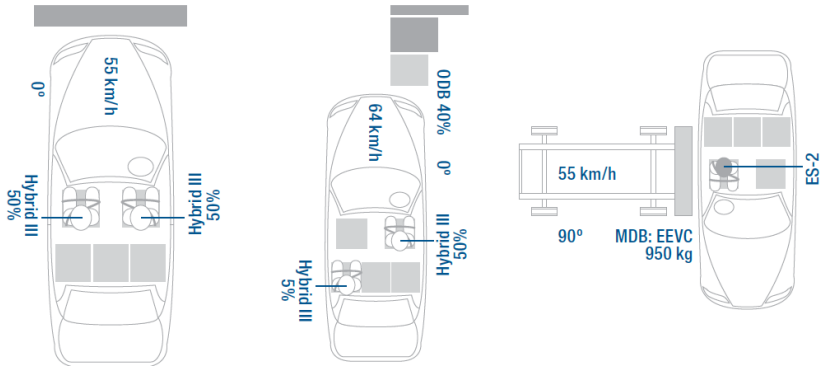	• Pedestrian test; • Whiplash mitigation tests; • Assistance systems.
K- **NCAP**	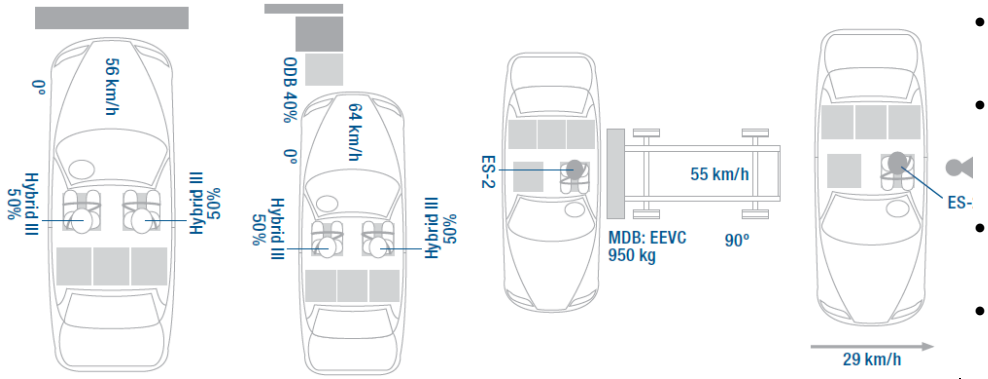	• Pedestrian test; • Whiplash mitigation test; • Rollover resistance; • Assistance systems
C- **NCAP**	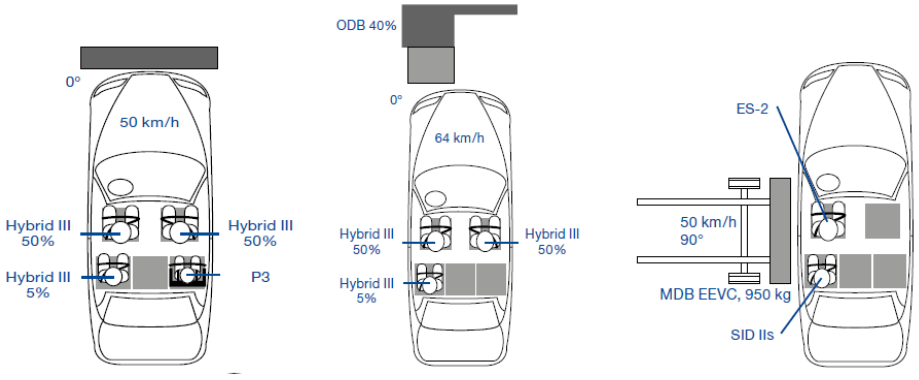	• Rollover resistance; • Whiplash mitigation tests; • Assistance systems.

IIHS	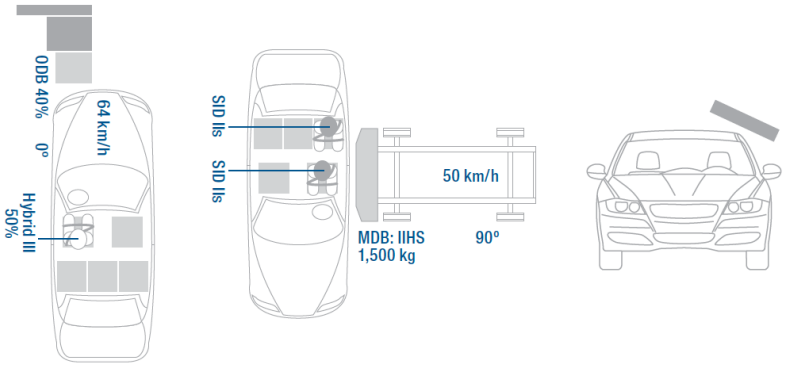	• Whiplash mitigation tests; • Low-speed damageability tests; • Assistance systems.
A-NCAP	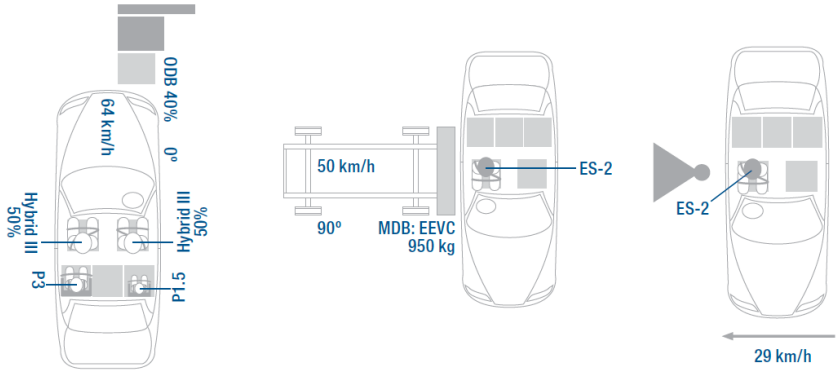	• Pedestrian tests; • Child tests; • Assistance systems.
ASEAN-NCAP	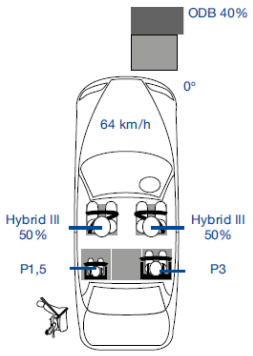	• Child safety tests;
LATIN-NCAP	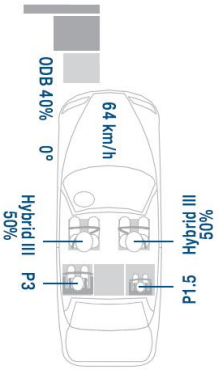	• Child safety tests;

In the research study of this PhD thesis, Federal Motor Vehicle Safety Standard (FMVSS) regulation has been selected as reference standard and will be discussed later.

3.3 Side impact crashworthiness evaluations

Federal Motor Vehicle Safety Standard (FMVSS) regulation is the reference one in the research study of this PhD thesis, the target vehicle is Toyota Yaris 2010 as mentioned before; and the movable deformable barrier is from Federal Motor Vehicle Safety Standard (FMVSS). Regulation FMVSS 214 and dimensions of MDB simulator are shown in Figure 3.3-1 and Figure 3.3-2 respectively [14]. This side impact regulation for passenger cars established minimum requirements for protection of occupants, including head, thorax, abdomen and pelvis. The MDB is moving at a velocity of $54\ Km/h$ with an angle $27°$ in order to simulate the relative motions between target and bullet vehicles in real side accident.

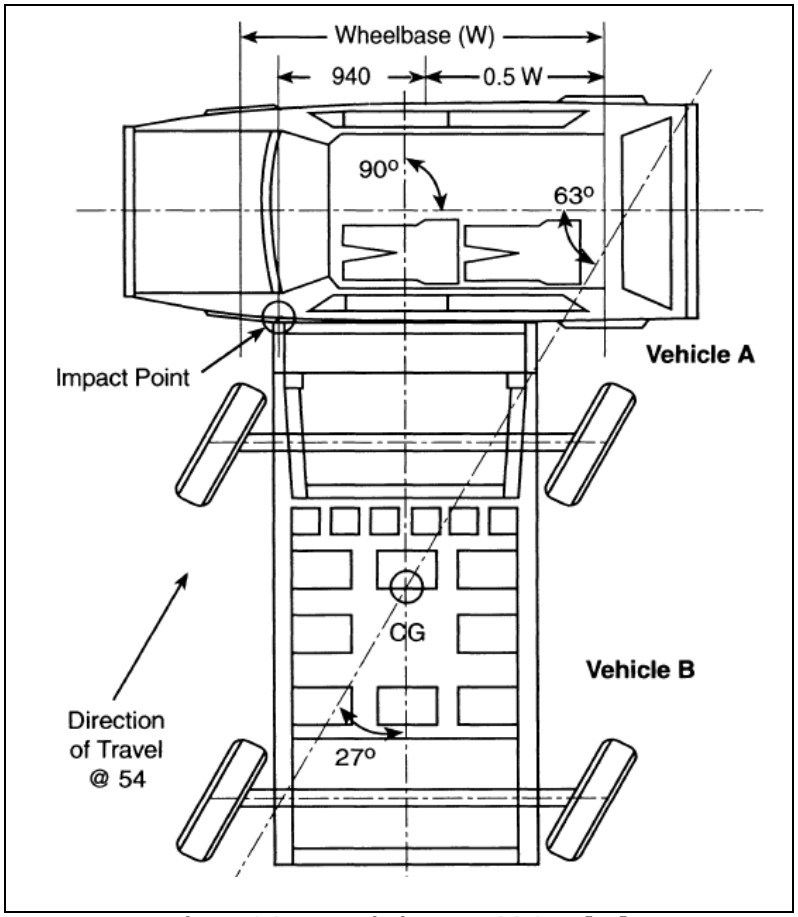

Figure 3.3-1 Regulation FMVSS 214. [14]

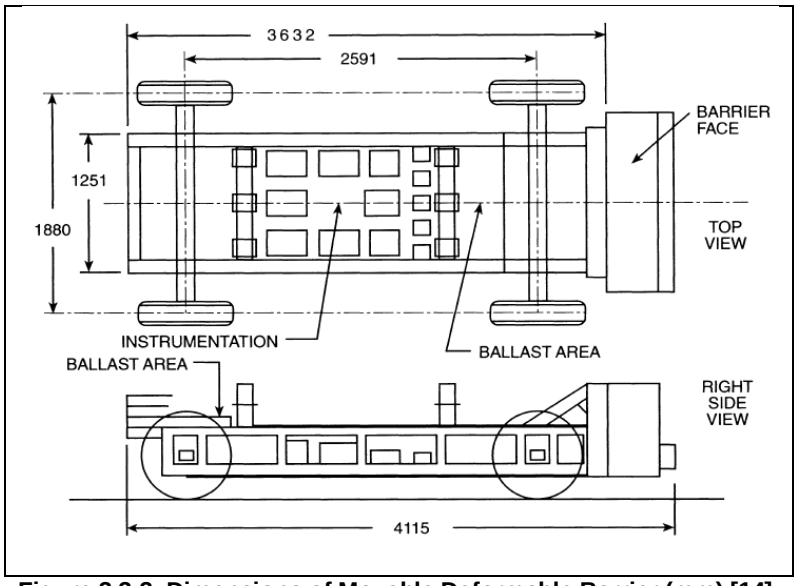

Figure 3.3-2 Dimensions of Movable Deformable Barrier (mm) [14].

Generally, there are some highlight characteristics of vehicle side impact [15]:

- Most vehicles are travelling perpendicular to each other when side impact are happening; the 27 deg angle is intended to take into account the effect of the relative motion of the two vehicles;
- Usually target car is travelling slower than the bullet vehicle;
- Comparing to frontal collision, side accidents have longer crash time.
- Occupants who are seated on the sides of occupant compartments of target car are at highest risk of serious injury in side impacts [16].

3.3.1 Injury risk and assessment

Injuries in head, spine, abdomen and pelvis are devastating, which could result fatality or different forms of permanent physical problems. Direct impacts in the head can severely affect the brain and most of the sensory organs located within it.

Head Injury Criteria (HIC) is the most commonly used criteria for head injury in automotive design engineering, which is based on head acceleration. HIC could be calculated by the following equation:

$$HIC = \left[\frac{1}{t_2 - t_1}\int_{t_1}^{t_2} a(t)dt\right]^{2.5}(t_2 - t_1)$$

where a is the resultant head acceleration, $(t_2 - t_1) \leq 36\,ms$ and the time interval t_2 and t_1 are selected such that HIC is maximum. In other standards, time interval is limited to $15\,ms$ instead of $36\,ms$.

Injuries of thorax are difficult to investigate exactly because there are many important organs inside it, as heart, lungs, aorta, cava and so on. Any damage to them could generate fatal injuries. So the intrusion displacements of ribs are very critical during crash impact and rib deflection is the most important index used to assess injuries of thorax, including all ribs: upper, middle and lower.

In case of abdomen, injuries to the liver, spleen, kidney and other organs could be also fatal, some research results showed that in near-side impacts, the liver is most vulnerable body part for right-front passengers and spleen is most frequently injured body part for drivers. In far-side impacts, kidney is the most critical body part for driver and liver is the most frequently injured body part for right-front passengers [17].

Injuries in the legs usually are not a cause of death in a road accident; however, injuries in this region of the human body could provoke permanent physical impairment. Legs of occupants are not constrained when people are sitting inside vehicle, so legs could strike interior surfaces of vehicle easily even when car is moving with a low speed, which is the principal reason why injuries happen. In this case, pubic symphysis force is measured in order to assess the damage caused to legs, peak force value should be smaller than limits that human body could tolerate.

3.3.2 Rating programs

Both legislation standard and consumer protection laws are designed to provide a fair, meaningful and objective assessment of the impact performance of cars. As we know, no crash test procedure could fully reflect the safety protection provided by a car in the different various accidents occurred on roads. However, vehicles that have better performances in test are expected to provide better protection in accidents than those performed worse in test procedures. There are no anthropometric dummies available which can demonstrate all the potential risks of injury to occupants and it is very difficult to assess the protection level for different occupants in various seating positions.

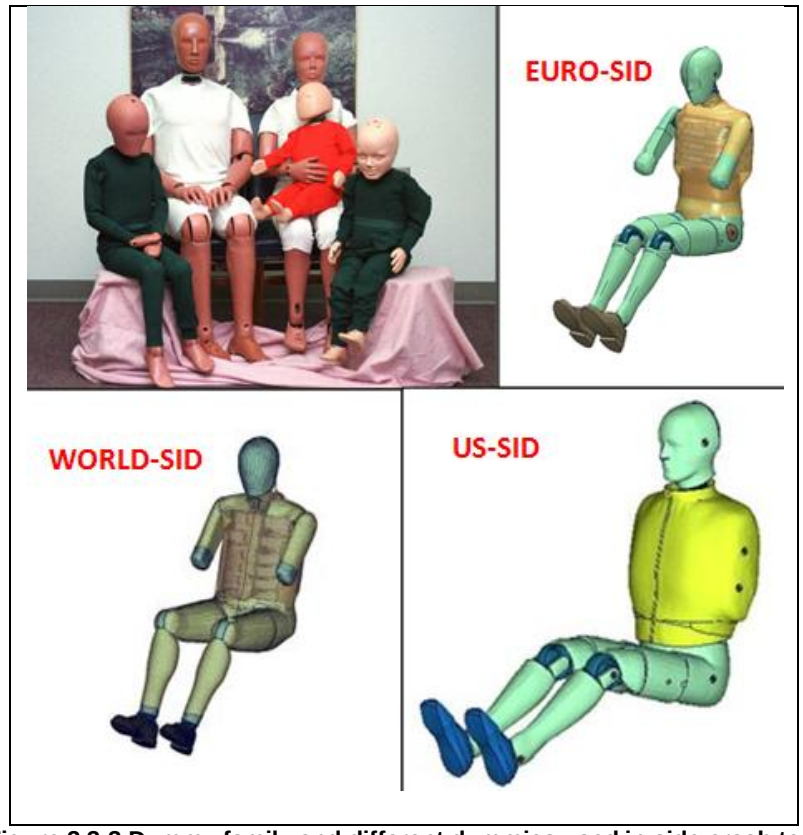

Figure 3.3-3 Dummy family and different dummies used in side crash test

The crash test dummy is a calibrated test instrument used to measure human injury potential in vehicle crash events. It simulates human response to impacts, accelerations, deflections, forces and moments generated during a crash. The different crash test dummies in use represent many sizes and ages and with the capability to be used in different crash orientations. They offer the vehicle designer a safe, repeatable test instrument for the furthering of transport safety. Figure 3.3-3 shows dummy family and three most common side dummies used in the world at the moment: EURO-SID, WORLD-SID and US-SID.

The USSID dummy and EUROSID-1 dummy are used since many years ago in order to assess side impact safety of passenger cars in U.S and EU standards, respectively. In 2003 the ES-2 was developed by replacing the ES-1 dummy in EURO-NCAP to assess the performance for side impact crash with MDB. There are small differences between the ES-1 and ES-2, although the USSID and the ES-2 dummy differ in many ways, such as arm positions, jacket material properties, number of ribs and pelvis model. In recent years ES-2re has substituted the USSID in a revised FMVSS 214 regulation. The ES-2re is derived from the ES-2 by altering the rib modules and the

back plate. The dummies ES-2 and ES-2re could give similar results in some ways except ES-2re could provide much more opportunities for load measurements [18].

In this research, 50% percentile male dummy of ES-2 was placed at the driver's seat inside Yaris model with sitting foam in order to investigate the protections provided by Yaris structure during MDB test.

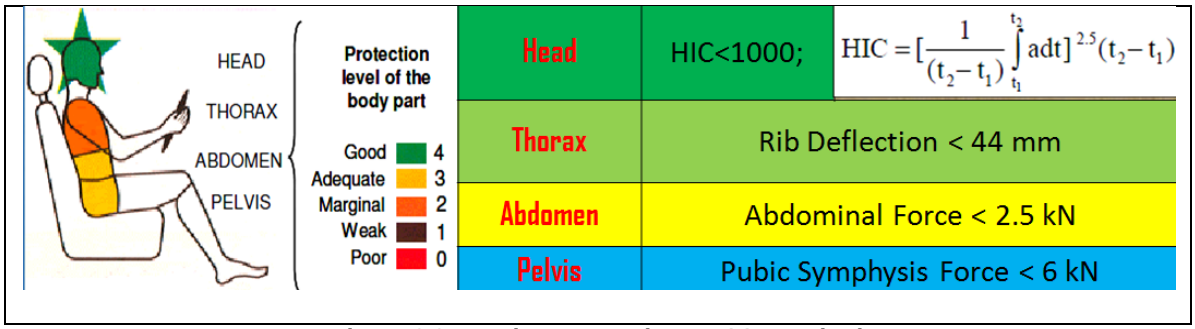

Figure 3.3-4 Rating system in FMVSS standard

Figure 3.3-4 is showing the index assessments of head, thorax, abdomen and pelvis: head injury criteria of $36\,ms$ should be not more than 1000, rib deflection should be smaller than $44\,mm$, resultant abdominal peak force must not exceed $2.5\,kN$, and the limit of pubic symphysis peak force is $6\,kN$, respectively. These limitations are established in FMVSS 214 with EU-2re dummy, which is considered as the reference standard in this research work.

3.4 Composite door solutions

Traditionally, the car door structure is built from steel material, including outer panel, inner panel, belt reinforcements, and impact beam. The use of alternative material with respect to the traditional steel has been studied by different researchers [14, 15, 16]. In the paper [14] Aimar and co-workers presented a door solution completely made by magnesium. This innovative design was specially aimed to weight saving, but also possible part integration is pointed out. Behavior of the composite side-door impact beams for passenger cars was investigated by Seong S. C, Dai G. L and Kwang S. J in 1997 [15], it was concluded that the composite impact beams (glass fiber and epoxy matrix) not only reduce the weight of the impact beams by more than 50% but also had a constant impact energy absorption capability with respect to environmental temperature variation. Then fiber-reinforced composites in the car side structure was studied by Patberg and co-workers

in 1999 [6], in that paper a sandwich door panel was formed by joining the inner and outer panel (multilayered axial fabrics and epoxy-based resin) and the preformed foam (PUR) layer by adhesive bonding, it came out that the requirements concerning stiffness and strength can be met when adopting the composite door structure and that the weight of the structure can be reduced considerably. A multi-material solution is taking place as very interesting one, the joining technology problem has to be carefully considered. In order to be able to join parts of different materials (metallic and composite), the most promising is adhesive technology [17, 18]. Adhesive bonded joints for composite material structures have been detailed analyzed in 2009 [18], the authors described the influence of many factors the designer should consider during the joint design.

Composite solutions of door structure are developed in this research activity, the following steps have been done:

1. Composite structural joint is the starting point and five joints have been developed and simulated for static loading cases. Based on the result, two simple door FE models are developed.
2. From the industry point view, solution 1 is only theoretical and could not be integrated into Yaris structure directly, consequently material substitution of Yaris side door is considered. In Yaris model, original materials of outer panel, inner panel and impact beam are substituted by carbon fiber reinforced plastics (CFRP) without any geometry change; and composite solutions are investigated in three design aspects: static lateral stiffness, NVH design, and crashworthiness evaluation.
3. An innovative composite door structure is developed, one multi-purpose panel was created in order to replace traditional impact beam and belt reinforcement, which is made with composite materials.

There are many types composite materials which are considered in this research, such Carbon Fiber Reinforced Plastic (CFRP), E-glass fiber reinforced epoxy, Glass Mat Thermoplastic (GMT), GMT_UD, GMT_TEX and Semi Impregnated Micro Sandwich (SIMS). All these materials will be introduced in next section.

3.5 Reference

[1]. European Aluminum Association, “The Aluminum Automotive MANUAL-Hang on parts”, 2013.

[2]. Daniel E.Whitney, MIT Engineering System Division and Cambridge MA, “Design and Manufacturing of Car Doors: Report on Visits Made to US, European and Japanese Car Manufacturers in 2007”, March 2008.

[3]. National Crash Analysis Center, http://www.ncac.gwu.edu/

[4]. World Health Organization, “Global Status Report on Road Safety”, 2013.

[5]. Volvo Trucks, “European Accident Research and Safety Report 2013”.

[6]. National Highway Traffic Safety Administration, “An Analysis of Recent Improvements to Vehicle Safety”, DOT HS 811 572, June 2012.

[7]. EVALUE Project, “Testing and evaluation methods for active vehicle safety”, http://www.evalue-project.eu/.

[8]. Final report of ELVA Project, “Societal scenarios and available technologies for electric vehicle architectures in 2020”, Grant Agreement Number 265898.

[9]. Nat’l Highway Traffic Safety Admin., DOT § 571.214, Dec. 13, 1979.

[10]. Juan M. A. G, PhD thesis, “A study to improve the crash compatibility between cars in side impact”, Marzo 2008.

[11]. Samaha RR, Elliott DS, “NHTSA side impact research: motivation for upgraded test procedures”, 18th International Technical Conference on the Enhanced Safety of Vehicles, Nagoya, Japan, 2003.

[12]. Kathleen D. K., Carol A. C. F., Kristen N., Lawrence W. S. and Jonathan D. R., “Abdominal injury in motor-vehicle crashes”, UMTRI-2008-40, Nov. 2008.

[13]. Peter S., Uli F., Sebastian S., Markus P., Arno E., DYNAmore GmbH, MAGNA STEYR, “Comparison of ES-2re with ES-2 and USSID Dummy” , DYNAmore GmbH, 2014.

[14]. Aimar A., Molina G. and Volpenge M., “The magnesium door project”, proc. of Int. Conf. Florence ATA 2003, Florence (1), paper 03A1039.

[15]. Seong S. C, Dai G. L and Kwang S. J., “Composite side-door impact beams for passenger cars.” Composite Structures Vol. 38, No. 1-4, 1997, pp. 229-239.

[16]. Patberg L., Philipps M. and Dittmann R., “Fiber-reinforced composites in the car side structure”, Proc Instn Mech Engrs, 1999, Vol.213 part D, pp. 417-423.

[17]. Belingardi G., “Recent advances in joining technology for car body applications”, proc. Int. Conf. MVM 2006 (Motor Vehicle and Motors), Kragujevac (Serbia), 4-6 October 2006.

[18]. Banea M. D. and Da Silva L. F., “Adhesively bonded joints in composite materials: an overview”, Proc Instn Mech Engrs, 2009, Vol.223 part L, pp.1-18.

4 Chapter 4 Materials characterization

4.1 Introduction

In general, composite materials are composed by at least two materials, one is reinforcing phase and the other is the matrix. There are two classification ways of composite materials. First way is based on the matrix materials: metal matrix composites (MMC), ceramic matrix composites (CMC) and polymer matrix composites (PMC), see Figure 4.1-1; second is based on the material physical structure: random orientation of particles, short-fiber reinforced composites, long-fiber reinforced composites and laminate composites (shown in Figure 4.1-2).

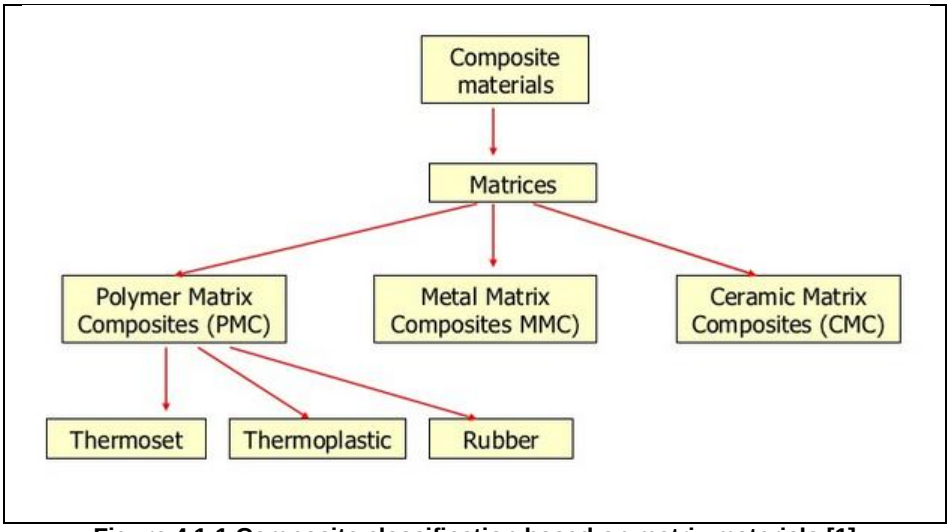

Figure 4.1-1 Composite classification based on matrix materials [1]

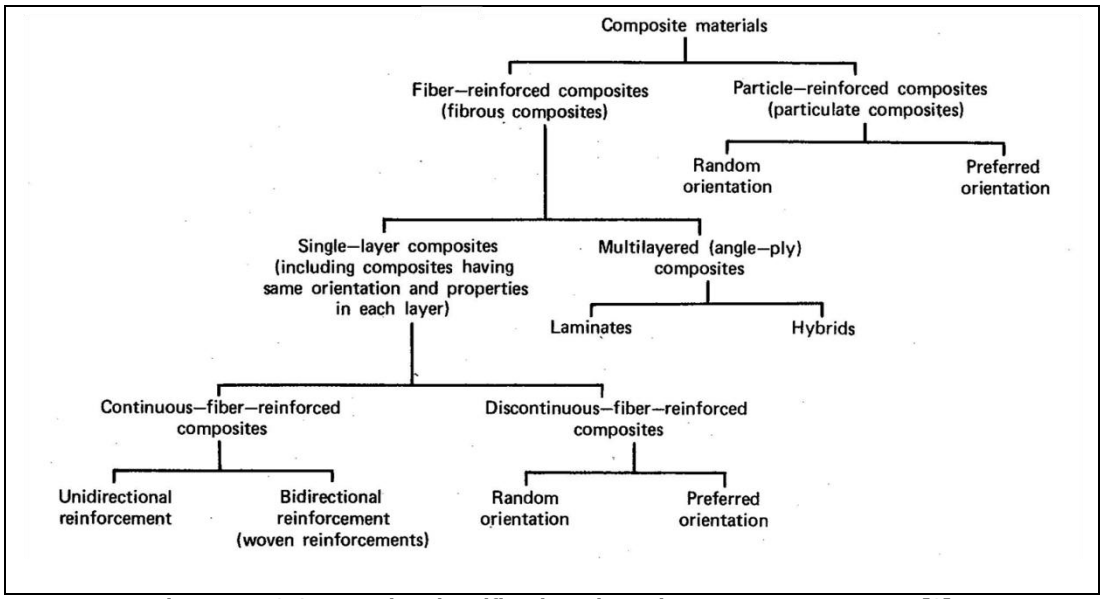

Figure 4.1-2 Composite classifications based on structure property [2]

The choice of fiber and resin type is of greatest importance when designing a structural component. Four common fibers are listed in following:

- Glass fiber [3]

  This type of fibre is characterised by a high strength (about $s_R = 3500 - 4600\ MPa$), nearly the double of the most resistant steels, and a high value of the elastic modulus ($E = 72 - 85\ GPa$, that is close to the aluminium values), relatively low cost and thermal and electrical conductivity.

  There are three different types of glass fibers: E, S and other types:

  - type **E** is constituted essentially of silica (SiO_2), alumina (Al_2O_3) and calcium carbonate ($CaCO_3$), at the beginning it was used in the electric industry (**E** means its original **e**lectric use);
  - type **S** is constituted essentially of silica (SiO_2),), alumina (Al_2O_3) and magnesia (MgO), it is characterised by higher strength (**S** stays for **s**trength);
  - type **C, M, A** and **D** are special-purpose glass fibers, not common.

  Although the fiber diameter can vary in a quite range of values, the most used diameter is equal to about $12\ \mu m$.

- Carbon fibers [4]

  Carbon fibres are characterised by a high strength ($s_R = 2100 - 2500\ MPa$), just a little lower than the glass fibres, but a higher value of the elastic modulus ($E = 240 - 390\ GPa$, around three times the glass fibre values), together with a relatively high thermal and electrical conductivity.

  They are characterised by high flammability, high electrolytic potential, higher than for example that of the aluminium. So, when joining with aluminium parts it is important to pay attention to possible corrosion phenomena.

  Practically two types of fibers are produced, which could be obtained by changing the production parameters:

  - type **1 or HS** is characterised by a high strength ($s_R = 2500\ MPa$);

- type **2 or HM** is characterised by a high value of the elastic modulus ($E = 390\ GPa$);

The characteristic value of the fiber diameter is about $7\ \mu m$.

- Boron fibers [5]

  This kind of fiber is characterised by quite high diameter (about $125\ mm$) that put limitations to the minimum bending radius during manufacturing (typically $8\ mm$). The high value of the fibre diameter gives to this composite material a good compressive strength, as the limit compressive load due to instability is consequently higher. The average tensile strength of boron fiber is $3 - 4\ GPa$, while its Young's modulus is between 380 and $400\ Gpa$.

  Boron fiber composites are in use in a number of U.S. military aircraft, notably the F-14 and F-15, and in the U.S. Space Shuttle. Increasingly, boron fibers are being used for stiffening golf shafts, tennis rackets, and bicycle frames. One big obstacle to the widespread use of boron fiber is its high cost compared to that of other fibers.

- Kevlar fibers [6]

  The Kevlar fibres (Kevlar is the commercial name used by the DuPont firm) are developed in recent years comparing to glass and carbon fibers. They are aramid (polymer) fibres which are usually used in vehicle tires manufacturing, two common types are:

  - the Kevlar 29 is used in industrial applications, such as cables, asbestos replacement, brake linings, and body/vehicle armour;
  - the Kevlar 49 type is used for the production of helmets and anti-bullet jackets;

  However, Kevlar fibbers are quite expensive and are very difficult to manufacture with respect to the glass and carbon fibres.

Mechanical properties of different fibers are shown in Table 4.1-1, While ***E*** is elasticity modulus, $\boldsymbol{\sigma_b}$ is tensile strength and $\boldsymbol{\rho}$ is the density.

Table 4.1-1 Properties of Composite Reinforcing fibers [7]

Material	E, GPa	$\sigma b, GPa$	$\rho, kg/m3$	$E/\rho, MJ/kg$	$\sigma b/\rho, MJ/kg$	$Cost, \$/kg$
HS-carbon	253	4.5	1800	140	2.5	$66-110$
HM-carbon	520	2.4	1850	281	1.3	$220-660$
E-glass	72.4	2.4	2540	28.5	0.95	1.1
S-glass	85.5	4.5	2490	34.4	1.8	$22-33$
Aramid	124	3.6	1440	86	2.5	$22-33$
Boron	400	3.5	2450	163	1.43	$330-440$

Advantages and disadvantages of different matrix materials are summarized in Figure 4.1-3, two biggest groups used in automotive industry are thermosetting resins and thermoplastic resins, especially thermosetting resins.

Matrix Type	Positive Attribute	Negative Attribute
Thermoset resins	Low cost processing	Brittle
Thermoplastic resins	Tough Formable	Low thermal and solvent resistant High cost to process for filament
Carbon	Very high temperature applications	Very high cost to process
Light metals	Thermal resistant Conductive Electrical and thermal	Reacts with most fibers
Superalloys	Oxidation resistant	Heavy
Refractory	High temperature strength	Heavy No oxidation Resistant
Glass	Corrosion resistant Thermal expansion	Brittle
Glass/ceramics	Corrosion and temperature resistant	Brittle and expensive
Ceramic	Very high temperature Oxidation	Expensive

Figure 4.1-3 Summary of matrix materials [2]

Several common thermosetting plastics are listed in following:

- Epoxy resins

  The epoxy resins give an excellent link fibre-matrix and consequently a high strength to fracture. Also the resistance to environment and corrosion is very good. The main

disadvantages are in the high value of viscosity that makes not easy the complete wetting of the fibres by matrix and the relative high cost and the low critical temperature (max temperature at work) that is equal to about $180° C$ [8];

- Polyester resins

  The polyester resins have a low viscosity that makes easy the complete wetting of the fibres by matrix, together with a low cost. The resistance to environmental agents is good and manufacturing is quite easy. Disadvantages are a quite weak link fibre-matrix, some brittle behaviour when submitted to shear loads and a quite high shrinking during cure that causes a low adhesion of the matrix to the fibres. The max allowable temperature is between $60° C$ and $80° C$ [9];

- Phenol resins

  These resins have the same advantages of the epoxy resins (good adhesion between fibre and matrix, good resistance to corrosion, and so on) with the possibility of higher operating temperature. The major disadvantages are due to the high pressure required during the polymerisation process, the high voids content and the characteristic black colour.

- Vinyl resins

  These resins have the same positive properties of the polyester resins (low viscosity, low cost and so on), but with a stronger link fibre-matrix.

According to some research work [10], the orientations and weave patterns of fibers in a composite component are very important, which influence the laminate properties too much. The most common orientation is unidirectional (UD) where all the fibers in a single ply lie in one direction, which results that load capacity in this direction is outstanding but very poor in the transverse direction. Also the fibers can alternatively be weaved in a regular pattern. There are three types of weave style widely known in fabric composite production: plain, twill and satin, as shown in Figure 4.1-4.

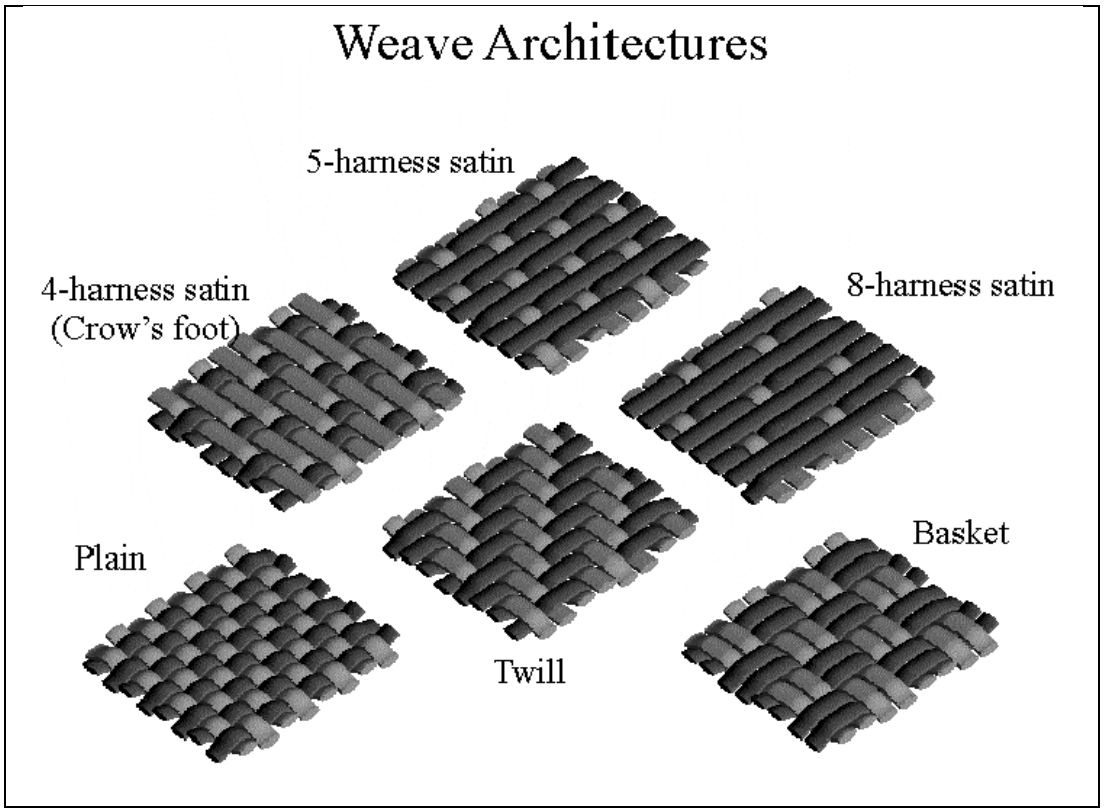

Figure 4.1-4 Weave types: plain weave, twill weave and satin weave [11]

4.2 Composite door materials characterizations

Figure 4.2-1 Vehicle deformation after crash

Vehicle side door structure is an important structural component of automobiles to prevent or reduce physical damage transferred to occupants during not only low-speed collisions but also high-speed collisions, see Figure 4.2-1. The selection of composite for side door structure should not only consider stiffness of bending, strength limit and some other static structural performances,

but also dynamic behavior, such as NVH design and crashworthiness. NVH design is offering comfort to passengers and crashworthiness can protects people when crash event is happening. Beside the original steel already used in door structure, which is considered as reference solution, this research is also proposing to trying to use several composite materials into door structure, focusing on outer panel, inner panel and impact beam. Considered composite materials are listed as follow:

- CFS003/LTM25 (CFRP) and E-Glass/epoxy

  CFS003/LTM25 is a 2 by 2 twill fabric using Amoco $T300$ fiber and impregnated with $LTM25$ epoxy resin. It exhibits lower density, about $1.45\ g/cm^3$, outstanding value of strength and elastic modulus in both longitudinal and transverse direction, together with a relatively high thermal and electrical conductivity. Also as mentioned before, epoxy resins give an excellent link fibre-matrix and consequently a high strength to fracture.

  E-Glass/epoxy considered here is also manufactured in fabric way. It performed lower strength and modulus with higher density of $1.85\ g/cm^3$, but it still has an excellent structural response with respect to other composites. Furthermore it cost less than CFS003/LTM25.

- Glass Mat Thermoplastics (GMT), GMT-UD and GMT-TEX

  Glass Mat Thermoplastic (GMT) is also one of composite candidate, which is already used widely in automobiles [13]. GMT here is a polypropylene laminate which possesses continuous random intertwined glass fibers. It exhibits an isotropic behavior, which allows to exploit this composite properties in various situations, as shown in Figure 4.2-2a.

  GMT-TEX and GMT-UD are two particular physical modification of GMT. GMT-UD is a polypropylene laminate with a filler consisting of a lot of short and randomly intertwined glass fibers layer, reinforced by layers of continuous randomly interwined glass fibers and by two layers of continuous and unidirectional aligned glass fibers. It has the peculiarity of presenting excellent mechanical properties along the direction which the oriented fibers develop, so this composite materials is mainly used for structural components, as shown in Figure 4.2-2b.

GMT-TEX is a laminate consisting of layers of random oriented short glass fibers, reinforced by layers of continuous random oriented glass fibers and by a layer of woven glass fibers. The excellent mechanical properties offered by the presence of the fabric make this composite suitable for structural applications, where it is required high loads endurance, see Figure 4.2-2c.

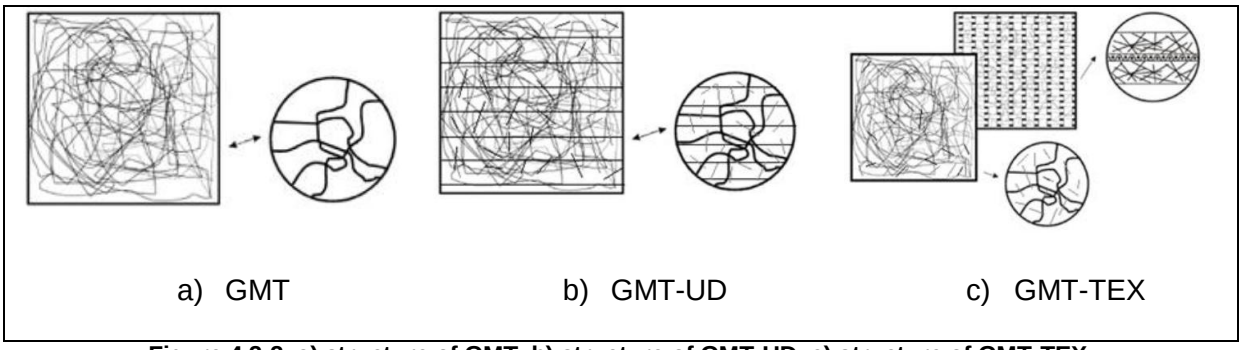

Figure 4.2-2 a) structure of GMT, b) structure of GMT-UD, c) structure of GMT-TEX.

- Carbon Semi Impregnated Micro Sandwich (CSIMS) and Glass Semi Impregnated Micro Sandwich (GSIMS)

  Semi Impregnated Micro Sandwich (SIMS) is a novel material that has been devised and proposed by DELTAtech company. This sandwich material contains long fiber composite skins and low-cost fleece core, porosity that often remains within the fleece is expected, while the non-woven fleece is needed to be completely wetted and bonded by the matrix both inside the fleece itself and to the composite skins in order to obtain the desired stiffness, as shown in Figure 4.2-3. Such structures are actually thinner and easier to manufacture than the traditional one and have been widely used in the past, both in automotive and sporting good applications including helmet and footwear [14].

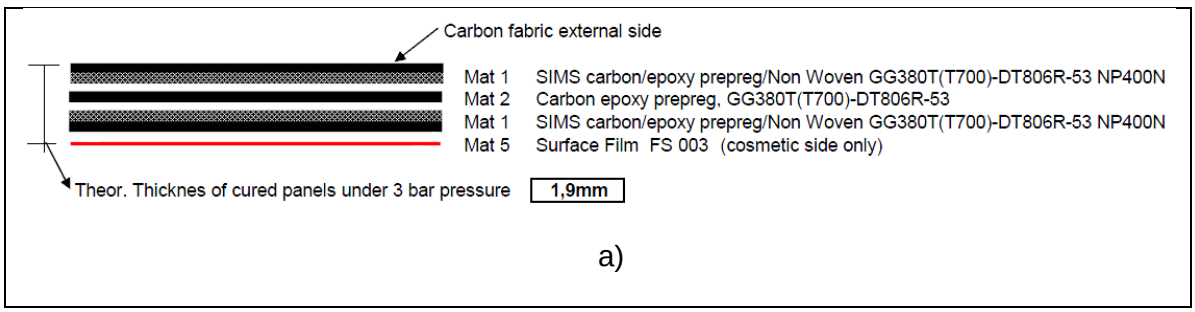

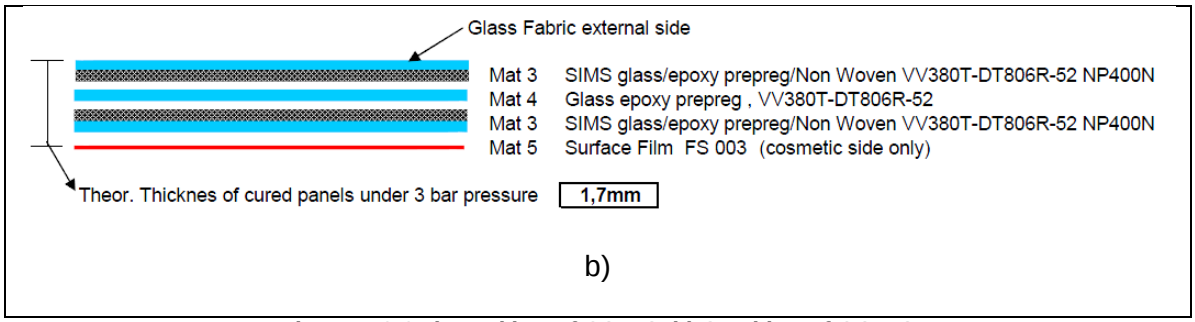

Figure 4.2-3 a) stacking of CSIMS, b) Stacking of GSIMS

Carbon and glass fibers are both used in this sandwich structures, see Figure 4.2-3a and Figure 4.2-3b respectively. The microstructure achieved during the manufacturing process could influence the mechanical properties of SIMS widely, so it is needed to limit the amount of dry fiber in the structure. With such proper impregnation, the materials can exhibit very high toughness due to the deformation mechanism in the dry regions of the non-woven fleece. According to the report of DELTAtech [15], in comparison with the traditional thin sandwich structures, SIMS is relatively thicker but is low-cost and has high impact performance, consequently it is an interesting candidate for automotive applications in impact absorbing substructure.

In order to model numerically the appropriate material card with all necessary properties that are significantly influencing structural response, some data are available in literature and others are characterized by research group of Prof. G. Belingardi [10, 17]. The mechanical properties of steel used to make two panels and impact beam in Yaris model are shown in Figure 4.2-4, which are taken from Yaris model directly [16], while composite materials considered in this research activity are summarized in Table 4.2-1.

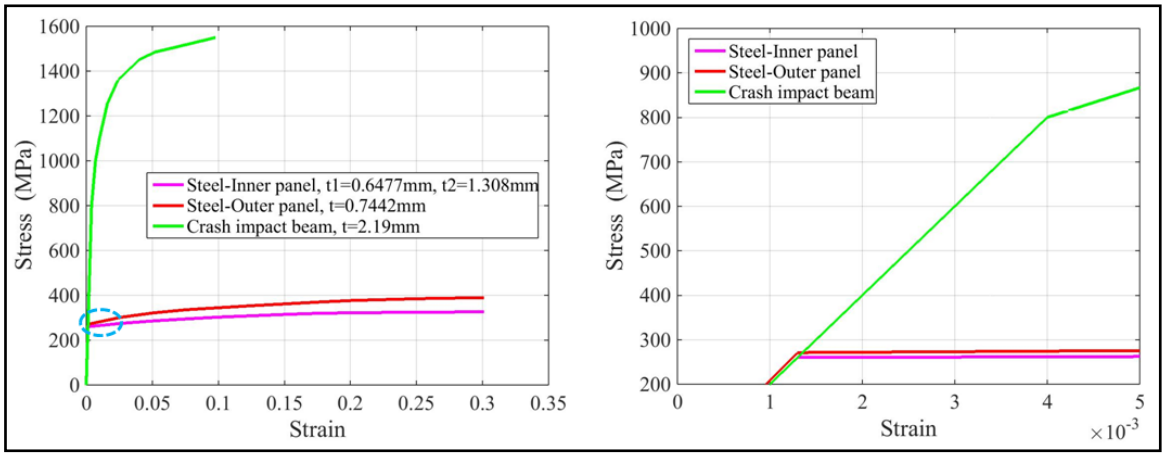

Figure 4.2-4 Properties of materials of Yaris door outer panel, inner panel and impact beam. [16]

Table 4.2-1 Summary of composite materials [10, 17]

	RHO *g/cm3*	*EA* *GPa*	*EB* *GPa*	*PR*	*GAB* *GPa*	*GAC* *GPa*	*GBC* *GPa*	*XT* *MPa*	*XC* *MPa*	*YT* *MPa*	*YC* *MPa*	*S* *MPa*
CFS003/LTM5208	1.45	53.6	55.2	0.042	2.85	2.85	1.425	618	642	652	556	84
E-Glass/epoxy	1.85	29.7	29.7	0.17	5.3	5.3	5.3	369	549	369	549	97
GMT	1.21	5.81	5.81	0.284	5.81	5.81	5.81	80.7	77.6	80.7	77.6	50
GMT_UD	1.23	11.07	6.48	0.307	4.21	2.1	4.21	180	100	80.7	58.5	50
GMT_TEX	1.20	9.24	6.00	0.389	3.5	1.75	3.5	174	70	70	57	45
CSIMS	1.22	27	23	0.105	6	3	6	411	128	396	125	62
GSIMS	1.35	11	10	0.21	5.2	2.6	5.2	154	113	142	106	66

Meaning of parameters listed in Table 4.2-1 is as follows:

RHO— density of composite material;

EA— Young's modulus of longitudinal direction, a direction;

EB— Young's modulus of transverse direction, b direction;

PR— Main Poisson's ratio, related to a direction and b direction;

GAB— Shear modulus of a direction and b direction;

GAC— Shear modulus of a direction and c direction, direction c is perpendicular to the plane of ab;

GBC— Shear modulus of b direction and c direction;

XT— Longitudinal tensile strength;

XC— Longitudinal compressive strength;

YT— Transverse tensile strength;

YC— Transverse compressive strength;

S— Shear strength of ab plane.

4.3 Reference

[19]. http://www.slideshare.net/BKLR/polymer-matrix-composites.

[20]. Giovanni B. , presentation of course “Progettazione di strutture meccaniche in materiale composito”, Politecnico di Torino, 2014.

[21]. Frederick T. W., James C. W. and Hong Li, PPG Industries, Inc, “Glass Fibers”, ASM Handbook, Vol. 21: Composites (#06781G), 2001.

[22]. Paul J. W., Zoltek Corporation, “Carbon Fibers”, ASM Handbook, Vol.21: Composites, 2001.

[23]. http://www.angelfire.com/ma/ameyavaidya/b_fiber.htm#boron

[24]. Reashad B. K. and Nasrin F., “Kevlar-The Super Tough Fiber”, International Journal of Textile Science 2012, pp78-83.

[25]. David Roylance, “Introduction to composite materials”, March 24, 2000.

[26]. Curt A., “NM EPOXY HANDBOOK”, third edition,2004.

[27]. http://www.netcomposites.com/guide/polyester-resins/8

[28]. Ermias G. Korico., “Implementation of Composites and Plastics Materials for Vehicle Lightweight”, PhD thesis,2012.

[29]. MIL-HDBK-17-5, “Composite Materials Handbook”, 17 June, 2002.

[30]. http://composite.about.com/library/data/blc-cfs003ltm25-rtd.htm

[31]. Giovanni B. and Brunetto M., “Recent research results in composite materials and adhesive applications for vehicle lightweight”, Int. Cong. Motor Vechiles&Motors 2014,October 9th-10th.

[32]. Patent US2002/0064640A1, “Thin composite laminate and use thereof in making sports articles, especially boots”.

[33]. P. Nieri, I. Montanari, A. Terenzi, L. Torre and J. M. Kenny, “A novel composite configuration for low-cost panels with improved toughness”, 29th International Conference and Forum- SECO 08, March 31st –April 2nd .

[34]. http://www.ncac.gwu.edu/

[35]. Giovanni B., Alem T. Beyene and Ermias G. Korico., “Geometrical optimization of bumper beam profile made of pultruded composite by numerical simulation”, Composite Structures, 2013.

5 Chapter 5 Finite Element Model Simulations

5.1 Finite Element Models

Numerical simulation gives an efficient tool for the analysis of deformation behavior of structural components in different industries, which could provide clear results of different alternative models at the initial designing stage in order to get the best structure. Due to high cost of prototypes when developing new vehicle models, computer simulations of vehicle dynamics become more and more important in the product development process. As we know that automotive components are geometrically complex, consequently, some assumptions and approximations need to be made in order to make the computer simulation more practical.

There are several common software on the market today used for vehicle dynamic simulations. ABAQUS [1] is one of several large software FE code on the market today for solving problem in multiphysics, which are including fluid, thermal, mechanical, electrical couplings and so on. As seen in [1] the ABAQUS product suite consists of three core products: ABAQUS/Standard, ABAQUS/Explicit and ABAQUS/CAE. ABAQUS/Standard is a general-purpose solver that uses traditional implicit integration scheme to solve finite element analyses. ABAQUS/Explicit uses explicit integration scheme to solve highly nonlinear transient dynamic analysis. ABAQUS/CAE provides an integrated modeling (preprocessing) and visualization (post-processing) environment for the analysis products.

LS-DYNA [2] is a general-purpose finite program capable of simulating complex real world problem. It is used by the automobile, aerospace, construction, military, manufacturing and bioengineering industries. The code's origins lie in highly nonlinear, transient dynamic finite element analysis using explicit time integration. Nonlinear means at least one of the following complications: changing boundary conditions, large deformations and nonlinearity of the materials behavior that therefore does not exhibit ideally elastic behavior. Transient dynamic means analyzing high speed, short duration events where inertial forces are important, including automotive crash, explosions and manufacturing process. Also it could provide many types models of different materials, such as metals, plastics, composite, foams and so on.

Also PAM-CRASH, RADIOSS, ADAMS and CarSim are used in vehicle dynamic simulations; all of these tools have different advantages and applications are different in different areas. In this research activity, ABAQUS and LS-DYNA are selected for simulation of vehicle side door structure.

5.2 Finite Element Simulation theory

This section describes the theory for solving different types of simulations in ABAQUS and LS-DYNA. More and more information about the simulation techniques are available in support documents.

5.2.1 Static analysis

A static analysis is sufficient if the interest is to investigate the long-term response of a structure to applied load and the inertia effects can be neglected. The equation of equilibrium governing static linear problems is:

$$[K]\{x\} = \{F\}$$

where $[K]$ is the elemental stiffness matrix, $\{F\}$ is the external load vector, $\{x\}$ is the node displacements vectors.

The problem can be both linear and nonlinear. Nonlinearities can arise from large displacement effects, material nonlinearity, and/or boundary nonlinearities such as contact and friction. If problem is nonlinear Newton's method will be used to solve equation above.

5.2.2 Dynamic analysis

In this case, dynamic analysis has load and response that vary with time and the duration of load application in the case of interest (i.e. impact) is very short in time. Usually vehicle crash event could finish within 100 milliseconds. When nonlinear dynamic response is investigated direct integration must be used, and this procedure can be done applying either implicit direct integration or explicit direct integration.

The equation of equilibrium governing the nonlinear dynamic response of a system, according to the finite element technique:

$$[M]\{\ddot{x}\} + [C(x,\dot{x})]\{\dot{x}\} + [K(x,\dot{x})]\{x\} = \{F(t)\}$$

Where: $[M], [C], [K]$ are the mass, damping and elemental stiffness matrices, $\{F(t)\}$ is the external load vector; $\{x\}, \{\dot{x}\}, \{\ddot{x}\}$ are the displacement, velocity and acceleration vectors of the nodes of the finite element mesh at time "t".

To solve this system means to calculate the time history of the displacements, velocities and accelerations, and also the time history of constraint forces. It is possible to use the modal transformation only if the coefficient of the matrices of mass, damping and stiffness are constant in time and the constraint are constant in time, otherwise the modal transformation method cannot be applied. Generally the coefficients of the mass matrix are constant in time, although this is not strictly right. It is possible that mass of the system is increasing or decreasing. The coefficients of the stiffness matrix may vary in time because of nonlinear behavior: material, geometrical and constraints, therefore the coefficients of the stiffness matrix are function of the present value of the displacement$x$. Also some materials are strain-rate sensitive, which means that the materials mechanical properties depend not only on the displacement but also on the velocity. Similar situations may affect the coefficients of the damping matrix.

To solve the equation system it is possible to use a step by step procedure, discretising the equation in time. The application of this method is based on some ideas:

- Calculate the kinematic quantities at the step $(t_i + \Delta t)$ on the basis of the quantities computed at the time instant t_i;
- Update the coefficients of the stiffness, damping and mass matrices according to the present situation;
- Assume the variation of the displacements, velocities and accelerations within each time interval "Δt". Obviously, the choice criteria on these assumptions determine the accuracy, stability and cost of the solution procedure.

5.2.2.1 Implicit method

Suppose that at the time instant t_i the nodal accelerations and the velocities are known

$$\{\dot{x}(t = t_i)\} = \{\dot{x}\}_i \qquad \{\ddot{x}(t = t_i)\} = \{\ddot{x}\}_i$$

Then the dynamic equilibrium equation at the time t_i can be considered as

$$[k(x)]_i\{x\}_i = \{F(t)\}_i - [M]\{\ddot{x}\}_i - [C]\{\dot{x}\}_i$$

$$[k(x)]_i\{x\}_i = \{F(t)\}_i - \{F_{iner}\}_i - \{F_{damp}\}_i$$

And then solved as

$$\{x\}_i = [k(x)]_i^{-1}\left\{\{F(t)\}_i - \{F_{iner}\}_i - \{F_{damp}\}_i\right\}$$

We could see some implications of that procedure:

- At each step the stiffness matrix (naturally if it is variable due to nonlinearities) must be inverted and the inversion procedure of this kind of matrix is so time consuming;
- The present (at the time t_i) value of the stiffness matrix coefficients depends on the result $\{x\}_i$, therefore inside each time step an iterative procedure for the update of the stiffness matrix coefficients is needed;
- The value of velocities and accelerations at the time $(t_i + \Delta t)$ must be calculated, through a forecasting process.

There are a lot of procedures for this and it is clear that we have to forecast the values of velocities and accelerations at the time $(t_i + \Delta t)$ on the basis of the known values at the time t_i. The most used procedures are: Houbolt method, Wilson θ method and Newmark method [3]. Implicit integration procedures are unconditionally stable and research work reveals that implicit numerical integration procedures does not assure the conservation of the total energy because some energy is dissipated by the numerical procedure itself, which could impact the accuracy of the solution. The convergence of solution is influenced by time-step period according to research work [3], the results would be more precise if time step Δt is smaller.

5.2.2.2 Explicit method

Let's now suppose that at the time instant t_i the nodal displacements and the velocities are known

$$\{x(t = t_i)\} = \{x\}_i \qquad \{\dot{x}(t = t_i)\} = \{\dot{x}\}_i$$

Then the dynamic equilibrium equation at the time t_i can be rearranged as

$$[M]\{\ddot{x}\}_i = \{F(t)\}_i - [C]\{\dot{x}\}_i - [k(x)]_i\{x\}_i$$

$$[M]\{\ddot{x}\}_i = \{F(t)\}_i - \{F_{damp}\}_i - \{F_{stiff}\}_i$$

And then solved as

$$\{\ddot{x}\}_i = [M]^{-1}\left\{\{F(t)\}_i - \left\{F_{damp}\right\}_i - \left\{F_{stiff}\right\}_i\right\}$$

Some implications are:

- At each step the stiffness matrix (that generally is changed due to nonlinearities) must not be inverted, avoiding the inversion procedure. Even the stiffness matrix can be simply calculated element by element and immediately multiplied by the known displacement vector $\{x\}_i$ to get the stiffness force vector;
- The present (at the time t_i) value of the stiffness matrix coefficients depends on the known displacement vector $\{x\}_i$, therefore inside each time step they are known;
- Then the value of displacements and velocities at the time $(t_i + \Delta t)$ must be calculated.

To match the stability requirement the time step Δt should be less than a critical value that is related to the largest eigenvalue of the discretised structure:

$$\Delta t_{stable} = \frac{2}{\omega_{max}}$$

Where ω_{max} is the highest frequency in the system.

An approximation to the stability is written as the smallest transit time of dilatational wave across any of the elements in the mesh:

$$\Delta t_{stable} = \frac{L_{min}}{c_d}$$

Where L_{min} is the smallest element dimension in the mesh and c_d is wave speed of the material (determined by elastic modulus and density).

In this explicit situation, a very big number of integration steps are needed, but each of them are quite quick as they does not require neither the inversion of the stiffness matrix nor the convergence procedure for the stiffness matrix evaluation. And the small size of the time step is generally sufficient to assure also the quality of the solution against the accuracy and convergence requirement.

5.3 FE Simulation models of vehicle side door

5.3.1 FE Model of Traditional door structure

The entire finite element model of Toyota Yaris 2010 (key version file) is available from the NCAC website [4], the model format is according to the rules of the software LS-DYNA. At first I have separated the front lateral door model away from the whole structure model. Then several components inside the door structure, for example, spacing foam, foam support, window movement mechanical arms and some brackets, have been deleted because they give no contribution to the integrity or the stiffness of the door. Finally the simplified door model contains 12 components.

The 12 components are: outer panel and two inner panels, impact bar and its two extremity brackets, and six reinforced supports of frame or panels. These components are made with steel and have different shapes and wall thickness. The left picture in Figure 5.3-1 is showing the door component without the two inner panels, and the right one is showing the door component without outer panel.

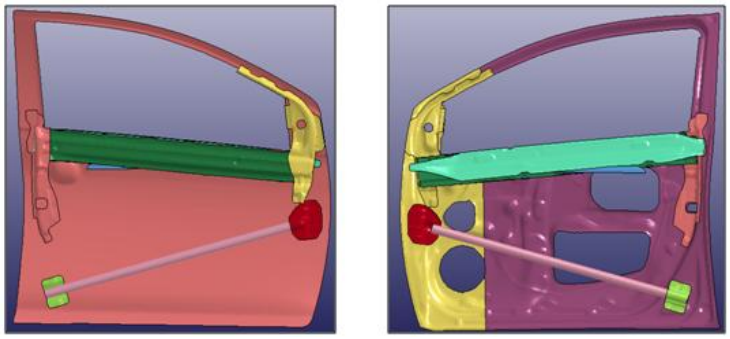

Figure 5.3-1 Simplified FE Model of Yaris door [4]

By means of software HyperMesh, the input file has been prepared according to the rules of ABAQUS code's language. Then the model could be imported correctly into ABAQUS. This process is shown in Figure 5.3-2.

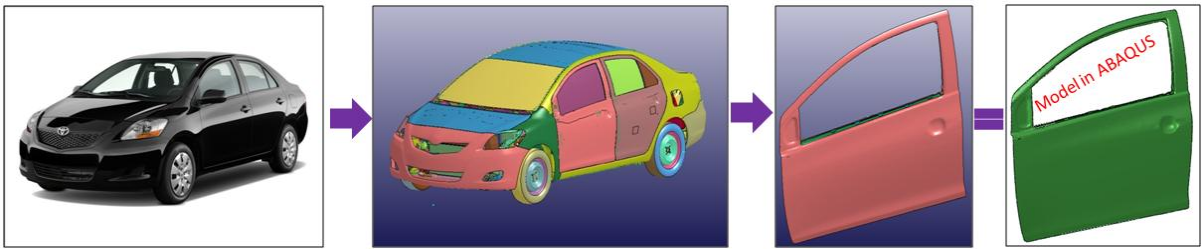

Figure 5.3-2 Extraction process to get traditional door model [4]

In this steel model, all the information about element type, element size, and the number of elements is same as that in the original key file. There are two shell element types in this steel model: $S3$ (i.e. with three nodes) and $S4$ (i.e. with four nodes). The total number of elements in this simplified model is 38256. The total mass of the simplified model is around$17.2kg$.

5.3.2 Composite door models

In general, there are some different ways to connect composite material parts together, and adhesive bonding is used widely in different areas because of many advantages. In this research activity adhesive bonding technology is adopted. In the two developed composite door models, there are three parts: beams of door frame and the internal reinforcing beam that are made with composite materials, corner structural joints that are made with aluminum alloy and joined to the composite structure by means of epoxy adhesives. These parts are described in the following sections.

5.3.2.1 Composite beams

Door frame beams and the internal reinforcement beam are made with composite material; all the sizes of these beams are defined according to the sizes of the traditional steel door. In this research work, one composite model is a plane door and the other one has the curved profile form (see Figure 5.3-4).

I have chosen the beam section as squared tube $43 \times 43mm$ and beam wall thickness is$2mm$, all the beams in these two composite models have same section size as shown in the left image of Figure 5.3-3. The relative position of the door beams is shown in the right image of Figure 5.3-4.

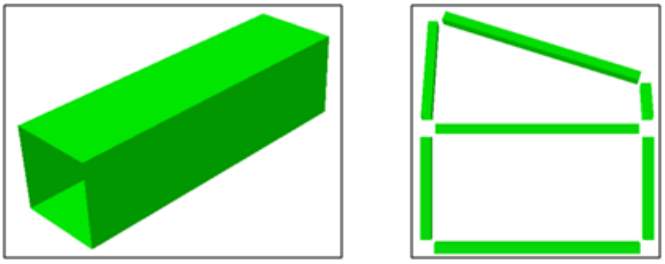

Figure 5.3-3 Composite beams

For the two composite door models, beam distribution and length of each beam are listed in Figure 5.3-4 and Table 5.3-1.

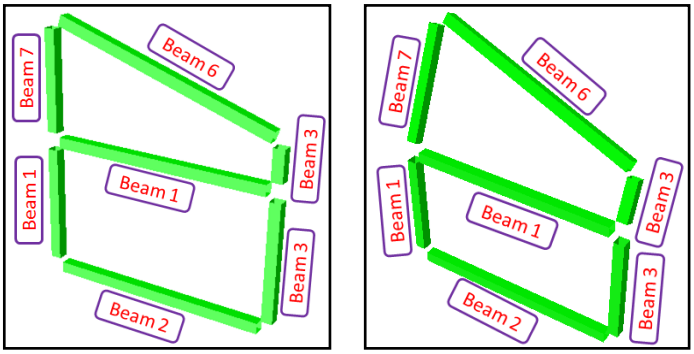

Figure 5.3-4 Composite beams distribution in plane and curved models

Table 5.3-1 Length of each beam

	Beam1 (mm)	**Beam2 (mm)**	**Beam3 (mm)**	**Beam4 (mm)**	**Beam5 (mm)**	**Beam6 (mm)**	**Beam7 (mm)**
Curved	427	854	427	854	157	906	462
Straight	457	854	457	854	120	897	398

For these beams, composite material $T300-5208$ is used, which consists of carbon fiber and epoxy matrix, with lower density$1600\ kg*m^{-3}$. This kind of composite has high strength and stiffness performance; it is used widely in automotive engineering as well as in aeronautical engineering, and has been considered suitable for door design. The fibers have unidirectional layout which is along the axis of the beam. Material data are taken from the company Hexcel website. The main mechanical property information is shown in Table 5.3-2.

Table 5.3-2 Mechanical properties of T300/5208 [5]

Fiber	**Matrix**	**Form**	**Volume of fiber**
T300 Carbon	5208 Epoxy	Unidirectional	0.7

E11	**E22**	**G12**	**Nu12**
$181GPa$	$10.3GPa$	$7.17GPa$	0.28
F1t	**F1c**	**F2t**	**F2c**
$1500MPa$	$1500MPa$	$40MPa$	$246MPa$

The meaning of the variables listed in Table 1-2 is as follows: E11=longitudinal modulus, E2=transverse modulus, G12=in-plane shear modulus, Nu12=major Poisson's ratio, F1t=longitudinal tensile strength, F1c=longitudinal compressive strength, F2t=transverse tensile strength, F2c=transverse compressive strength.

5.3.2.2 Aluminum alloy joints

The corner joints are used for connecting beams together through proper adhesive bonding, shapes of the joint are depending on the directions of beams which are to be connected. In order to contribute to the lightweight design, joints have hollow structure with a wall thickness of$2\ mm$, fillet radius of the joints is $10\ mm$. The FE model of some of these joints and their positions in the door model are shown in Figure 5.3-5. There are 6 joints in each composite door model.

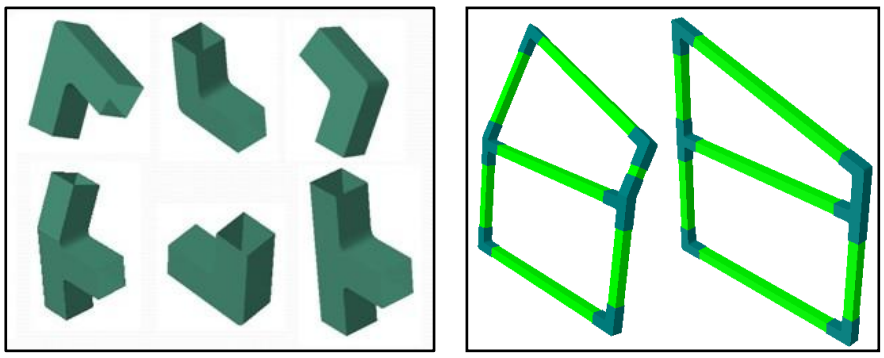

Figure 5.3-5 Joints shapes and position in composite door models

These joints are made with aluminum alloy$AW6016$. This material is mostly used in automotive car body manufacturing, especially for outer panels. It exhibits very good formability with low spring back, very good hemming capability, good weld ability, high corrosion resistance, stretcher-strain free surfaces, stabilized formability in temper, generally well balanced properties (formability, strength, and bake hardening). Main mechanical properties are reported in Table 5.3-3.

Table 5.3-3 Mechanical properties of aluminum alloy AW6016 [6]

E(MPa)	**v**	**ρ** $(kg * m^{-3})$	**RMN**(MPa)	**RM**(MPa)
69500	0.33	2700	-	100

Variables in Table 5.2-3: E=Modulus of elasticity, v=Poisson's ratio, ρ=density, RMN=min ultimate tensile strength, RM=ultimate tensile strength.

5.3.2.3 Adhesives

In the models adhesives are used for bonding composite beams and aluminum corner joints together. The bonding method is structural four sided bonding and the adhesive layer thickness is defined as $0.2mm$, with the bonding length is $60mm$.

Epoxy adhesive Loctite Hysol 3425 material is used in the models, which is a two components, high viscosity, thixotropic epoxy adhesive which cures at room temperature after mixing. It is a general purpose, non sag adhesive which develops high strength on a wide range of substrates. The thixotropic properties enable this adhesive system to bond rough vertical surfaces made from metal, ceramic, rigid plastics or wood through gaps of up to 3mm.

The main mechanical characteristics of Hysol 3425 are reported in Table 5.3-4.

Table 5.3-4 Mechanical characteristics of epoxy adhesive Hysol3425 [7]

Appearance	Yellow/White Paste
Working life of mixed adhesive 25 degree (6-10g mix), minutes	120
Maximum Gap Fill, mm	3
Mix Ratio by Volume	1:1
Mix Ratio by weight (g) (Resin/Hardener)	100:100
Fixture Time (light handling, 0.1N/mm^2) @23°C, minutes	240
Coefficient of Thermal Conductivity, (ASTM C177), $W/(m*K)$	0.28
Coefficient of Thermal Expansion, (ASTM E831-93), K (19.4°C to 33°C) (55.4°C to 199.4°C)	44×10^{-6} 173×10^{-6}
Hardness (shore D)	70-80
Glass Transition Temperature Tg °C (ASTM E1640-99)	72
Tensile strength (ASTM D882), N/mm^2	27.2
Elongation (ASTM D882), %	2.9
Modulus (ASTM D882), N/mm^2	1353

5.3.3 Final door models

Finally the three developed finite element models prepared in Abaqus6.10 environment are shown in Figure 5.3-6.

The weights of these three models are $17.2kg$, $3.6kg$ and $3.5kg$ respectively. Because in the two composite models there are no inner or outer panels, in order to consider this factor and to give more realistic values, the current weight values could be doubled, obtaining $7.2kg$ and $7.0kg$. As we can see, the weight is still remarkably reduced in comparison with that of traditional steel door model.

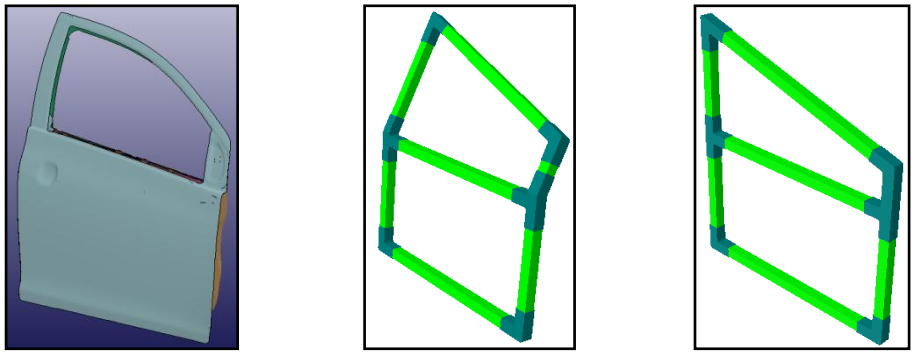

Figure 5.3-6 Three FE Models of lateral frontal door

5.4 Model of door substitution materials

In order to reduce the risk of injuries of the driver and passengers during vehicle side crash, vehicle side doors generally have an additional beam beside the outer panel and inner panel, three of them are playing a very important role in decreasing external forces applied to the on-board human beings by absorbing a certain amount of side impact energy and by reducing the bullet vehicle intrusion into the passenger compartment. Seong et al. [8] investigated the behavior of composite side-door impact beam for passenger cars and they concluded that the composite impact beams made of glass fiber and epoxy matrix not only reduce the weight of impact beams by more than 50% but also have a constant impact energy absorption capability with respect to environmental temperature variation. Side door outer panel, inner panel and impact beam are considered in this research.

5.4.1 Model for static and modal analysis

In this section, the traditional steel material was substituted with composite materials in side door panels and impact beam without changing figures of them. The first innovative composite solution is that only the outer panel and inner panel materials are substituted with composite material; not only panels but also impact beam material is replaced by composite material is the second solution. Side model is the same as the one used in previous solution, see Figure 5.4-1. Outer panel, inner panel and impact beam are three most important parts designed to protect passengers from injuries during the side impact event by reducing force and absorbing energy, see Figure 5.4-2. Design targets are lightweight, high strength and high energy absorption. Element type and

element size of simplified model are exactly the same as they are in original Yaris model, shell element are selected for outer panel, inner panel and impact beam.

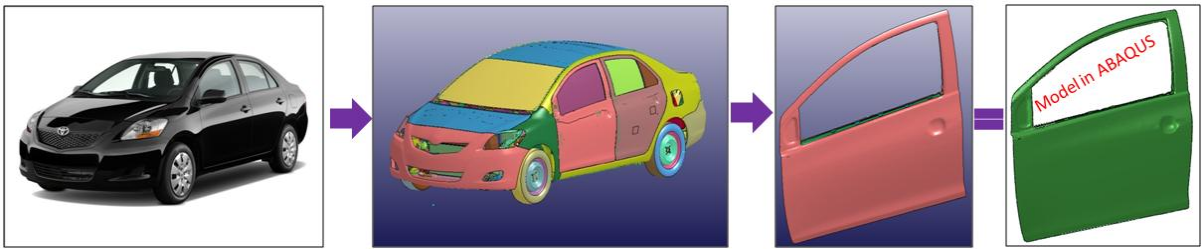

Figure 5.4-1 Yaris side door model [4]

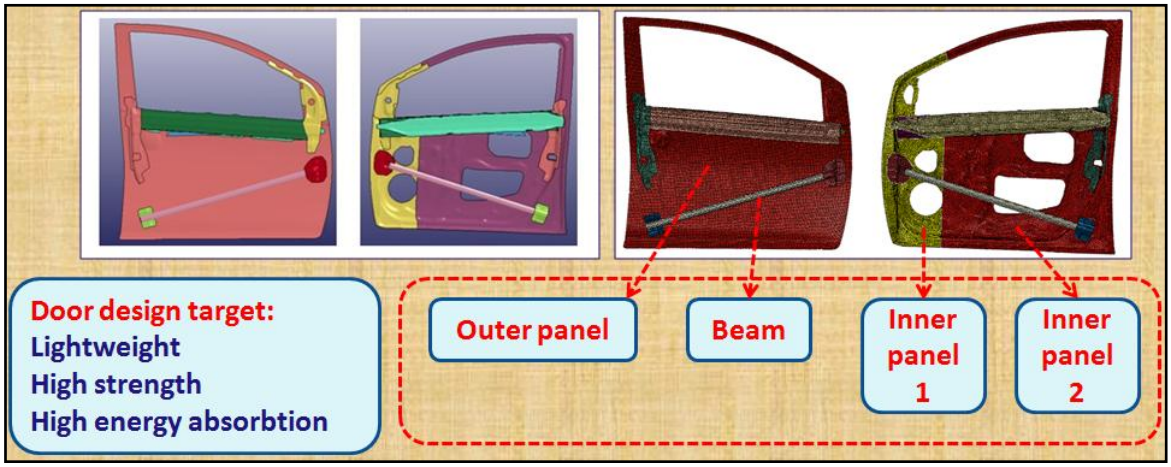

Figure 5.4-2 Parts considered: outer panel, inner panel and impact beam

5.4.2 Model of Crashworthiness evaluation

As dynamic crash step, crash analysis was performed to study the behavior of the door when the impacting barrier is equipped with its frontal bumper subsystem, that includes bumper beam, fascia, water cooler support, rails and energy absorber (as shown in Figure 5.4-4). The mass of the considered barrier is 1600 kg applied at the center of gravity of the striking vehicle, with impact velocity of$30\ km/h$.

At this stage, the side frame of Yaris (blue part in Figure 5.4-3) is simulated as a rigid body and its most important role is to contribute to boundary contact conditions for the perimeter areas of the door inner panel, that is an approximate simulation way for side frame behavior in a side crash impact. The side frame is completely constrained (six degrees of freedom are constrained).

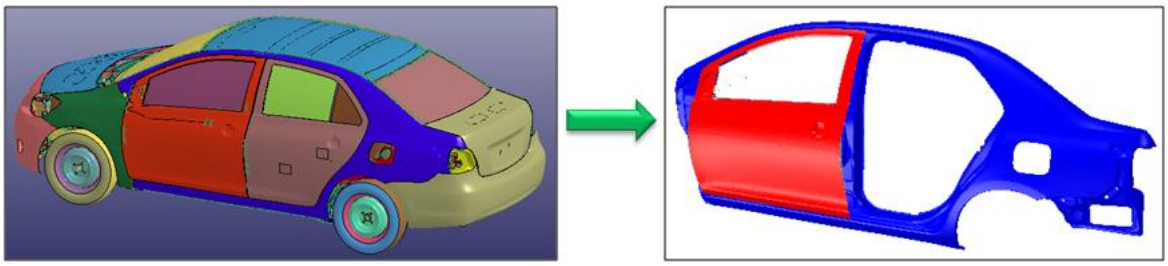

Figure 5.4-3 Crash model of side door [4]

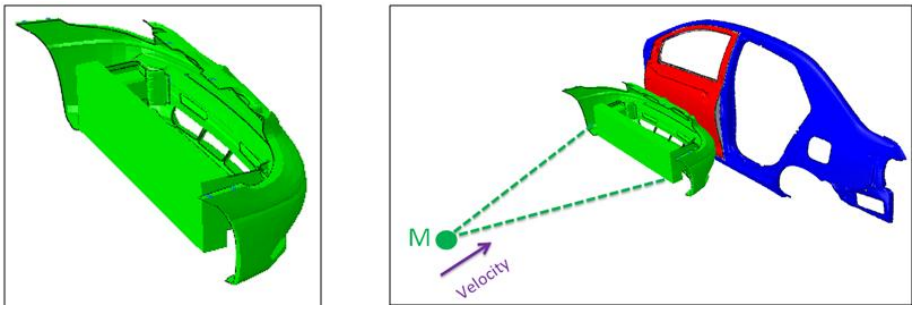

Figure 5.4-4 Simulation of side impact: deformable bumper and side door structure.

5.5 Model of crashworthiness evaluation on total Yaris structure level

The whole simulation was based on the FEM model of whole vehicle Toyota Yaris 2010 (see Figure 5.5-1b), which was available in the NHTSA web site and imported into LS-DYNA environment. Besides, 50 percentile male dummy of ES-2 (see Figure 5.5-1d) was properly placed by authors on the driver's seat with deformed sitting foam. In this work the movable deformable barrier (MDB, see Figure 5.5-1c) was the FMVSS214 (Regulation rule is shown in Figure 5.5-1a) shell version 2.0, with a mass of about $1360kg$. Evaluation of the dummy response was the way to estimate the crashworthiness of vehicle structure for the reference steel material and for the considered composite materials.

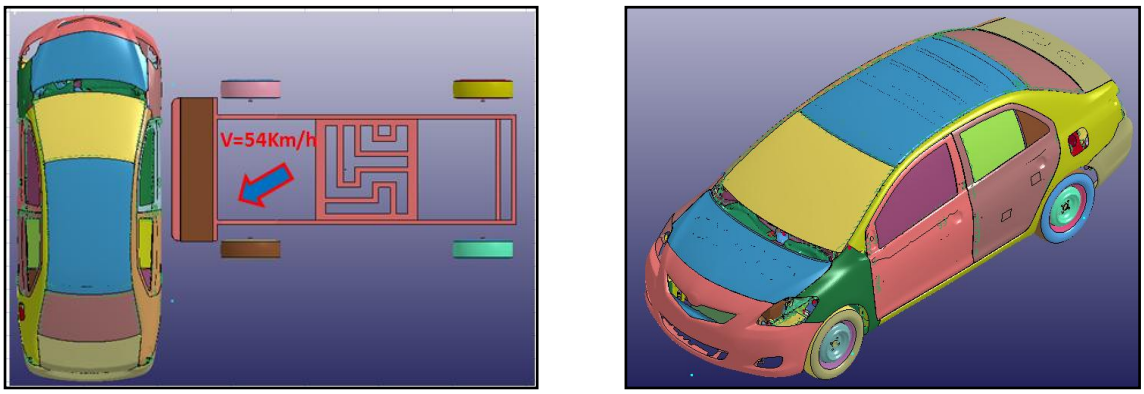

a) b)

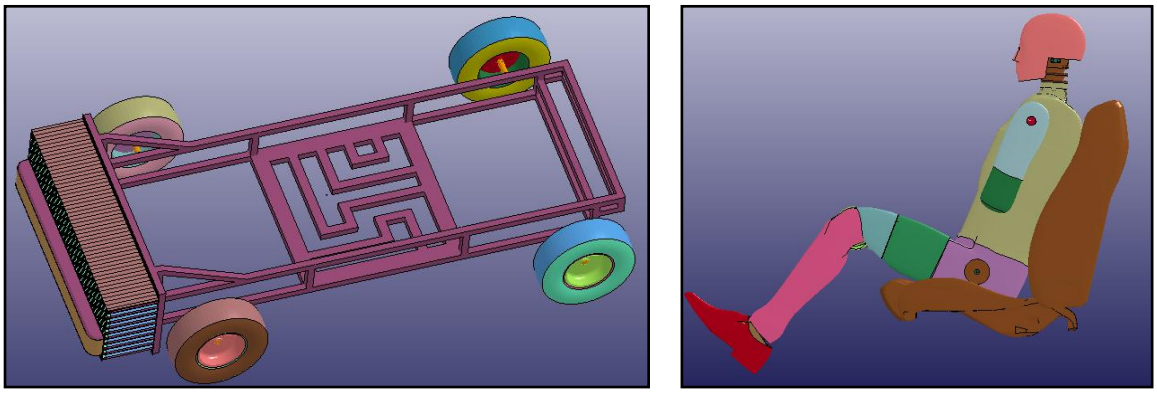

c) d)

Figure 5.5-1 Simulation model, a) Regulation FMVSS 214, b) Yaris model, c) Movable Deformable Barrier (MDB), d) dummy of EURO-SID 2

5.6 Innovative composite panel of Yaris side door

As discussed in Chapter 2, substitution of aluminum for steel can reduce mass in automotive closures. Nowadays, aluminum sheet has been most commonly used in hoods, where the limited formability of aluminum is not a significant barrier to efficient manufacturing. In research work [9], James G.S proposed an innovative door structure, which was composed of an inner panel, an outer panel and a multi-purpose “Simplified Total Aluminum Reinforcement” (STAR), shown in Figure 5.6-1.

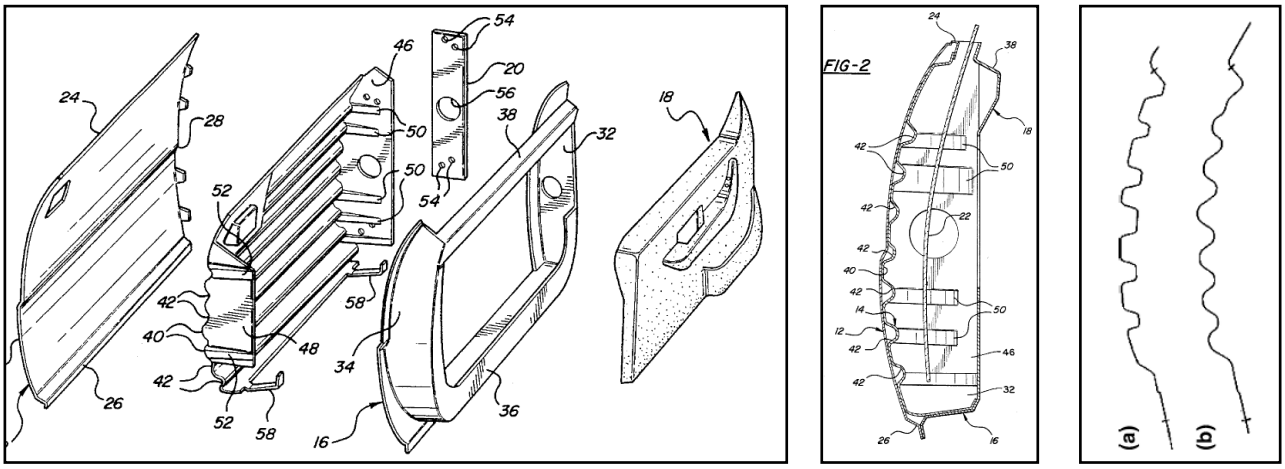

a) b) c)

Figure 5.6-1 a) Schematic aluminum door construction including a Simplified Total Aluminum Reinforcement (STAR) panel; b) Vertical door section showing the inner, outer, and STAR panel; c) STAR panel corrugation geometries. [9]

Actually the innovative solution was presented in patent work of Rashid earlier in 1997 [10]. A vehicle door was reinforced by an internal reinforcement panel that was fixed to and reinforced side portions of the inner door panel. This innovative design was tested successfully for static stiffness and static door intrusion. In that concept, a box-like STAR panel replaced or contributed to the function of the door impact beam, the outer beltline reinforcement, the latch reinforcement, and the hinge reinforcement.

In this research, an innovative STAR panel made with composite materials was developed for Yaris model, see Figure 5.5-2a. Figure 5.6-2b and Figure 5.6-2c are showing original Yaris door model and innovative one respectively.

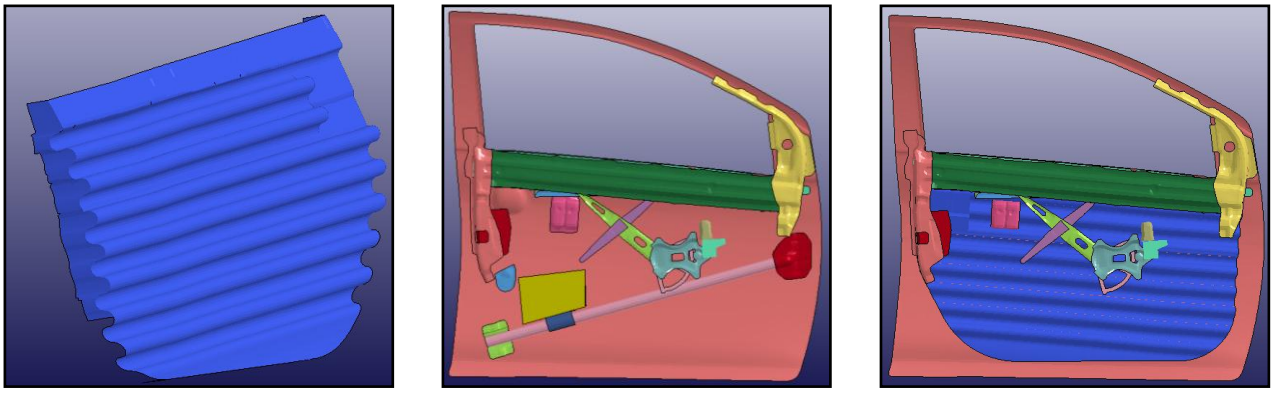

a) b) c)

Figure 5.6-2 a) STAR panel of Yaris; b) Original door model of Yaris; c) Innovative door model of Yaris

Figure 5.6-2c is showing that there is enough space between STAR panel and inner panel where several components could be built, such as window regulator and other brackets. Six components (shown in Figure 5.6-3a) in original door could be replaced by one composite part (see Figure 5.6-3b). Six parts include impact beam and outer belt reinforcement. Four red circles in Figure 5.6-3c are joining areas which are used to bond STAR panel, outer panel and inner panel together, adhesives bonding is proposed to use in this new model.

The choice of finite element type for this new panel is shell element in LS-DYNA because the innovative panel is a thin walled shell structure. Total number of shell element of this part is 34479.

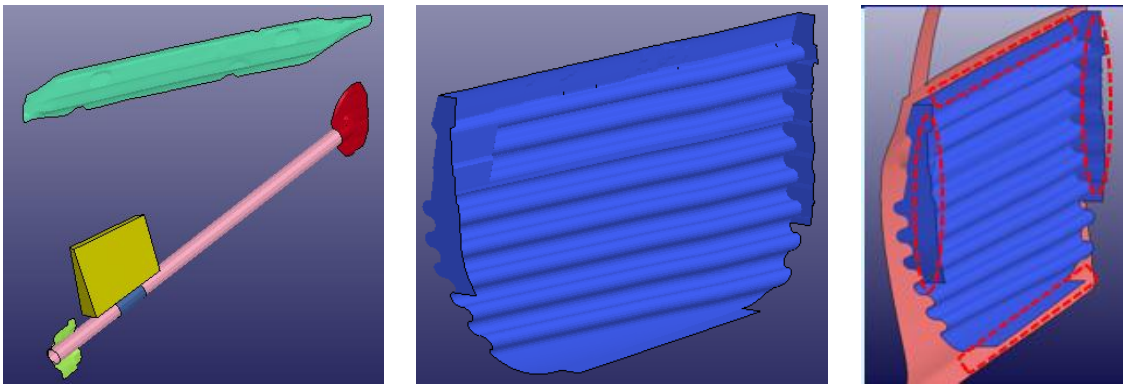

a) b) c)

Figure 5.6-3 a) Parts could be replaced; b) Innovative part made with composite; c) Four connecting areas

In order to investigate the protection level of new door structure during a side impact, this new STAR panel is integrated into Yaris door model and the crashworthiness is evaluated based on biomechanical response of dummy according to regulation FMVSS214. For the STAR panel material, several composite materials are modeled with LS-DYNA, and intrusion displacements of inner panel, injury of head, thorax, abdomen and pelvis are analyzed in the numerical simulations.

5.7 Models of failure criteria for composite materials

Models of Chapter 5.32 and Chapter 5.4 are developed in ABAQUS environment (see Figure 5.7-1) and models of Chapter 5.5 and Chapter 5.6 are simulated with tool LS-DYNA tool (see Figure 5.7-2).

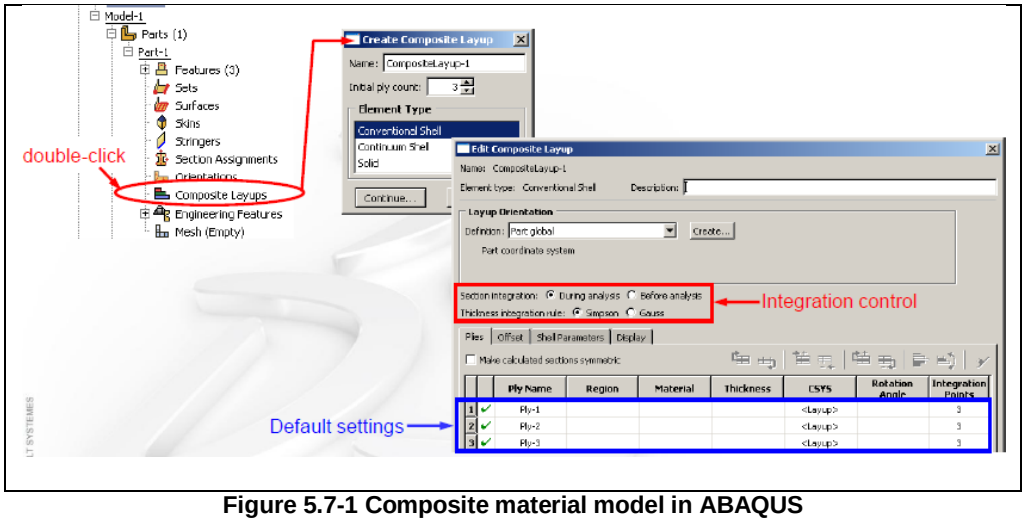

Figure 5.7-1 Composite material model in ABAQUS

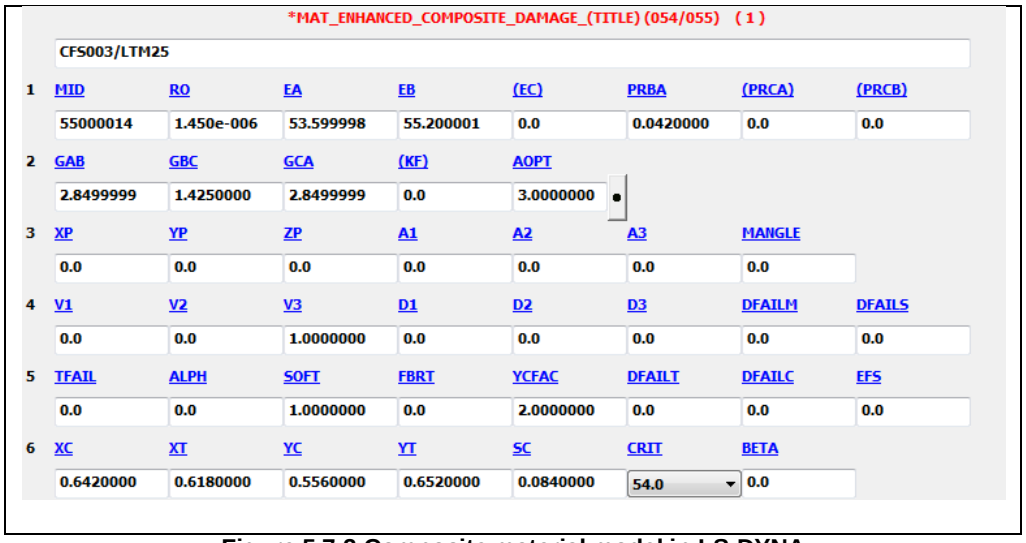

Figure 5.7-2 Composite material model in LS-DYNA

Composite materials display a wide variety of failure mechanisms as a result of their complex structure and manufacturing process, which include fiber failure, matrix cracking, buckling and delamination. Based on these failure mechanisms it can be more appropriate to consider the composite as a structure rather than as a material.

- Fiber failure, including fiber tension and fiber compression;
- Matrix cracking;
- Buckling, cause structural collapse;
- Delamination between different layers, cause significant structural damage, particularly in compression.

There are a lot of failure criteria of composite materials proposed during past 30 years in the scientific and technical literatures. These criteria can be classified in a number of ways, including whether they are based on strength or fracture mechanics theories, whether they predict failure in a general sense or are specific to aparticular failure mode, and whether they focus on in-plane or interlaminar failure. In this chapter, failure theories for in-plane and interlaminar failure are summarized, that are largely based on the stress components of an individual ply within the laminate.

5.7.1 Fiber failure

Fiber failure in tension happens due to the accumulation of individual fiber failures within plies, which becomes critical when there are not enough fibers remaining to carry the applied loads. Some researchers apply a maximum strength or maximum strain criterion at each ply, using simple material limit values taken from experimental activities. Hashin [11] applied a quadratic interaction criterion involving in-plane shear, Chang and Chang [12] used the Hashin quadratic interaction criterion but with nonlinear shear behavior, all of them are summarized in Table 5.7-1.

Table 5.7-1 Failure criteria for fiber failure in tension

Criterion	Equation	Additional terms
Max_stress_fiber_tens	$\sigma_1 \geq X_T$	
Max_strain_fiber_tens	$\varepsilon_1 \geq \varepsilon_{1T}$	
Hashin_fiber_tens (1980) [11]	$\left(\frac{\sigma_1}{X_T}\right)^2 + \frac{1}{S_{12}^2}(\tau_{12}^2 + \tau_{13}^2) \geq 1$	
Chang_Chang_fiber_tens (1987) [12]	$\sqrt{\left(\frac{\sigma_1}{X_T}\right)^2 + \frac{\frac{\tau_{12}^2}{2G_{12}} + \frac{3}{4}\alpha\tau_{12}^4}{\frac{S_{12_{is}}^2}{2G_{12}} + \frac{3}{4}\alpha S_{12_{is}}^4}} \geq 1$	α from nonlinear shear law $\gamma_{12} = \left(\frac{1}{G_{12}}\right)\tau_{12} + \alpha\tau_{12}^3$
Puck_fiber_tens (1998) [13]	$\frac{1}{\varepsilon_{1T}}\left(\varepsilon_1 + \frac{\nu_{f12}}{E_{f1}} m_{f\sigma}\sigma_2\right) \geq 1$	Subscript f denotes fiber values; $m_{f\sigma}$ is stress magnification factor

Table 5.7-2 is showing criteria for compressive fiber failure, where many authors use the maximum stress or maximum strain criteria based on limit value from experimental data, some of them is involving the effects of micro-buckling.

Table 5.7-2 Failure criteria for fiber failure in compression

Criterion	Equation	Additional terms
Max_stress_fiber_comp	$\sigma_1 \geq X_C$	
Max_strain_fiber_comp	$\varepsilon_1 \geq \varepsilon_{1C}$	
Greszczuk_fiber_comp (1974) [14]	$\sigma_1 \geq \frac{G_{12}^m}{1 - V_f}$	G_{12}^m: matrix shear modulus V_f: fiber volume fraction
Chang_Lessard_fiber_comp (1991) [13]	$\sigma_1 \geq \bar{X}_C$	$\bar{X}_C$: microbuckling strength, equation in separate paper
Puck_fiber_comp (1998) [13]	$\frac{1}{\varepsilon_{1C}}\left\|\left(\varepsilon_1 + \frac{\nu_{f12}}{E_{f1}} m_{f\sigma}\sigma_2\right)\right\| \geq 1 - (10\gamma_{12})^2$	Subscript f denotes fiber values; $m_{f\sigma}$ is stress magnification factor

5.7.2 Matrix failure

Matrix failure in laminated composites is very complicated. Cracks initiate typically at defects or fiber–matrix interfaces. A lot of literatures were published on the analysis of matrix cracking and failure, and many researchers have developed approaches for predicting the initiation of matrix cracks, using fracture mechanics theories to predict the growth or accumulation of damage from existing cracks. Except for the maximum stress and maximum strain criteria, the simplest proposal is the quadratic interaction criterion of Hashin and Rotem [15], and nonlinear shear terms are included in other criteria, as shown in Table 5.7-3. An exception to this is the criterion of Cuntze and Freund, which is only based on the transverse tensile stress and strength and through-thickness shear stress. The criteria for matrix failure in compression, given in Table 5.7-4, are similar to those for tension failure.

Table 5.7-3 Failure criteria for matrix failure in tension

Criterion	Equation	Additional iterms
Max_stress_matrix_tens	$\sigma_2 \geq Y_T$	
Max_strain_matrix_tens	$\varepsilon_2 \geq \varepsilon_{2T}$	
Hashin_Rotem_matrix_tens (1973) [15]	$\left(\frac{\sigma_2}{Y_T}\right)^2 + \left(\frac{\tau_{12}}{S_{12}}\right)^2 \geq 1$	
Hasin_3D_matrix_tens (1980) [11]	$\frac{(\sigma_2+\sigma_3)^2}{Y_T^2} + \frac{{\tau_{23}}^2 - \sigma_2\sigma_3}{S_{23}^2} + \frac{{\tau_{12}}^2 - {\tau_{13}}^2}{S_{12}^2} \geq 1$	
Chang_Chang_matrix_tens (1987) [10]	$\sqrt{\left(\frac{\sigma_2}{Y_T}\right)^2 + \frac{\frac{\tau_{12}^2}{2G_{12}} + \frac{3}{4}\alpha\tau_{12}^4}{\frac{S_{12_{is}}^2}{2G_{12}} + \frac{3}{4}\alpha S_{12_{is}}^4}} \geq 1$	α from nonlinear shear law $\gamma_{12} = \left(\frac{1}{G_{12}}\right)\tau_{12} + \alpha\tau_{12}^3$
Chang_Lessard_matrix_tens (1991) [16]	Chang and Chang (1987) with in situ strength $Y_{T_{is}}$ instead of Y_T	
Shahid_Chang_matrix_tens (1995) [17]	$\left(\frac{\bar{\sigma}_2}{Y_T(\phi)}\right)^2 + \left(\frac{\bar{\tau}_{12}}{S_{12}(\phi)}\right)^2 \geq 1$	$\bar{\sigma}$: effective ply stress ϕ: matrix crack density Y_T, S_{12} : use crack density

Table 5.7-4 Failure criteria for matrix failure in compression

Criterion	Equation	Additional terms
Max_stress_matrix_comp	$\sigma_2 \geq Y_C$	
Max_strain_matrix_comp	$\varepsilon_2 \geq \varepsilon_{2C}$	
Hashin_Rotem_matrix_comp (1973) [15]	$\left(\frac{\sigma_2}{Y_C}\right)^2 + \left(\frac{\tau_{12}}{S_{12}}\right)^2 \geq 1$	
Hasin_3D_matrix_tens (1980) [11]	$\frac{\sigma_2}{Y_C}\left[\left(\frac{Y_C}{2S_{23}}\right)^2 - 1\right] + \left(\frac{\sigma_2}{2S_{23}}\right)^2 + \left(\frac{\tau_{12}}{S_{12}}\right)^2 \geq 1$	
Chang_Lessard_matrix_comp (1991) [16]	$\sqrt{\left(\frac{\sigma_2}{Y_C}\right)^2 + \frac{\frac{\tau_{12}^2}{2G_{12}} + \frac{3}{4}\alpha\tau_{12}^4}{\frac{S_{12_{is}}^2}{2G_{12}} + \frac{3}{4}\alpha S_{12_{is}}^4}} \geq 1$	α from nonlinear shear law $\gamma_{12} = \left(\frac{1}{G_{12}}\right)\tau_{12} + \alpha\tau_{12}^3$

5.7.3 Shear failure

Some common criteria applied in analyzing in-plane shear failure are summarized in Table 5.7-5, Hashin and Chang criteria considered the relationship between fiber and matrix.

Table 5.7-5 Failure criteria for fiber-matrix shear failure

Criterion	Equation	Additional terms
Max_stress_shear	$\tau_{12} \geq S_{12}$	
Max_strain_shear	$\gamma_{12} \geq \gamma_{12}^u$	γ_{12}^u: ultimate shear strain
Hashin-shear (1980) [11]	$\left(\frac{\sigma_1}{X_T}\right)^2 + \left(\frac{\tau_{12}}{S_{12}}\right)^2 \geq 1$	
Chang_Lessard_shear (1991) [16]	$\sqrt{\left(\frac{\sigma_1}{X_C}\right)^2 + \frac{\frac{\tau_{12}^2}{2G_{12}} + \frac{3}{4}\alpha\tau_{12}^4}{\frac{S_{12_{is}}^2}{2G_{12}} + \frac{3}{4}\alpha S_{12_{is}}^4}} \geq 1$	α from nonlinear shear law $\gamma_{12} = \left(\frac{1}{G_{12}}\right)\tau_{12} + \alpha\tau_{12}^3$

5.7.4 Ply failure

Some authors have developed criteria which could predict the ply failure in laminates, such as “fully interactive” criteria such as Tsai and Wu [21], where all the data is used to generate a failure surface, summarized in Table 5.7-6.

Table 5.7-6 Interactive failure criteria for ply failure

Criterion	Equation
Tsai_Hill_ply_inter (1965) [18, 19]	$\left(\frac{\sigma_1}{X}\right)^2+\left(\frac{\sigma_2}{Y}\right)^2+\left(\frac{\tau_{12}}{S_{12}}\right)^2-\frac{\sigma_1\sigma_2}{X^2}\geq 1$ X, Y are either X_C, Y_C or X_T, Y_T depending on sign of σ_1, σ_2
Hoffman_ply_inter (1967) [20]	$\left(\frac{1}{X_T}-\frac{1}{X_C}\right)\sigma_1+\left(\frac{1}{Y_T}-\frac{1}{Y_C}\right)\sigma_2+\frac{{\sigma_1}^2}{X_TX_C}+\frac{{\sigma_2}^2}{Y_TY_C}+\left(\frac{\tau_{12}}{S_{12}}\right)^2-\frac{\sigma_1\sigma_2}{X_TX_C}\geq 1$
Tsai_Wu_ply_inter (1971) [21]	$\left(\frac{1}{X_T}-\frac{1}{X_C}\right)\sigma_1+\left(\frac{1}{Y_T}-\frac{1}{Y_C}\right)\sigma_2+\frac{{\sigma_1}^2}{X_TX_C}+\frac{{\sigma_2}^2}{Y_TY_C}+\left(\frac{\tau_{12}}{S_{12}}\right)^2-2f_{12}\sigma_1\sigma_2\geq 1$ $f_{12}=-\frac{1}{2}\sqrt{f_{11}f_{22}}$ *or* $f_{12}=-\frac{1}{2}\sqrt{\frac{1}{X_TX_CY_TY_C}}$

5.7.5 Delamination failure

Table 5.7-7 is showing a lot of criteria proposed to predict the initiation of delamination using the stress values of an individual ply or interface element. All the criteria listed in the table are using combinations of the through-thickness tensile and shear parameters, in linear, quadratic or curve-fit relationships, with a small number also considering the stress in the fiber direction.

Table 5.7-7 Failure criteria for delamination initiation

Criterion	Equation
Max_stress_delam	$\sigma_3\geq Z_T, \tau_{31}\geq S_{31}, \tau_{23}\geq S_{23}$
Hashin_delam (1980) [11]	$\left(\frac{\sigma_3}{Z_T}\right)^2+\left(\frac{\tau_{23}}{S_{23}}\right)^2+\left(\frac{\tau_{31}}{S_{31}}\right)^2\geq 1$
Lee_delam (1982) [22]	$\sigma_3\geq Z_T$ or $\sqrt{{\sigma_{12}}^2+{\sigma_{13}}^2}\geq S_{23}$
Kim_Soni_delam (1986) [23]	$F_{13}{\sigma_{13}}^2+F_{23}{\sigma_{23}}^2+F_{33}{\sigma_3}^2+F_3\sigma_3\geq 1$ F_{i3} and F_3 are general functions of the interlaminar strengths
Long_delam (1991) [24]	$\left(\frac{\sigma_3}{Z_T}\right)+\left(\frac{\tau_{23}}{S_{23}}\right)^2\geq 1$ and $\left(\frac{\sigma_3}{Z_T}\right)^2+\left(\frac{\tau_{23}}{S_{23}}\right)^2\geq 1$
Tsai_delam (1997) [25]	$\frac{{\sigma_1}^2-\sigma_1\sigma_3}{{X_T}^2}+\left(\frac{\sigma_3}{Z_T}\right)^2+\left(\frac{\tau_{23}}{S_{23}}\right)^2\geq 1$
Tong_Tsai_delam (1997) [25]	$\frac{{\sigma_1}^2-\sigma_1\sigma_3}{{X_T}^2}+\left(\frac{\sigma_3}{Z_T}\right)+\left(\frac{\tau_{23}}{S_{23}}\right)^2\geq 1$
Degen_Tong_Tsai_delam (1997) [25]	$\left(\frac{\sigma_1}{X_T}\right)^2+\left(\frac{\sigma_3}{Z_T}\right)+\left(\frac{\tau_{23}}{S_{23}}\right)^2\geq 1$
Zhang_delam(1998)[26]	$\sigma_3\geq Z_T$ or $\sqrt{{\tau_{31}}^2+{\tau_{23}}^2}\geq S_{23}$

In the failure criteria summarized above: $\sigma, \tau, \varepsilon$ and γ are used for stress and strain in the normal and shear directions; X, Y, Z and S are strengths in the fiber, matrix, through-thickness directions and shear directions; subscripts 1,2 and 3 refer to the fiber, transverse and through-thickness directions; subscripts T and C denote limit values in tension and compression; subscript "is" refers to in situ strengths, and all other symbols and abbreviations are explained in the table or in the reference papers.

5.8 Reference

[1]. Dassault Systemes, Getting Started with Abaqus: Interactive Edition version 6.12.

[2]. Livermore Software Technology Corporation, "LS-DYNA THEORY MANUAL", March 2006.

[3]. Bathe KJ, "Finite Element Procedures",

[4]. http://www.ncac.gwu.edu/

[5]. http://composite.about.com/library/data/blc-t300-5208.htm

[6]. http://aluminium.matter.org.uk/aluselect/03_physical_browse.asp

[7]. Technical Data Sheet Hysol 3425, LOCTITE, Tallaght Business Park, Dublin, Ireland, February 2004.

[8]. Seong S. C, Jin H.C and Dai G.L, "Development of the composite bumper beam for passenger cars", Composite Structures 32 (1995) 491-499.

[9]. James G.S, Hans M.B and Narinder P.G, " Quick Plastically Formed Aluminum Doors: Design and Performance", 2007.

[10]. Moinuddin S.R and Chongmin K, United States Patent 5536060, "Reinforced Vehicle Door", July 16, 1996.

[11]. Hashin Z, "Failure criteria for unidirectional composites", J Appl Mech 1980.

[12]. Chang F-K, Chang K-Y, "A progressive damage model for laminated composites containing stress concentrations", J Compos Mater 1987.

[13]. Puck A, Schurmann H, "Failure analysis of FRP laminates by means of physically based phenomenological models", Compos Sci Technol 1998.

[14]. Greszczuk LB, “Microbuckling of lamina-reinforced composites”. Composite materials: testing and design (third conference). ASTM STP, vol. 546. American Society for Testing and Materials,1974.

[15]. Hashin Z, Rotem A, “A fatigue failure criterion for fiber reinforced materials”, J Compos Mater, 1973.

[16]. Chang F-K, Lessard LB, “Damage tolerance of laminated composites containing an open hole and subject to compressive loadings”, part 1-analysis, J Compos Mater, 1991.

[17]. Shahid I and Chang F-K, “An accumulative damage model for tensile and shear failures of laminated composite plates”, J Compos Mater, 1995.

[18]. Hill R, “A theory of the yielding and plastic flow of anisotropic metals”, Proc Royal Soc London, 1994.

[19]. Tsai W, “Strength characteristics of composite materials”, NASA CR-224, 1965.

[20]. Hoffman O, “The brittle strength of orthotropic materials”, J Compos Mater, 1967.

[21]. Tsai S and Wu E , “A general theory of strength for anisotropic materials”, J Compos Mater, 1971.

[22]. Lee JD, “Three dimensional finite element analysis of damage accumulation in composite laminate”, Comput Struct 1982; 15(33):335-50.

[23]. Kim RY, Soni SR, “Failure of composite laminates due to combined interlaminar normal and shear stresses”. In: Kawata K, Umekawa S, Kobayashi A, editors. Composites 86: recent advances in Japan and the United States, Proceedings of Japan-US. CCM-III; 1986, p341-350.

[24]. Long RS, “Static strength of adhesively bonded ARALL-1 joints”, J Compos Mater 1991; 25: 391-415.

[25]. Tong L, “An assessment of failure criteria to predict the strength of adhesively bonded composite double lap joints”. J Reinf Plastic Compos 1997; 16(8):698-713.

[26]. Zhang X, “Impact damage in composite aircraft structures-experimental testing and numerical simulation”. J Aerospace Eng 1998; 212(4):245-59.

6 Chapter 6 Static and modal simulation results

6.1 Vehicle side door structure with composite frame

As mentioned in Chapter 5, two composite solutions (Figure 6.1-1b and Figure 6.1-1c) of Yaris side door are developed while the original steel side door structure (see Figure 6.1-1a) is considered as reference solution.

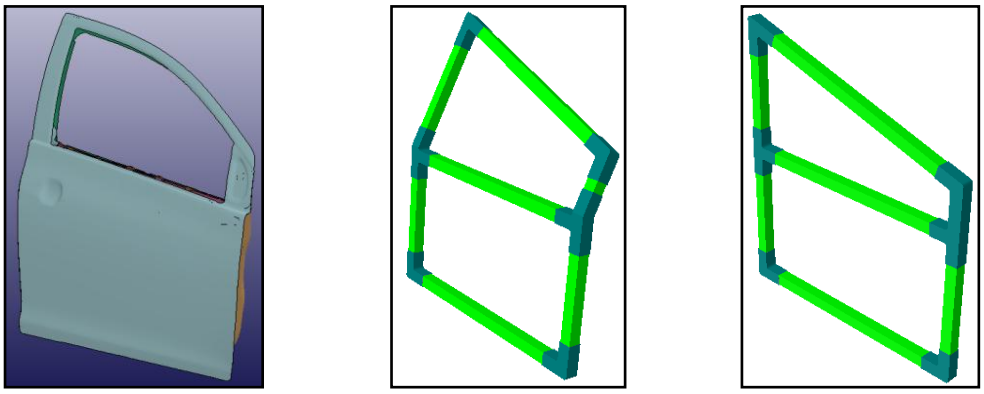

a) b) c)

6.1-1 Three FE Modes of vehicle side door

In these two composite door models, composite beam are simulated using conventional shell element $S4R$ because they are made of laminated material; aluminum joints are also simulated using shell element $S4R$; adhesives layers are simulated using brick element $C3D8R$. Surface to surface tie constraint is adopted for simulating the links between the surface of adhesive and the surface of beam, or the surface of adhesive and the surface of the joint. The surface of beam or structural joint is the master surface while the surface of adhesive is the slave surface.

In the considered loading case, door models are constrained by two hinges as in the reality. Hinges are simulated by hinge connector model which can be found in Abaqus connector library: the hinge connector has only one degree of freedom which is the rotational degree of freedom around the first axis direction of one coordinate system defined by user, the coordinate has been created according to the rotational direction of each door model.

Here are the three considered load cases (calculated by ABAQUS 6.10 standard).

6.1.1 Vertical load case

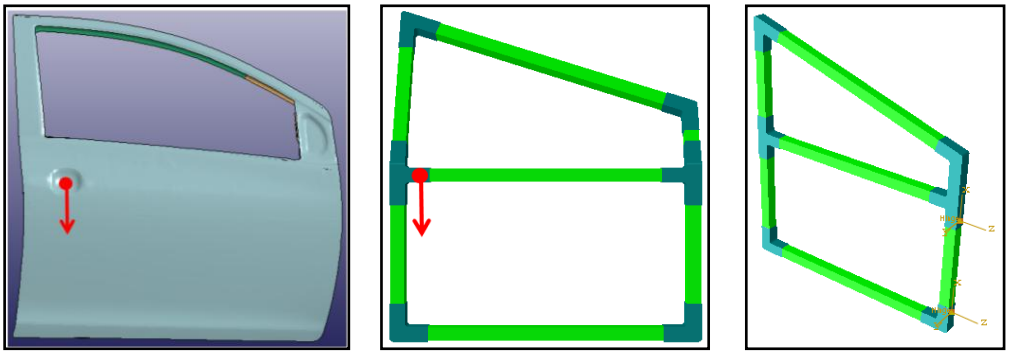

a) b) c)

6.1-2 - Force applied in vertical load case and hinge positions in composite models.

In this case, with $1g$ acceleration of gravity and a vertical concentrated force of $385N$ (Z-direction in steel model and Y-direction in composite models, as shown in Figure 6.1-2a and Figure 6.1-2b) has been applied at the outside handle point. The maximum vertical displacement of the door and the stress generated on door models are calculated. The two local coordinates in Figure 6.1-2c are used for defining hinges which are supposed to be installed on aluminum alloy joint, not on composite beams.

Boundary condition: two hinges (five degrees of freedom are constrained).

In this load case, the Von Mises stress of door shall be less than maximum yield strength of material in order to prevent permanent deformation of door [1].

In steel model all components are made with steel material, Von Mises equivalent stresses are extracted from the results; in composite material principal stresses are more important, in aluminum alloy and adhesives Von Mises stresses are extracted. Figure 6.1-3 shows the stress distributions in three models in this load case.

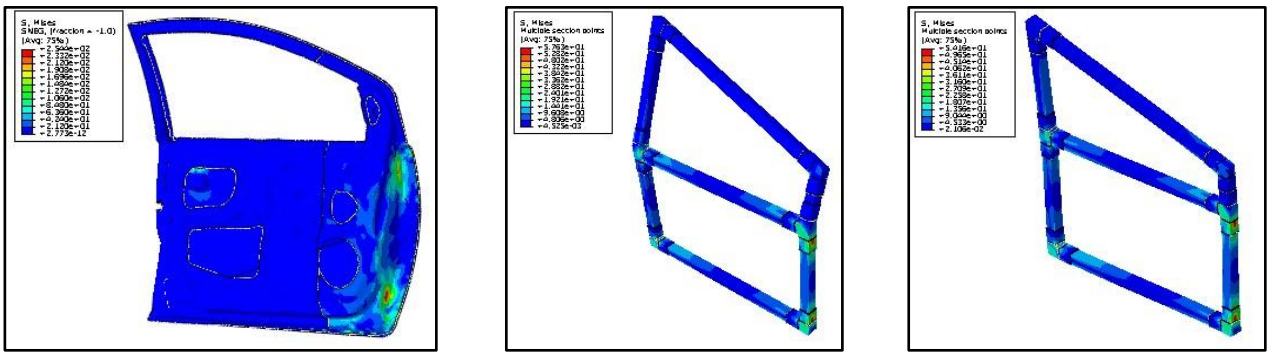

6.1-3 Von Mises stress distribution in three models for load case 1.

The maximum stresses are extracted from the result, and reported in Table 6.1-1.

Table 6.1-1 - Stresses extracted for load case 1.

	Maximum stress (MPa)		**Yield stress** (MPa)
Steel model	(V-Mises)	254	270
Curved composite model	Beams(Principal_stress)	33	40
	Joint (V-Mises)	54	100
	Adhesive (V-Mises)	5.7	27
Plane composite model	Beams(Principal_stress)	35	40
	Joint(V-Mises)	58	100
	Adhesive(V-Mises)	6.4	27

From Table 6.1-1, the stresses are less than the material yielding stress, so the strength condition is satisfied. In the two composite models the maximum stresses in different parts are almost the same, so there is not big difference between the two composite door models. The vertical displacement distribution is shown in Figure 6.1-4 and the extracted maximum displacements are shown in Table 6.1-2.

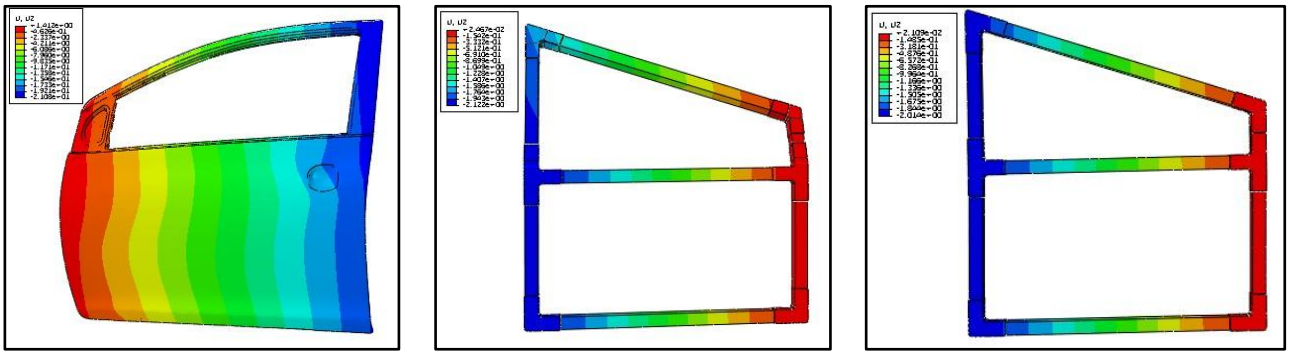

Figure 6.1-4 Vertical displacements distribution for load case 1.

Table 6.1-2 - Vertical maximum displacement in three models for load case 1.

	Maximun displacement (mm)
Steel model	3.5
Curved_composite	2.8
Plane_composite	3.0

From the maximum displacement point view, the composite models are almost the same, and a little smaller than the steel one.

Also the displacement of handle point of outer panel and the structural reaction force in vertical direction during the loading process have been collected, so the slope of the line in Figure 6.1-5 is the vertical direction stiffness of model for this load case.

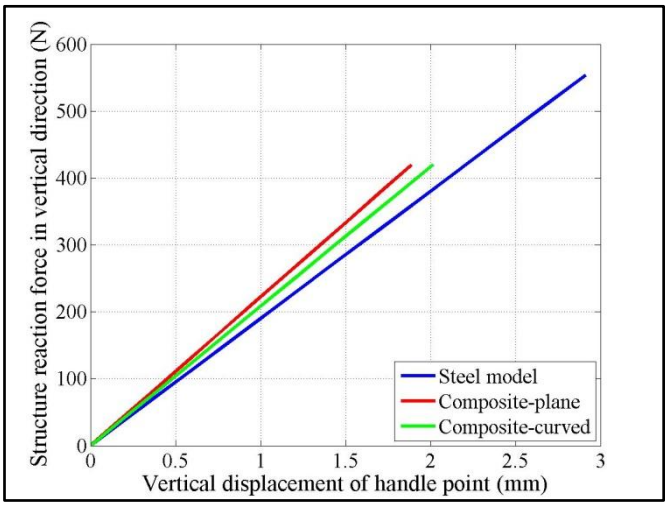

Figure 6.1-5 Vertical displacement and reaction force for load case 1.

In this vertical load case, the stiffness of composite door models are slightly higher (but higher) than that of the steel door model.

6.1.2 Horizontal load case

1g acceleration of gravity and a horizontal concentrated force of $385N$ (X-direction in three models) applied at outside panel handle point. The maximum vertical displacement of the door and the stress field generated on door models are calculated.

Boundary condition: two points where hinges are installed are completely constrained, which means that six degrees of freedom are all constrained.

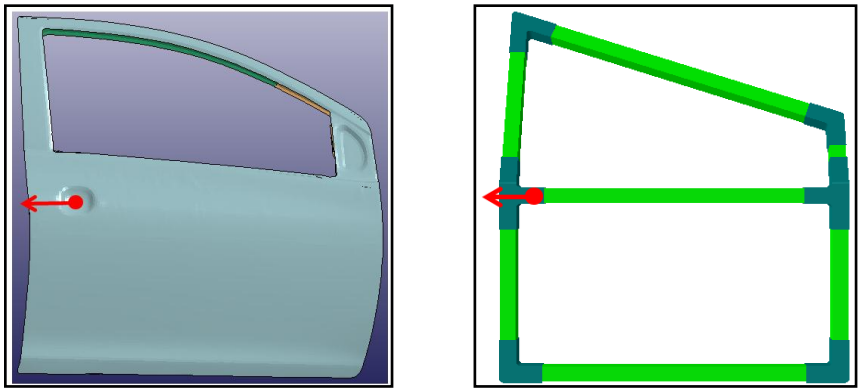

Figure 6.1-6 – Horizontal load case.

Under this load case, the stresses and the maximum displacement in the horizontal direction are extracted from the computed results, Figure 6.1-7 is showing stresses in three modes.

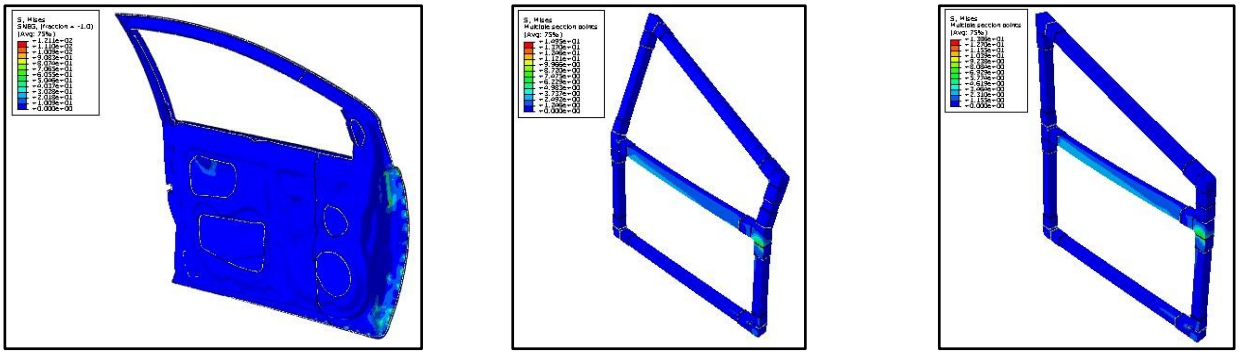

Figure 6.1-7 - Von Mises stress in three models under horizontal load.

Maximum stress are shown in Table 6.1-3.

Table 6.1-3 - Stresses extracted for horizontal load.

	Maximum stress (MPa)		**Yield stress** (MPa)
Steel model	(V-Mises)	119	270
Curved composite model	Beams(Principal_stress)	3.3	40
	Joint (V-Mises)	14	100
	Adhesive (V-Mises)	1	27
Plane composite model	Beams(Principal_stress)	3.2	40
	Joint(V-Mises)	15	100
	Adhesive(V-Mises)	1	27

The maximum stresses in different parts are almost same in two composite models. Horizontal displacement distribution and maximum displacement are shown in Figure 6.1-8 and Table 6.1-4.

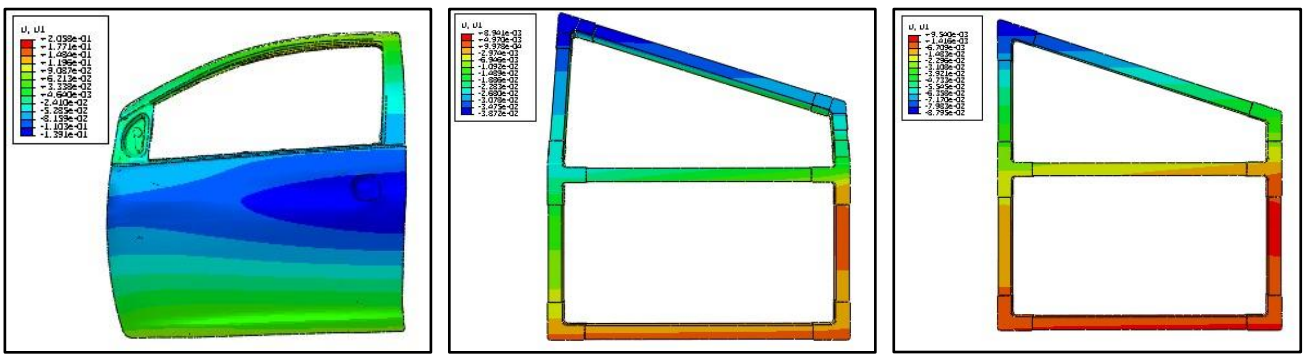

Figure 6.1-8 - Horizontal displacements in three models for horizontal load.

Table 6.1-4 - Horizontal maximum displacements in three models for horizontal load.

	Maximun displacement(mm)
Steel model	0.14
Curved_composite	0.04
Plane_composite	0.09

All the maximum displacements in this case are all very small, however the composite models have better behavior.

Also, the displacement of the handle point and the structural reaction force in the horizontal direction have been collected; the slope of the lines shown in Figure 6.1-9 is the stiffness.

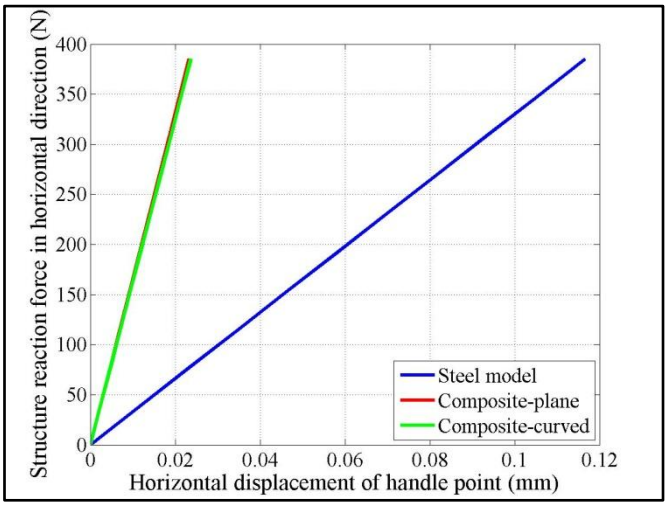

Figure 6.1-9- Horizontal displacement and reaction force for load case 2.

In this figure, for this load case, the stiffness of composite door models is much higher than that of steel door model.

6.1.3 Quasi static intrusion simulation

This load case is to simulate the quasi-static intrusion behavior of the door, based on the Euro NCAP Pole Test (the left image in Figure 6.1-10): the car is moving laterally with stated velocity while the pole is stationary, in this developed analysis, a static force is applied to the vehicle door by a cylindrical structure that is simulating the pole. Pole diameter is $254mm$, which is modeled as a rigid body, it can only translate in the direction perpendicular to the surface of the outer panel of the door (Y direction in Figure 6.1-10b).

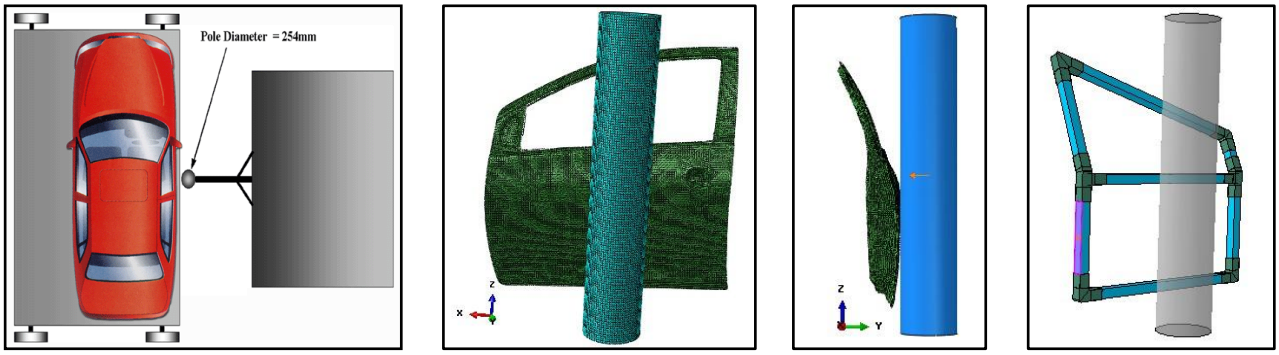

a) b) c) d)

Figure 6.1-10- Quasi static intrusion simulation model

A concentrated force is applied at the center of the pole in order to push the pole against the door; the contact condition is that the pole surface is the master surface while the outer surface of the panel is the slave surface during the whole intrusion process (Figure 6.1-10c). In the steel model, similar contact conditions are defined between the impact bar surface (the master surface) and the outer panel surface (the slave surface). Correlated to the Euro Pole test, the weight of the car model, which that is about $1100Kg$ according to the Toyota Yaris technical report, is used as the pushing force value.

Boundary condition: two hinge constraints and the lock point constraint, hinge constraints are the same as used before; the lock point is constrained in two translation directions, X-direction and Y-direction in the steel door model and X-direction and Z-direction in composite door models. The lock point is located at the center of the lower vertical beam in Figure 6.1-10d (same center point position in the plane composite model).

The displacement distributions in intrusion direction in different models are shown in Figure 6.1-11.

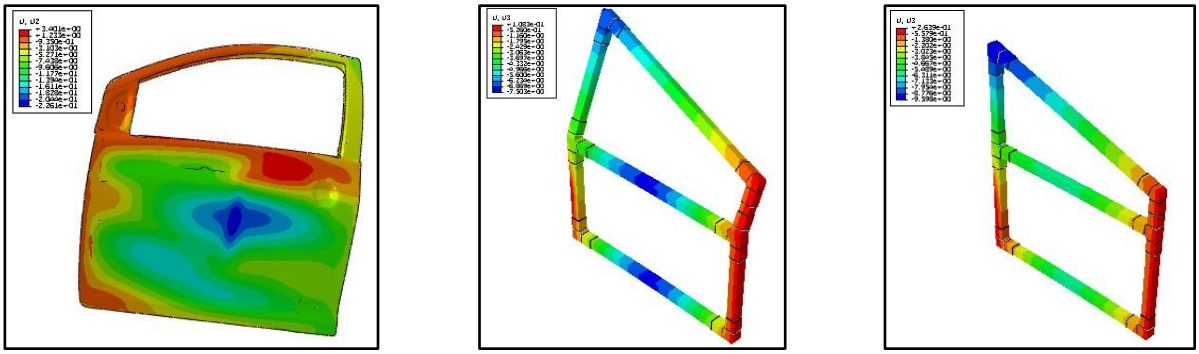

Figure 6.1-11- Displacements in extrusion direction in three models for load case 3.

In Table 6.1-5 the maximum displacements resulting for these three models are reported:

Table 6.1-5- Maximum displacements in extrusion direction in three models in load case 3.

	Maximun displacement (mm)
Steel model	22
Curved_composite	7.5
Plane_composite	9.6

The intrusion displacements of the composite models are much smaller than that of the steel one.

The displacement in intrusion direction of center point of the internal beam of the composite models have also been collected during the loading process; in steel door model the point which has maximum displacement is collected, together with the reaction force in intrusion direction. The slope of line in Figure 6.1-12 is the intrusion direction stiffness.

From the figure, it comes out that the stiffness of the composite door models is higher than that of the steel door model; the stiffness of the two composite door models is almost same.

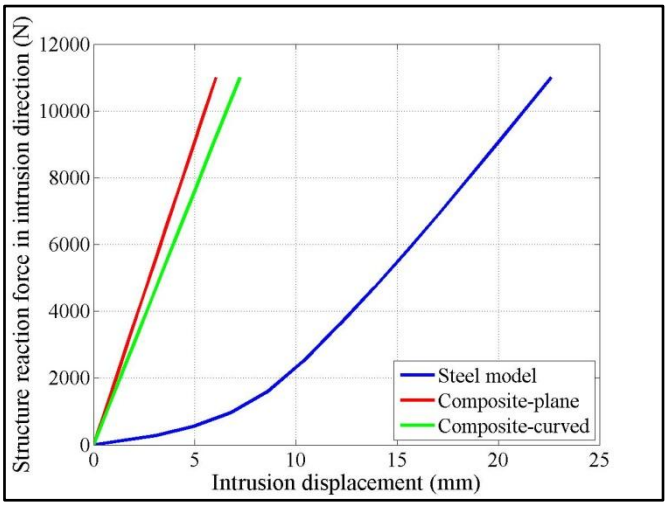

Figure 6.1-12- Displacement and reaction force in quasi static intrusion simulation.

6.1.4 Conclusion and discussion

The advantage that can be obtained by the use of a composite material structure for the lateral door of an automobile has been analyzed in comparison with the steel normal production solution.

Composite door models have been developed by the Finite element method and three different load cases have been considered, in order to explore the possible loading conditions encountered in the normal life. One of the considered load case is simulating through a quasi-static load

application, the impact of the side door against a pole. This is a very severe load condition to be taken into account with respect to international safety regulations.

The proposed composite solution satisfies the targets for the structure stiffness and strength and appears to behave even better than the steel reference solution. However the main result is the relevant weight reduction (the order of magnitude is at least 50%) in comparison with the steel door.

Furthermore, the proposed composite solution appears to behave in a satisfying way also in the case of the impact against pole conditions. Although the study has been conducted in a quasi-static loading condition the value of the applied load is of the order magnitude of the real one for this type of accident.

In the following sections, the dynamic crash process of composite door models will be studied, both at the subassembly level and after the inclusion of this innovative door into the car, at the whole structure level.

6.2 Materials substitution simulation results

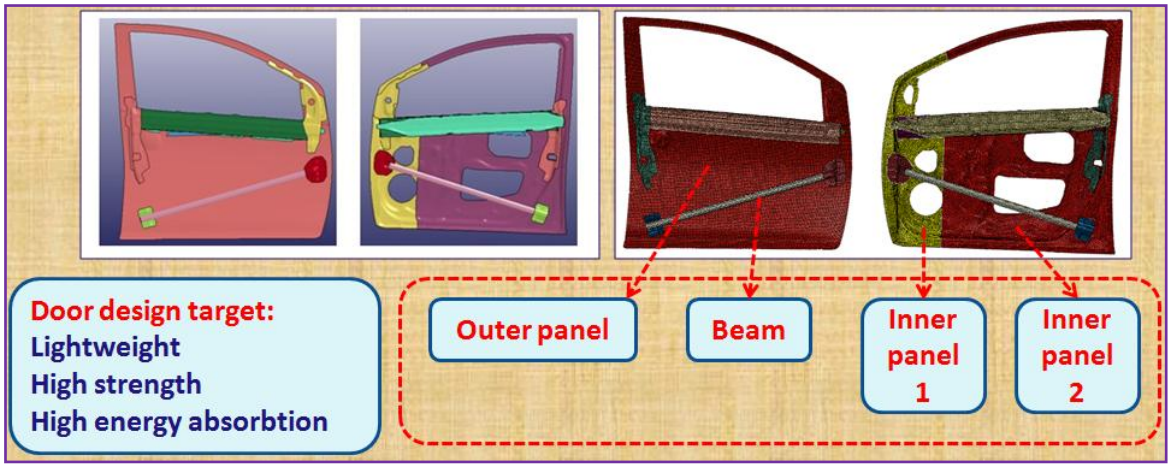

Figure 6.2-1 Side door structure model of Yaris

The thickness of composite panels and beam are evaluated approximately based on the equal stiffness criteria. A flat plate is considered for determination of the thickness for the given materials type under the same loading condition, in our case load case is assumed to be bending load (actually the loading case is too complicated during the side crash impact). In Figure 6.2-2, the plate with dimensions $b \times l \times h$, made of steel, is subjected to maximum bending moment M_{max} .

To choose the appropriate thickness for the proposed material, a simple equation has been used on the bases of maximum deflection formula (showed in the middle of Figure 6.2-2). In order to avoid excessive deformation and protect the remaining near components, the maximum deflection of composite component should be not greater than the reference steel component. So the thickness of composite material could be calculated from the right equation in Figure 6.2-1 [2].

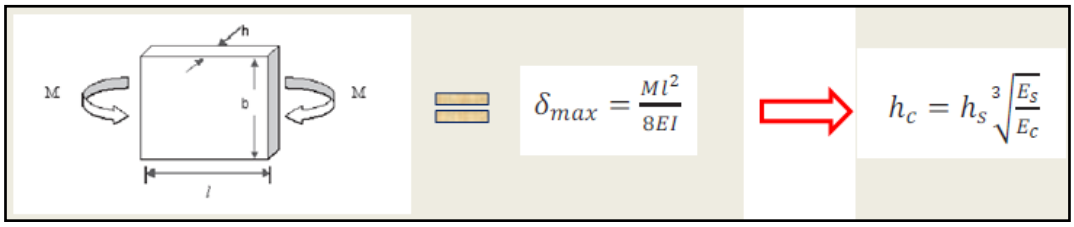

Figure 6.2-2 Equal stiffness criteria

The thickness value of outer panel and inner panel chosen in this model are $2\ mm$ and impact beam thickness is $3.6\ mm$, consequently the mass reduction of each component are showed in Table 6.2-1.

Table 6.2-1 Thickness of composite parts

	E_s (GPa)	h_s (mm)	M_s (Kg)	E_c (GPa)	h_c (mm)	h_c (mm)	M_c (Kg)	$Mass$ $reduction\ (Kg)$
Outer panel	200	0.7442	4.89	54	1.1514	2.0	2.42	2.47 (50%)
Inner panel 1	200	1.308	2.36	54	2.20	2.0	0.663	1.697 (72%)
Inner panel 2	200	0.6477	3.18	54	1.002	2.0	1.80	1.38 (43%)
Beam	200	2.19	1.62	54	3.38	3.6	0.491	1.129 (70%)

As a result, the total mass reduction of these three parts is about $6.7\ Kg$, which is around 39% of the total mass of reference steel door.

The front door subsystem was isolated from the complete car model and appropriate constraints have been imposed at locking mechanism and hinged joints of the front door. Lateral stiffness have been evaluated for four loading cases: F_{y1}, F_{y2}, F_{y3} and F_{y4} (as shown in Figure 6.2-2). In this case, the door model is fixed by two hinges constraints and one lock constraint at latch point as it is constrained in reality.

Also sagging behavior was investigated, when a vertical load of $500N$ in Z direction is applied on latch position. Hinges mechanism is fixed around its own axis (showed in Figure 6.2-3).

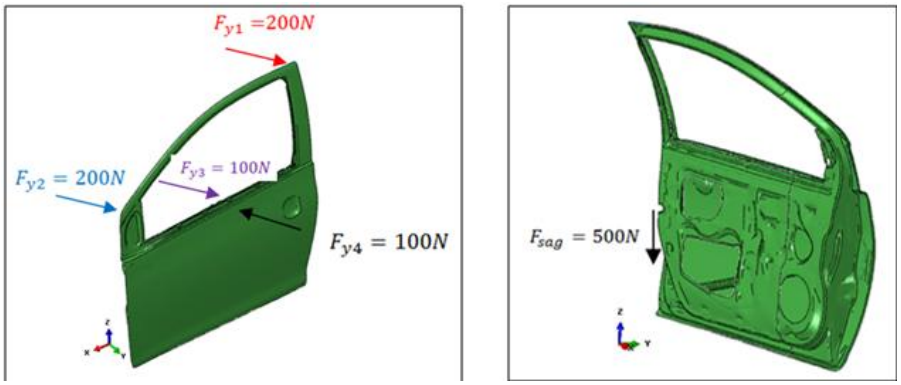

Figure 6.2-3 Lateral stiffness and sagging load case.

Von-Mises stress and principal stress predicted by numerical simulation are extracted for steel components and for composite components respectively, the resultant stress should be under the strength yield limit of each material (steel and CRFP), stress value are shown in Table 6.2-2.

Table 6.2-2 Critical stresses in different parts.

	Max stress		F_{y1} (MPa)	F_{y2} (MPa)	F_{y3} (MPa)	F_{y4} (MPa)	F_{sag} (MPa)	$Yield\ limit$ (MPa)
Steel Model		***V_mises***	243	113	99	111	209	271
Panel_CFRP Model	***Steel***	***V_mises***	202	63	34	102	187	271
	CFRP	***Principle***	77	32	19	28	70	84
Panel&Beam_CFRP Model	***Steel***	***V_mises***	204	63	34	102	188	271
	CFRP	***Principle***	78	32	19	28	70	84

Results show that all the simulated stresses at critical sections in different part are smaller than the material yield/failure stress, so the static design criteria is satisfied. In the sagging loading case, the hinge areas of the inner panel exhibited higher stress when the inner panel is made of composite material, but, even for the composite door case, the hinge areas will be made of steel or need to be properly reinforced.

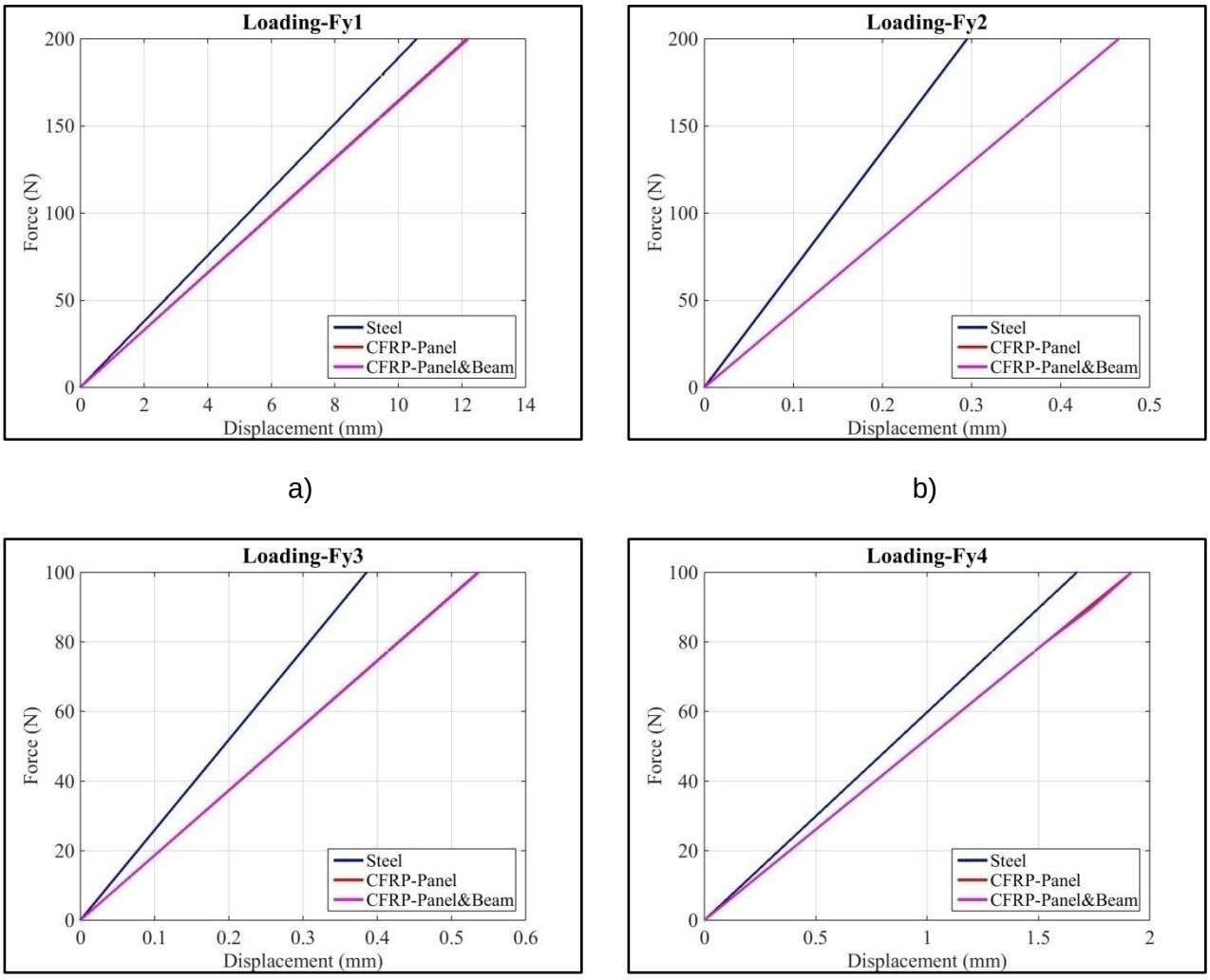

Figure 6.2-4 Load-displacement diagrams for different loading cases

The load-displacement curves, from which the stiffness values can be calculated, of the three FE models under loading cases F_{y1}, F_{y2}, F_{y3} and F_{y4} are shown in Figure 6.2-4a, Figure 6.2-4b, Figure 6.2-4c and Figure 6.2-4d respectively. In legend “Steel” means the reference steel solution; “CFRP-Panel” represents solution where materials of outer panel and inner panel are replaced by composite material; “CFRP-Panel&Beam” solution means that not only outer panel and inner panel but also impact beam are made with composite materials. Results show that each lateral stiffness of reference steel door solution is higher than the stiffness of two composite solutions, two composite solutions have almost same stiffness (curves with same shape). The same situation happens in sagging case, see Figure 6.2-5.

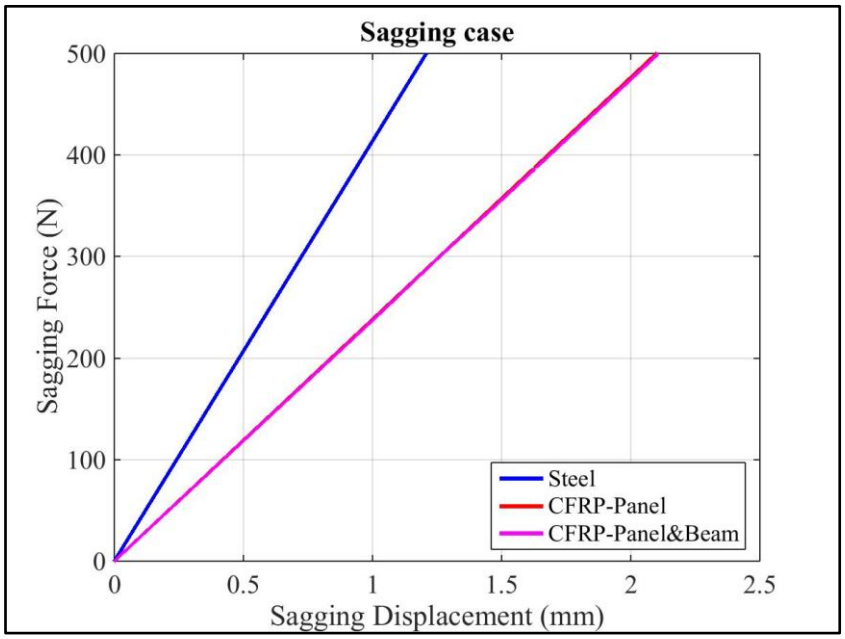

Figure 6.2-5 Load-displacement diagram for three models under sagging case

6.3 Modal analysis simulation

The noise, vibration and harshness requirements for the car door were defined by determining the lowest natural vibration frequency for the door in the close position. Modal is the natural vibration characteristic of mechanical structure, each modal has a specific natural frequency, damping ratio and mode shape. Solving problem of free vibration system characteristics (natural frequencies and modal shapes) means to calculate the matrices of the eigenvalues and eigenvectors. In this research activity, ABAQUS 6.12 solver is adopted to calculate the door modal and extract the first five of modal eigenvalues and modal eigenvectors. In order to separate the resonance frequency of the door away from the engine and road excitation frequency, the first modal frequency of the door assembly should be larger than road and engine excitation frequency.

Table 6.3-1 First five frequencies of three models

Frequency (Hz)	*Steel model*	*CFRP_Panel*	*CFRP_Panel&Beam*
1st order	29.6	34.3	34.3
2nd order	30.6	51.8	52.1
3rd order	49.6	63.6	66.0
4th order	55.4	70.0	70.2

5th order	60.0	73.3	78.4

First five frequencies of three models are summarized in Table 6.3-1, we could see that frequencies of two composite solutions are higher than that of reference steel solution, which meet the design requirement. Also there is small difference between two composite solutions. And Figure 6.3-1 is showing the modal shapes of side door structure related to first and second order vibration.

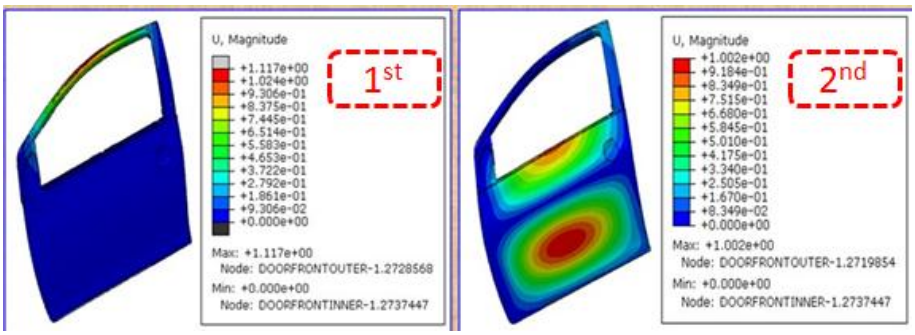

Figure 6.3-1 Modal shapes for first order and second order.

The results could be also explained from theory point view (see Figure 6.3-2). Frequency is increasing when structure mass is reduced while there is little change of stiffness of structure.

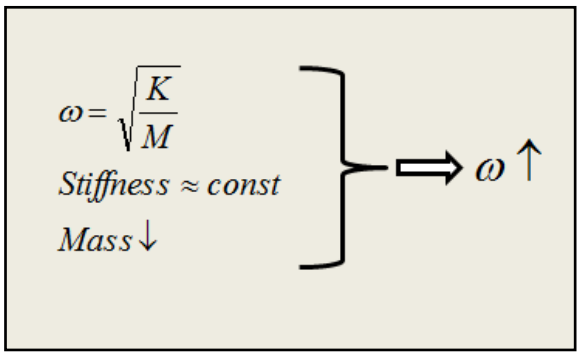

Figure 6.3-2 Frequency change theory

6.4 Reference

[1]. Kurtaran H, Buyuk M and Eskandarian A, “Ballistic impact simulation of GT model vehicle door using finite element method”, Theoretical and Applied Fracture Mechanics 40, 2003, pp. 113-121.

[2]. Ermias GK, PhD thesis, “Implementation of Composites and Plastics Materials for Vehicle Lightweight”, March 2012.

7 Chapter 7 Crashworthiness evaluation results

7.1 Crashworthiness evaluation of automotive composite side door

As dynamic crash step, crash analysis was performed to study the behavior of the door when the side impacting barrier is equipped with a frontal bumper subsystem instead of the standard MDB. The adopted bumper subsystem, includes bumper beam, fascia, cooling support, rails and energy absorber (as shown in Figure 7.1-2). The mass of the considered barrier is $1600\ k$g applied at the center of gravity of the striking vehicle, with a velocity of $30\ km/h$.

The side frame of Yaris (blue part in Figure 7.1-1) at first is simulated as a rigid body and it is contributing to boundary contact conditions for the perimeter areas of the door inner panel, that is a approximate simulation way for side frame behavior in a side crash impact. The side frame is completely constrained in this model (six degrees of freedom are constrained).

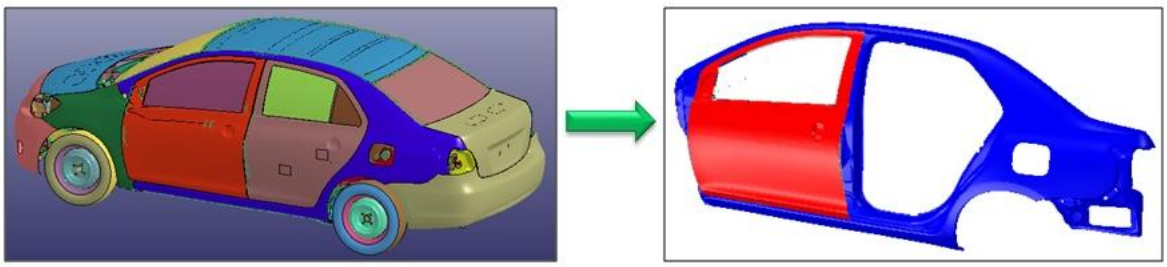

Figure 7.1-1 Yaris side door structure model.

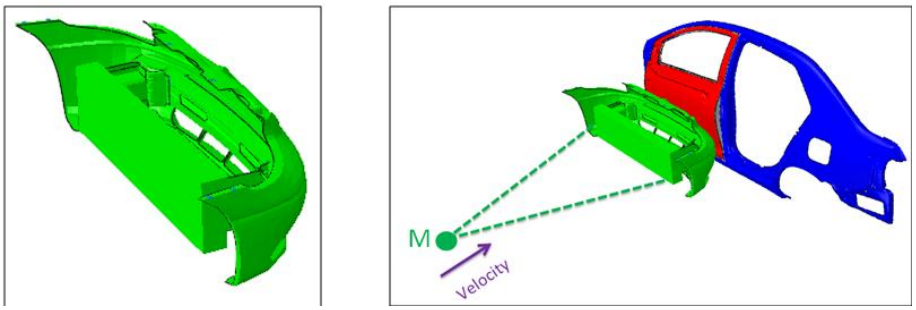

Figure 7.1-2 Crash model for crashworthiness evaluation.

7.1.1 Simulation results

During side crash, the intrusion displacement history of the vehicle occupant compartment is very important to evaluate the performance of crashworthiness of the door structure because many people got killed not because of the high force or acceleration transferred to human body during

side crash, but only because of huge intrusion displacement. Figure 7.1-3 shows a comparison of the intrusion displacements history among the three considered door solutions. And we could see that minimum intrusion around $150\ mm$ is found for CFRP_Panel model at time instant $100\ ms$, and also the intrusion displacements of two composite solutions are a little smaller than that of reference steel solution during the whole crashing process. Three solutions have almost same occupant compartment intrusion distance response.

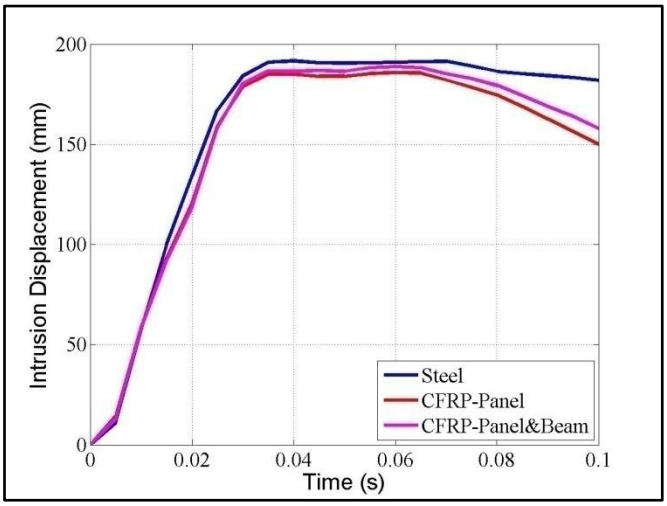

Figure 7.1-3 Intrusion displacement history of three models

As shown in Figure 7.1-4, material replacement on the bases of equal stiffness criteria gives similar curves of reaction force versus time with small different peak values. During crash scenario, the reaction force can be subdivided in two parts: the first part, which includes the first reaction force peak due to lock and hinges resistance; and the second part which includes the peak value of reaction force due to the side frame resistance.

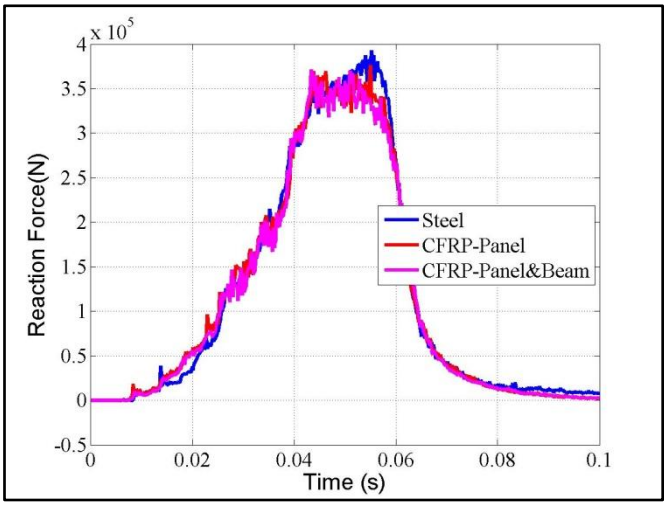

Figure 7.1-4 Reaction force history of three models

Evaluation of how much energy is absorbed by the door structure during a side impact event is so important because it is related to the potential damage induced to human body, the higher the absorbed energy, the safer the driver. The energy absorption diagram (Figure 7.1-5) is showing a relationship over the intrusion distance with some spring back at the end of side impacting process. As shown in the figure 7.1-5, the energy absorbed during the side crash process by two composite door solutions are much higher, about $6.2\ kJ$ and $6\ kJ$ respectively, while the energy absorbed by the reference steel door structure is only around $5\ kJ$. The capacity to absorb energy of the composite solutions is much higher than reference steel structure, about 20% increased. The maximum absorbed energy is found using panels and impact beam made with CFRP (CFRP_Panel&Beam) on the bases of equal stiffness criteria and is followed by CFRP_Panel door with steel material impact beam. The reference steel solution exhibited the lowest absorbed energy.

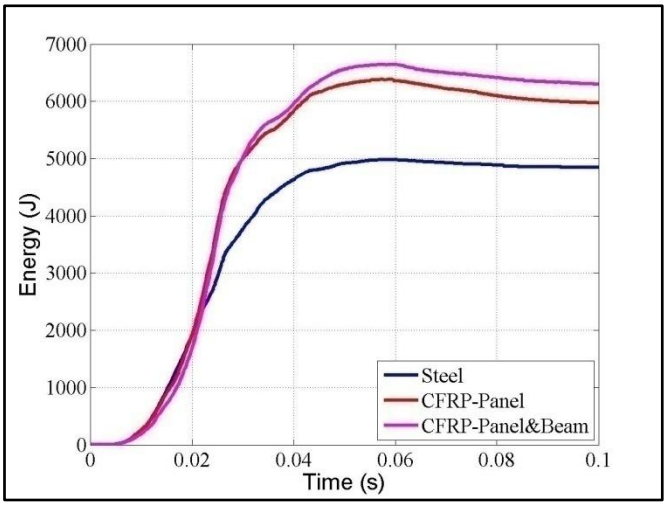

Figure 7.1-5 Energy absorbed by side door structures

We also would like to know how total energy is exchanged during side crash event, it is reasonable that kinetic energy of the bumper is absorbed not only by car side door structure and also by deformable bumper. Figure 7.1-6 shows that the energy absorbed by side door structure and by bumper, it is visible that the energy absorbed by bumper is dominating in comparison with the energy absorbed by side door, about 4 times higher. The rigid side panel is not deformable so the bumper needs to absorb some additional energy when the crash event is happening.

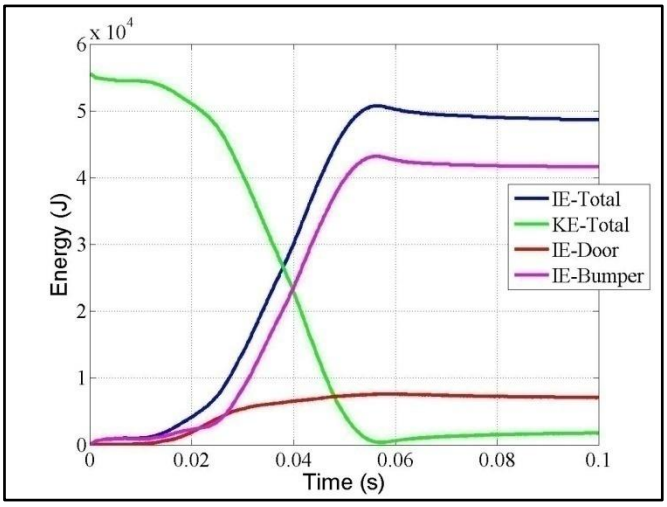

Figure 7.1-6 Kinetic energy and internal energy of model CFRP_Panel&Beam.

7.1.2 Discussion

Generally, it can be concluded that the composite doors can satisfy both the static design criteria and the side crash performance requirements, in better way comparing with the traditional steel door solution. It is also worth to mention that remarkably weight reduction - the total weight

decreases of about 6.7 kg, that is 39% of the steel solution - has been achieved using composite solution, which is one the relevant design aspect from point of lightweight vehicle design.

7.2 Crashworthiness evaluation of composite vehicle side door based on dummy response

The whole simulation was based on the FEM model of whole vehicle Toyota Yaris 2010, which was available in the NHTSA web site and imported into LS-DYNA environment. Besides, 50 percentile male dummy of ES-2 was properly placed on the driver's seat with deformed sitting foam. In this thesis work the movable deformable barrier was the FMVSS214 shell version 2.0, with a mass of about 1360kg. Evaluation of the dummy response was the way to estimate the crashworthiness of vehicle structure for the reference steel material and for the considered composite materials.

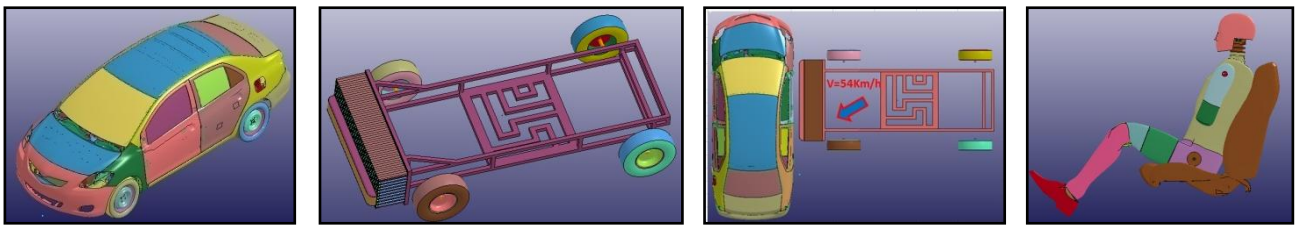

a) b) c) d)

Figure 7.2-1 Side crash model: a) Toyota Yaris 2010, b) Movable Deformable Barrier, c) Side impact regulation FMVSS214, d) ES-2 Dummy.

Side door car crash analysis was performed to study the behavior of the door when the impacting barrier is FMVSS214 shell version 2.0 (as shown in Figure 7.2-1b) according to the FMVSS214 regulation, barrier was moving with a velocity of $54km/h$ (as shown in Figure 7.2-1c).

The ES-2 dummy version 2.1 released in 2010 (as shown in Figure 7.2-1d) was imported and positioned at the driver seat inside the Toyota Yaris model. Crashworthiness results evaluation was based on the dummy response. Seat belt which can constrain the motion of dummy was not considered in this model for sake of model simplification since contribution of seat belt is negligible during the car side crash impact.

The outer and inner panels (Figure 7.2-2a and 7.2-2b) of the door contribute to reduce the intrusion displacement in order to protect occupants. Hence, optimized design approach of door panels

could have a vital influence on the bending stiffness of the door during the side crash event. Besides, impact beam (Figure 7.2-2c) is also mounted on the side door panels of passenger cars to guarantee passengers' safety from side impact damage. The impact beam is usually required to have high static strength and stiffness in order to allow controlled limited deformation and to absorb larger fraction of impact energy, respectively. One of the challenging tasks for the designer during material selection for impact beam application is to find the material that satisfies both requirements, which are conflicting properties in conventional steel materials.

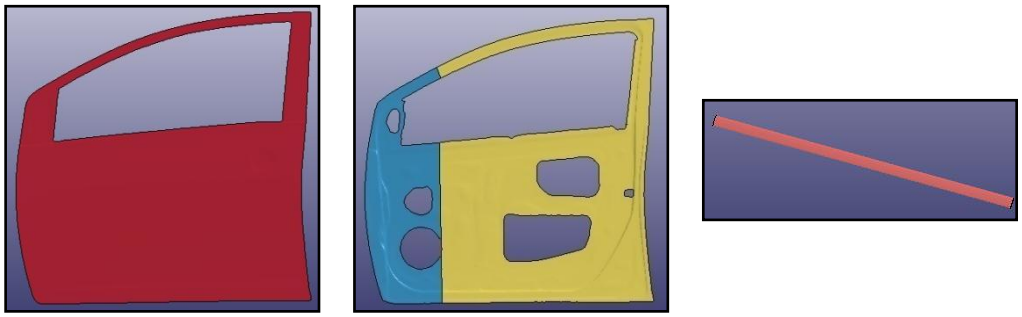

a) b) c)

Figure 7.2-2 Parts considered in Yaris door: a) Outer panel, b) Inner panels, c) Reinforcing impact beam.

Taking into account the desired targets, lightweight, high strength and high energy absorption, the present research work is proposing carbon fiber reinforced composite material as a solution to substitute the steel used for the door panels and for the impact beam. The wall thicknesses of the composite panel and beam are approximately calculated based on the same stiffness criteria, as stated in Chapter 6. The thickness of the inner panel as well as of the outer panel is $2\ mm$ and the thickness of the reinforcing beam wall is $3.6\ mm$. In this case, the weight reduction is about 50% and 70% respectively in comparison with the reference steel solutions.

Table 7.2-1 Deformation in different vehicle side profiles

Steel	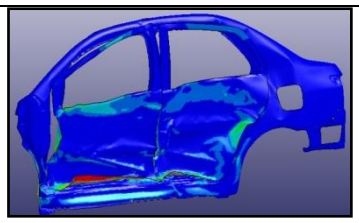	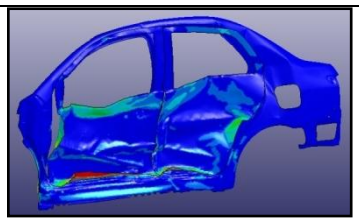	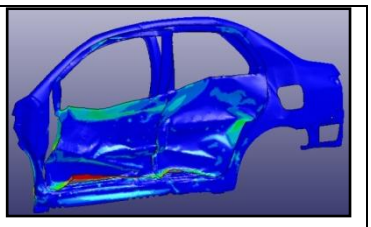

CFRP-Panel	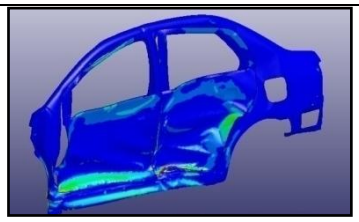	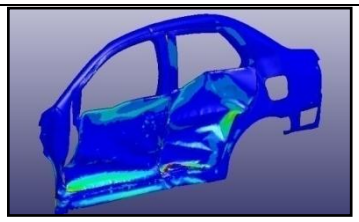	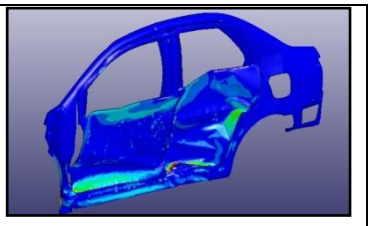
CFRP-Panel &Beam	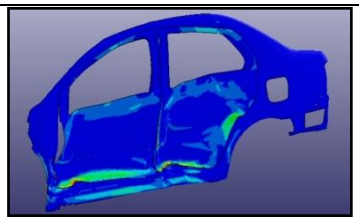	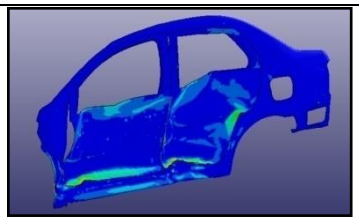	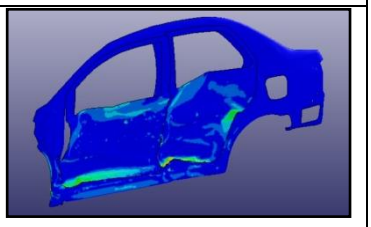
	$t = 40\ ms$	$t = 60\ ms$	$t = 80\ ms$

Table 7.2-1 is showing the deformation of vehicle profile for the three solutions at different time instants, three solutions deformed differently. Also the movements of dummy during side crash are shown in Figure 7.2-3.

$t = 30\ ms$ $t = 65\ ms$ $t = 85\ ms$ $t = 95\ ms$

Figure 7.2-3 Movements of dummy during side crash impact

7.2.1 Intrusion displacement

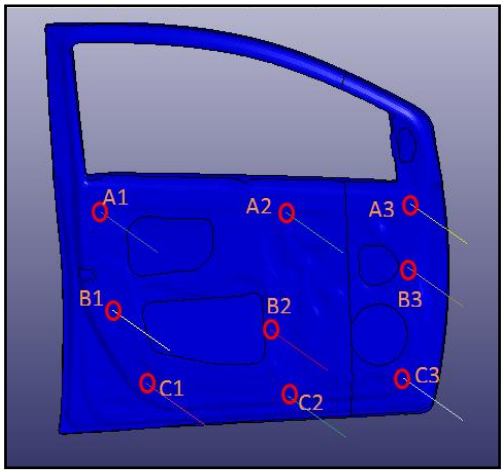

Figure 7.2-4 9 critical points for investigation of intrusion displacement on inner panel.

In this work, displacement history of 9 critical positions in three levels on the door inner panel were collected from the FEM results of simulation performed with models according to the three different solutions (see Figure 7.2-4), namely the NP steel solution, the solution with CFRP panels and the solution with panels and reinforcing beam made with CFRP. Figure 7.2-5 shows a comparison of the displacement history of 9 points among the three considered door solutions. Results show that in some position, such as point A2 and C2 smaller intrusion could be found using CFRP door; at the same time in other positions such as point B2, higher, but slight higher, intrusion displacements could be found using CFRP door; finally for other points, such as B1 and C1, steel door and CFRP door have almost same intrusion displacement values.

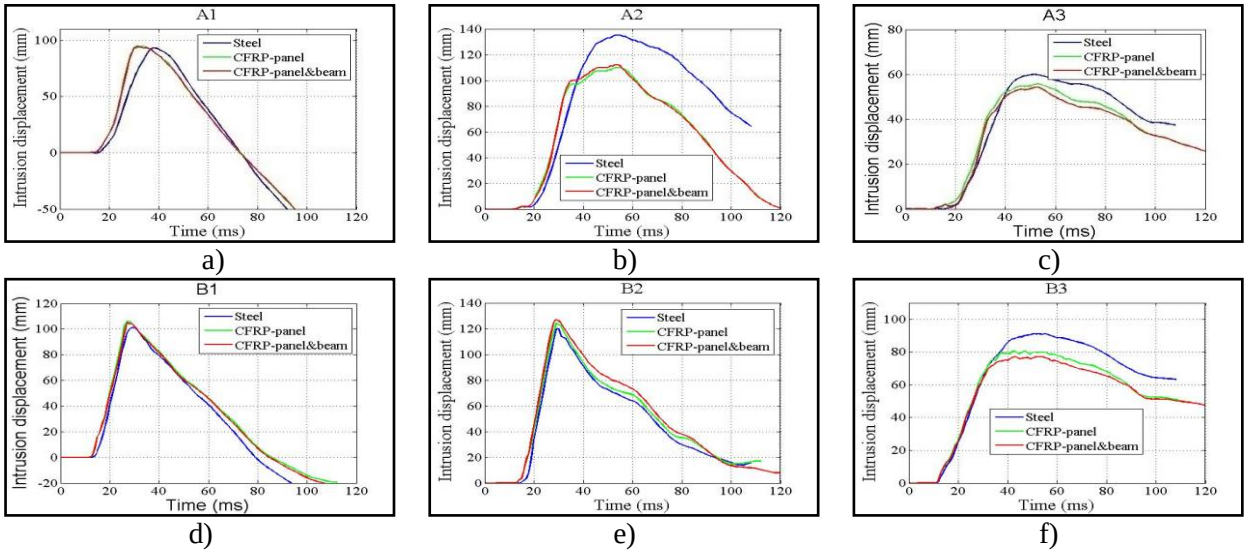

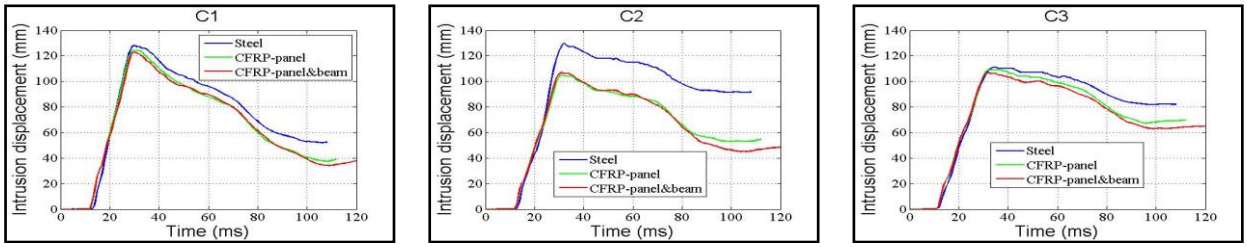

g) h) i)

Figure 7.2-5 Intrusion displacements of 9 critical points on inner panels of side door

7.2.2 Biomechanical response of dummy

As shown in Figure 7.2-6a, material replacement on the bases of equal stiffness criteria gives similar curves of reaction force versus time with almost same peak value. This force is the total force reacting between barrier and target car when the side crash is happening.

An estimated 40-75 percent of passenger vehicle occupant deaths in case of side impact crashes result from head injuries (IIHS, 2001) [1]. Injuries in neck and spine resulting from side impact are also devastating, and can lead either to a fatality or to various forms of permanent physical impairment. Direct impacts of head can severely affect the brain and most of the sensorial organs located within it.

The response of the dummy provides a critical assessment of each structure performance because the biomechanical measurements during such impacts are currently used in comparison of stated limit values as the approval criteria in regulation test procedures. Usually evaluation of dummy response in side impact crash should include head injury criteria (HIC), rib deflection, abdomen force, pubic symphysis force and some other indexes.

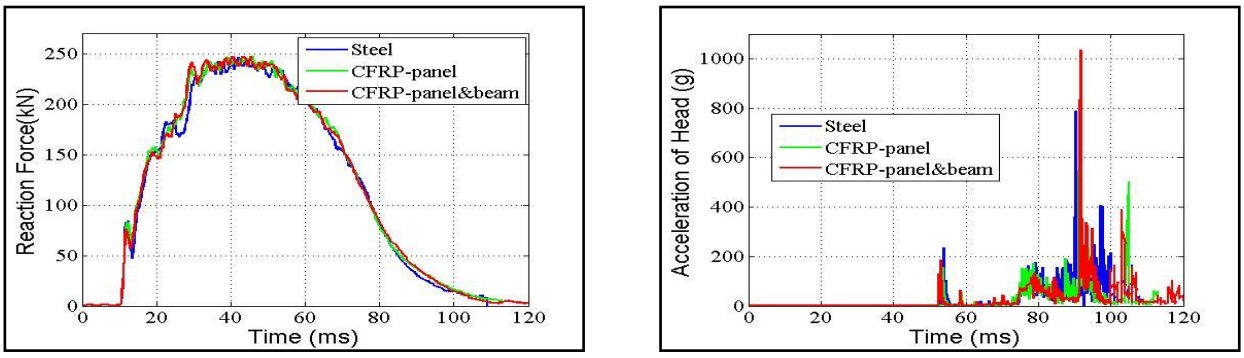

a) b)

Figure 7.2-6 Reaction force and head acceleration

Head acceleration history measured as gravity acceleration g multiple is shown in Figure 7.26b, the result shows that the head acceleration peak value of the three models are very high (more

than$800g$, and related HIC is much higher than usual limitation of regulation $HIC_{36} < 1000$). This is because the crash simulation in this work does not consider the lateral air bags and the dummy head impacts directly against the roof rail during the crash event, which is shown in the red circle area in Figure 7.2-7a. Actually there are two installations to reduce the acceleration pulse inside real vehicle structure, which are foam layer around roof rail and side air bags (see Figure 7.2-7b and Figure 7.2-7c, [2, 3]).

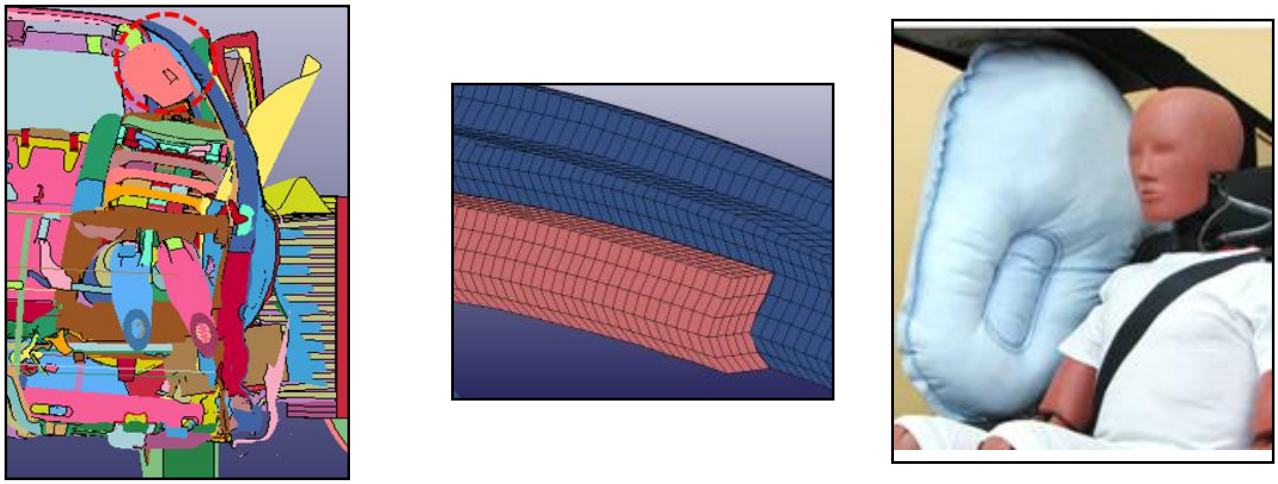

a) b) c)

Figure 7.2-7 a) Dummy head impact with roof rail, b) Foam around roof rail, c) Side air bags.

7.2.2.1 Thorax injury assessment

Injuries of chest could also be lethal for human during the side crash, most of organs residing within chest, as the heart and the lungs, or transiting it as the esophagus, the aorta and the cava are vital, so any damage to them has the potential to generate very serious or fatal injuries. The lungs occupy the majority of the chest cavity volume. The assessment for the chest injury is rib deflection value, which is shown in Figure 7.2-8. In the FMVSS214 Protection Criteria, the deflection of any of the upper, middle, and lower ribs shall not exceed$44\ mm$. From Figure 7.2-8, we can see that the rib deflection of the composite solution are higher than that of steel reference solution for upper and middle ribs, but all of them are smaller than $22mm$; for the lower rib, rib deflection of composite solution is even smaller than that of reference solution, and both of them are within limitation.

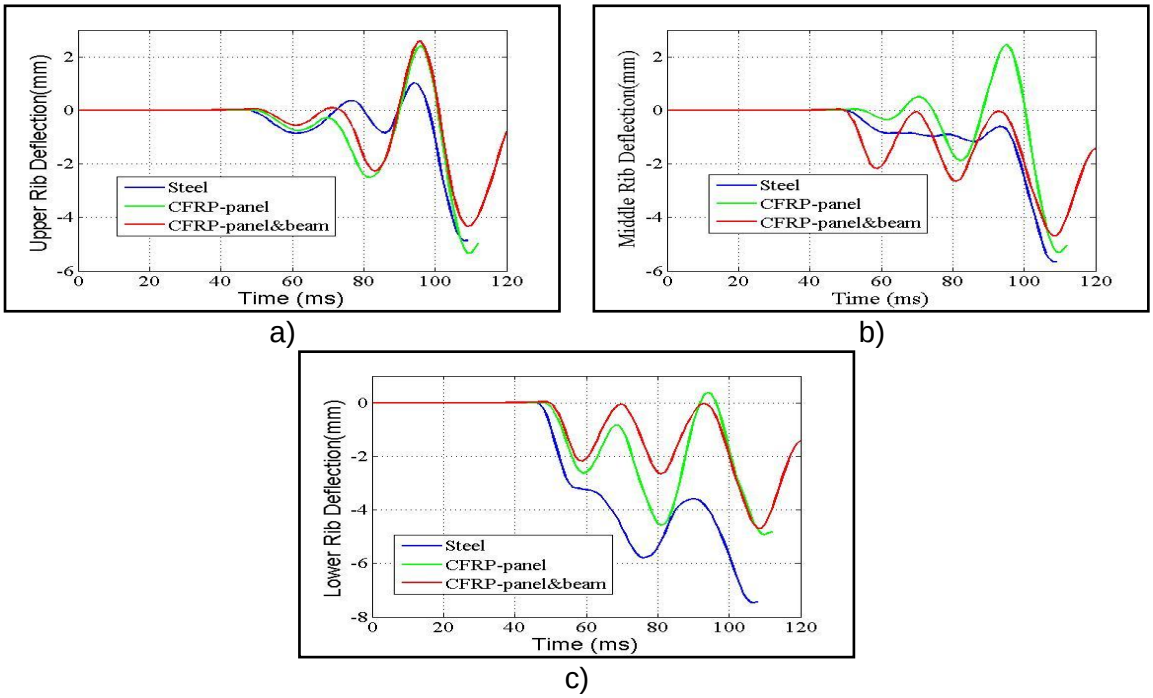

Figure 7.2-8 Rib deflections, a) Upper rib, b) Middle rib, c) Lower rib.

7.2.2.2 Abdomen injury assessment

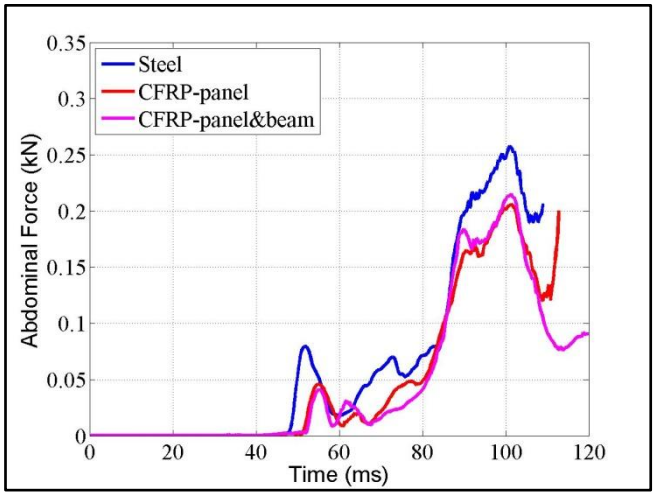

Figure 7.2-9 Abdominal Force.

As mentioned before, abdomen injury should be measured. The sum of the front, middle and rear abdominal forces, shall not exceed 2.5 kN, as required in regulation FMVSS214. From Figure7.2-9, it is obviously that the maximum of the abdominal force is around 0.25 kN, much smaller than that limitation value.

7.2.2.3 Pelvis injury assessment

The pelvis force peak value is also critical for causing invalidating injury to human body, Figure 7.2-10 shows that the pelvis forces presented in composite structure are much smaller than that in reference steel structure, according to the peak value, and all values are lower than the limit value in regulation. FMVSS214 requires that the pubic symphysis force must be smaller than $6\,kN$, Figure 7.2-10 shows that the highest peck is around $2.7\,kN$, which means that in all the examined solutions the high performance limits are full respected.

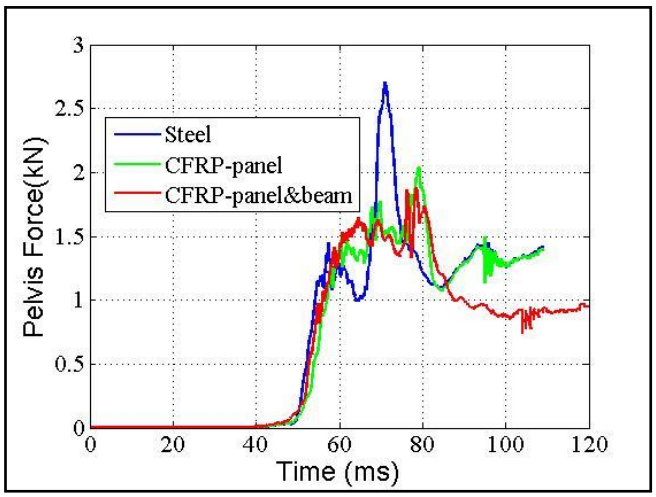

Figure 7.2-10 Pubic Symphysis Force.

7.3 Crashworthiness evaluation of innovative composite side door solution

This innovative solution of vehicle side door was already introduced in Chapter 5.6 and this section is focusing on crashworthiness evaluation based on intrusion displacement of occupant compartment and biomechanical response of dummy placed on driver's seat. The side impact regulation and analysis methods used in this section are same as solution 7.2.

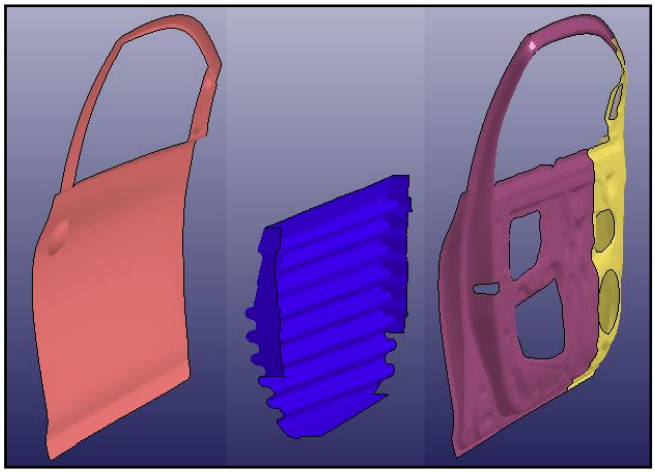

Figure 7.3-1 Outer panel, reinforced panel and inner panels.

For this innovative reinforced panel (see blue part in Figure 7.3-1), several composite materials are considered, including carbon fiber reinforced plastic, E-Glass fiber reinforced plastic, GMT, GMT_UD, GMT_TEX, CSIMS and GSIMS. Also from solution in Chapter 7.2, the materials of door outer panel and inner panels could be substituted by composite material CFS003/LTM25. So two composite solutions for each composite reinforced panel are developed in LS-DYNA, first one is steel door panels with composite reinforced panel and second one is composite side panels (CFS003/LTM25) with composite reinforced panel. The results are compared with reference steel door solution. Firstly composite material GMT was considered for innovative reinforced panel and crashworthiness is evaluated following. In this case the wall thickness of reinforced panel is $2.3\,mm$ with a mass of $2.26\,kg$.

7.3.1 Intrusion displacement

Following the already adopted procedure for the analysis of the results (see Figure 7.2-4), values for the 9 critical points are collected in order to investigate the intrusion displacements on inner panels. Figure 7.3-2 is showing the comparison between three vehicle door solutions: reference steel solution and two proposed composite solutions. GMT-reinforced panel is the one that uses GMT reinforced middle panel with reference steel outer and inner panels; GMT-CFRP panels is third solution that GMT reinforced middle panel with composite outer and inner panels (CFS003/LTM25), so this kind of solution have more mass reduction with respect to solution GMT-reinforced panel.

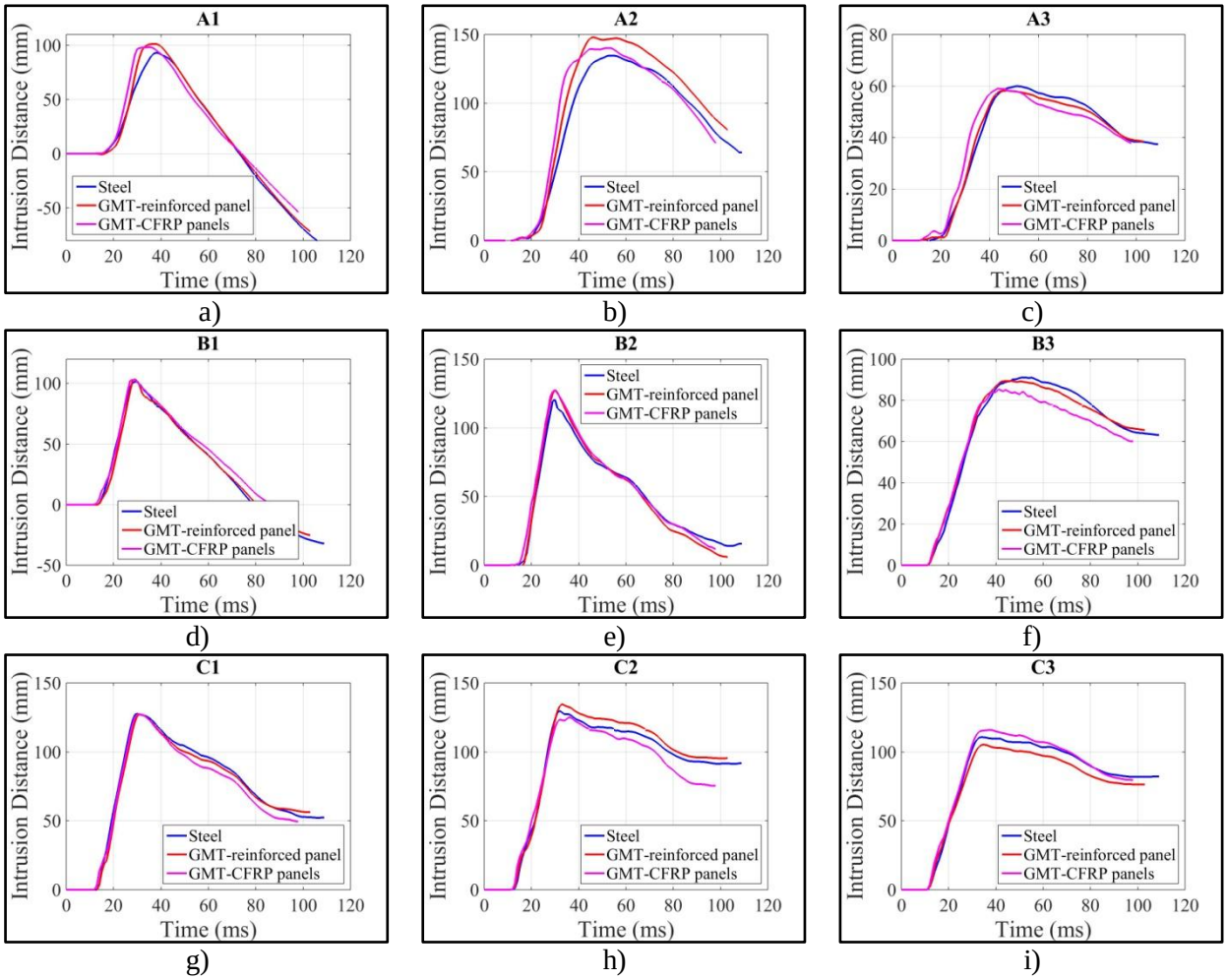

Figure 7.3-2 Intrusion displacements of occupant compartment

Results of intrusion displacements are showing that the two composite solutions have same intrusion displacements as steel reference solution, see point B1 and C1; composite door models have higher intrusion displacements at point A1 and A2. The two composite solutions have obvious different intrusion responses at point A2, C2 and C3, they have different advantages at different positions.

7.3.2 Biomechanical response of dummy

Rib deflections of three ribs are compared in Figure 7.3-3. Results give us that two composite solutions have same deflections compared with steel reference solution for all three ribs, and all deflections are smaller than the limitation value$44\ mm$, as required in regulation FMVSS214.

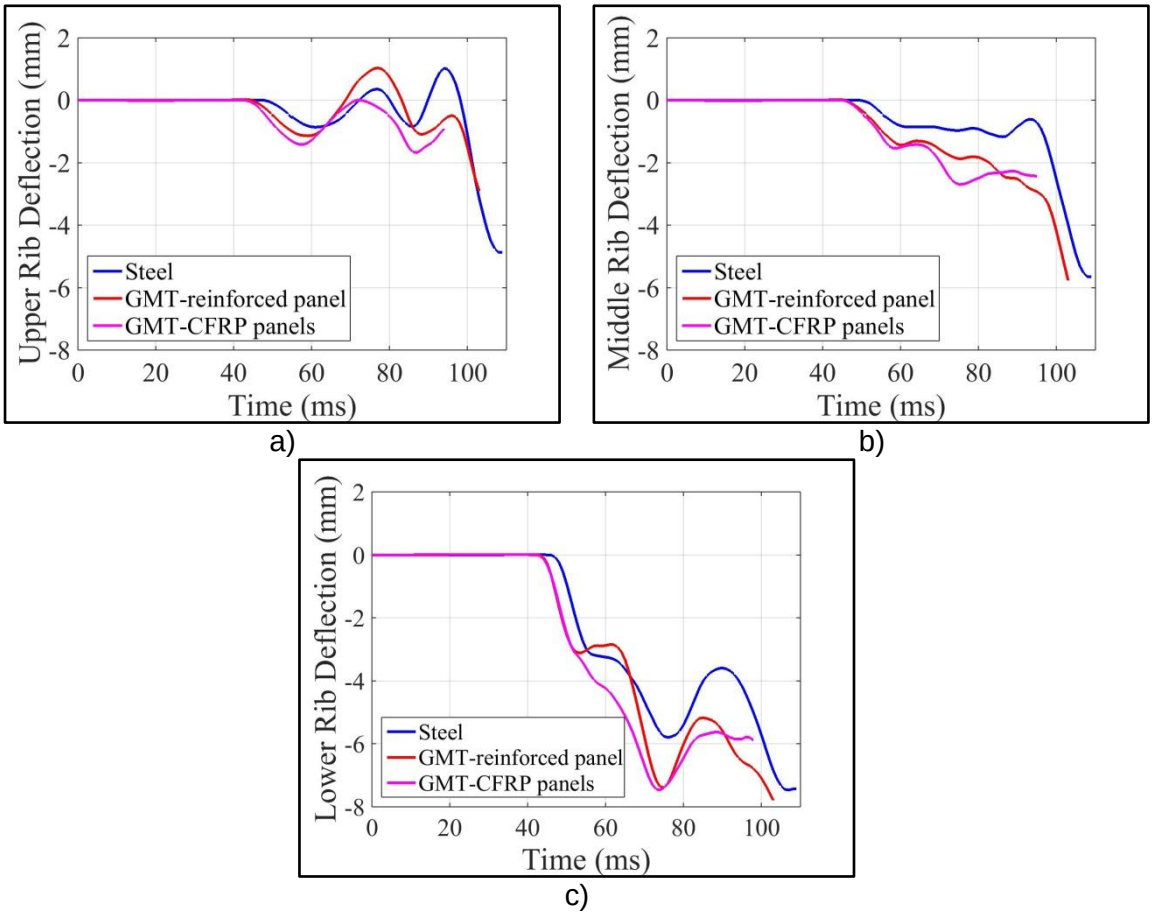

Figure 7.3-3 Rib deflections

Figure 7.3-4 is showing the abdominal force history resulting in abdomen part of dummy for three solutions. The maximum value for the steel solution is around $0.26\ kN$ and $0.33\ kN$ is the peak value for the two composite solutions, which are much smaller with respect to regulation value$2.5\ kN$, as required in FMVSS214 regulation. This means that all three solutions can protect driver well during side impact event.

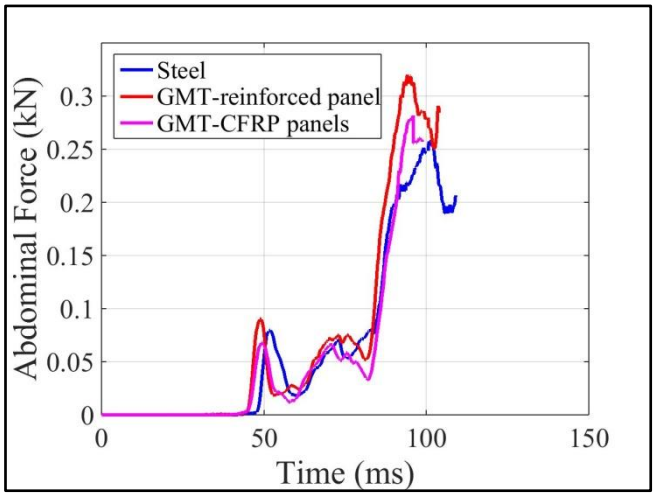

Figure 7.3-4 Abdominal resultant force

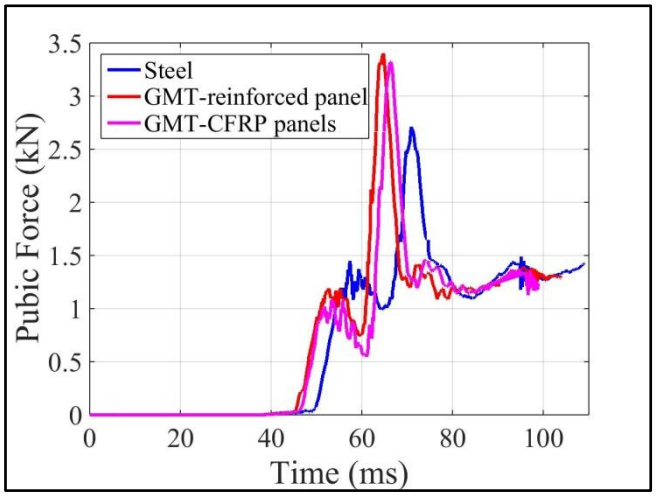

Figure 7.3-5 Pubic symphysis force

For assessment of pelvis injury, pubic symphysis force history is shown in Figure 7.3-5, peak value of two composite door models are around $3.4\ kN$ while the highest value for the steel reference solution is about$2.7\ kN$. This means that GMT solutions could cause more severe pelvis injury to driver during side crash, however all of the forces are almost half of the limit value in FMVSS214 regulation, which is$6\ kN$.

As mentioned in last section, beside carbon fiber reinforced plastic material CFS003/LTM25 was considered for this reinforced panel, GFRP, GMT, GMT-UD, GMT-TEX, CSIMS and GSIMS are also proposed for this innovative panel, at the same time materials of outer panel and inner panels could be substituted by composite material CFS003/LTM25.

In next sections, composite materials GMT-TEX, GMT-UD, CFRP, GFRP, CSIMS and GSIMS are considered as alternative options for innovative reinforcing panel. Results of these composite solutions are compared to steel reference door solution, through not only intrusion displacements of occupant compartment but also biomechanical indexes: rib deflection, abdominal resultant force and pubic symphysis force.

Composite lateral door made with GMT-TEX and GMT-UD are analyzed in section 7.3.3; CFRP and GFRP solutions are discussed in section 7.3.4; last group is sandwich materials CSIMS and GSIMS, which is presented in section 7.3.5. For all these results, the intrusion displacements are higher or lower than that of steel reference solution, but the difference are very small. The acceleration of dummy head generated in composite solutions are much higher than limit value

required in safety regulation because usual head protection strategies are not considered in this finite element simulation. The deflection value of three ribs, resultant abdominal force and pubic symphysis force resulted in composite door structures are larger or lower than that in steel door model, but all of them are satisfied with the requirement of FMVSS214 regulation. To sum up, these composite solutions also could protect driver well during side impact event compared with original Yaris vehicle. All the numerical results are listed in following sections.

7.3.3 GMT-TEX and GMT-UD

7.3.3.1 Intrusion displacements

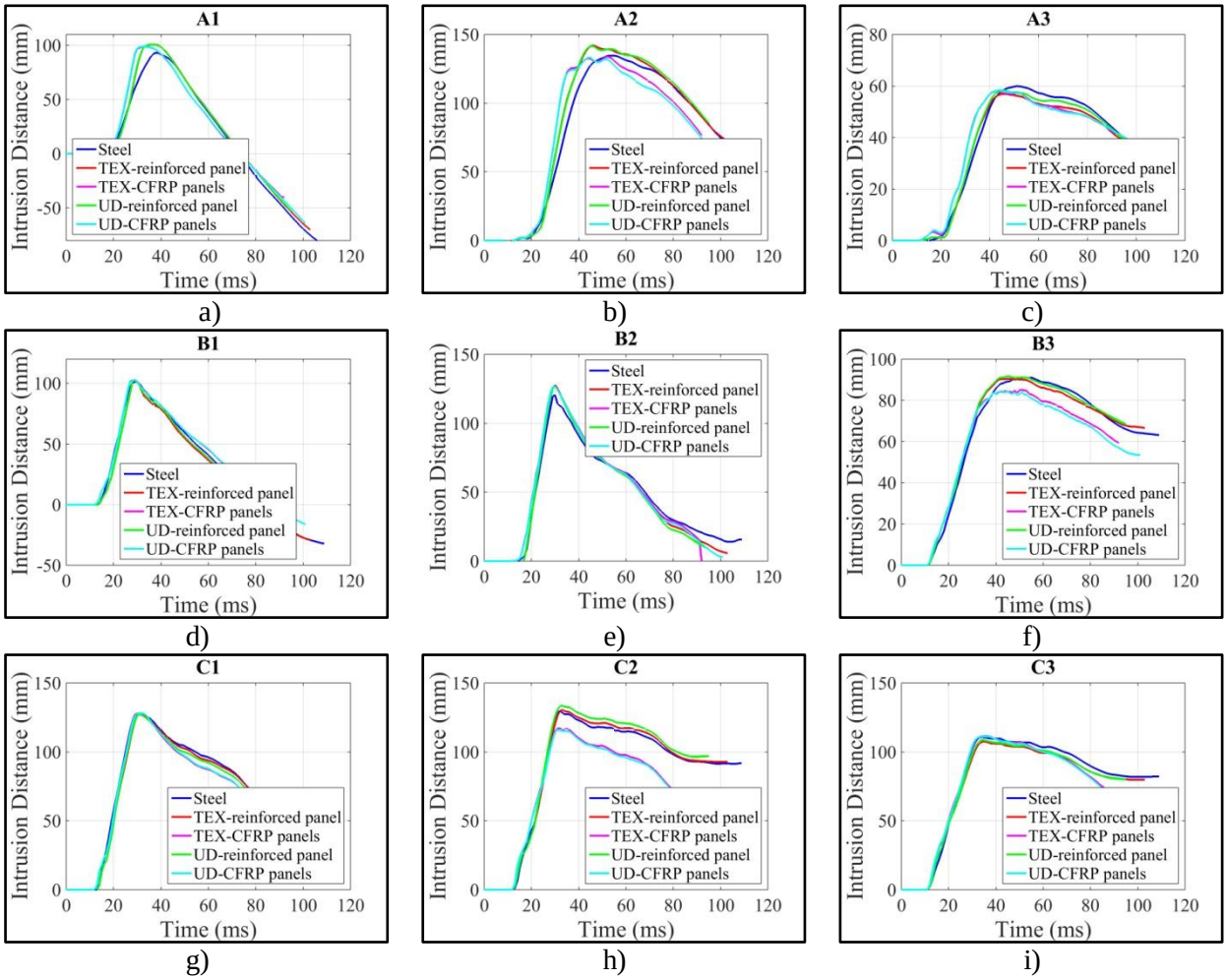

Figure 7.3-6 Intrusion displacements

7.3.3.2 Biomechanical response of dummy

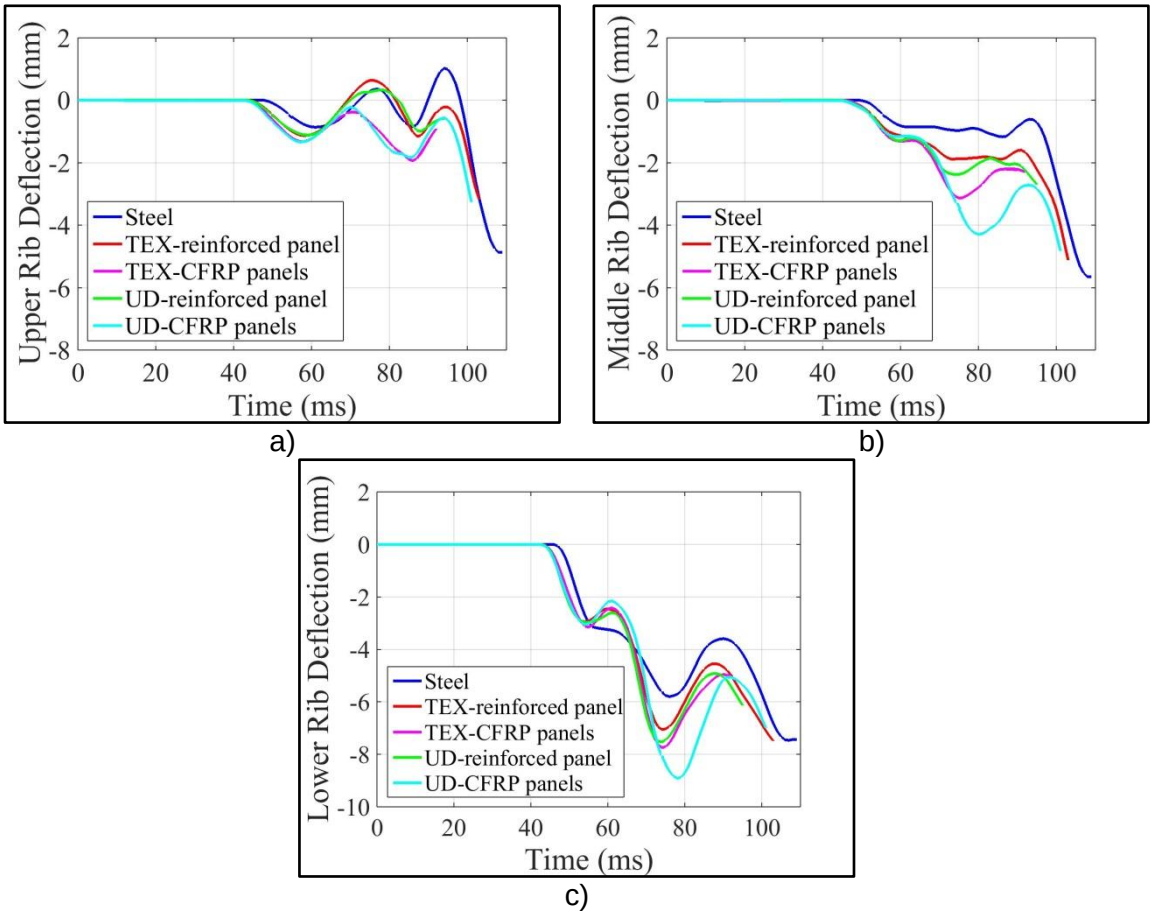

Figure 7.3-7 Rib deflection a) Upper rib, b) Middle rib, c) Lower rib

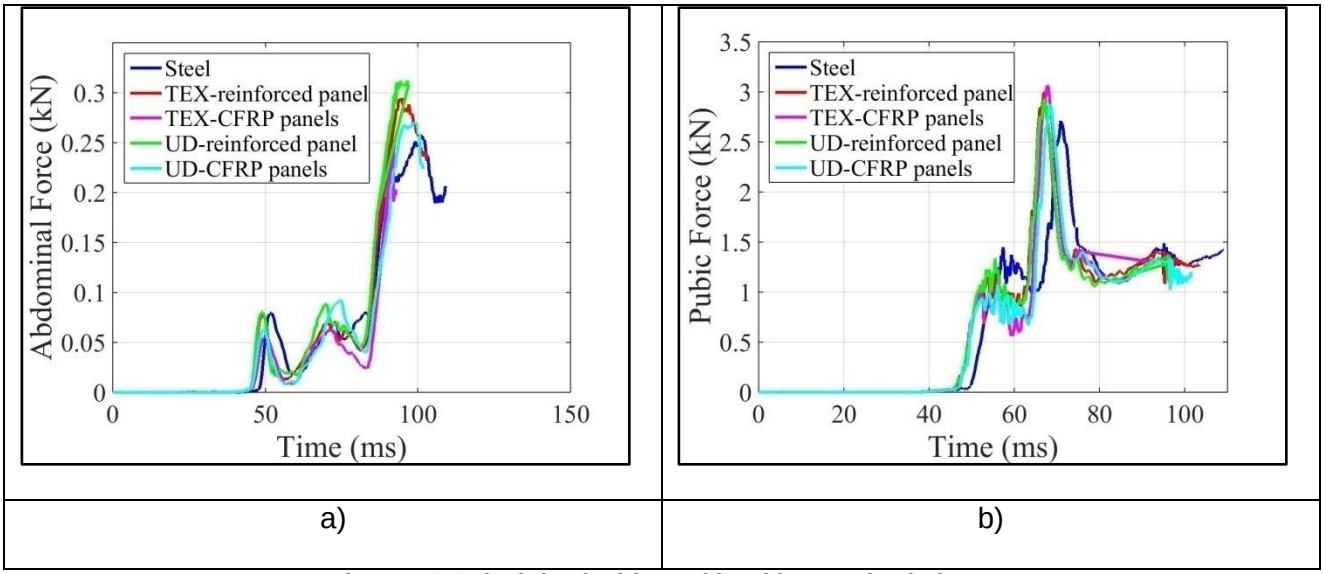

Figure 7.3-8 a) Abdominal force, b) Pubic symphysis force

7.3.4 Caron fiber reinforced plastic (CFRP) and glass fiber reinforced plastic (GFRP)

7.3.4.1 Intrusion displacement

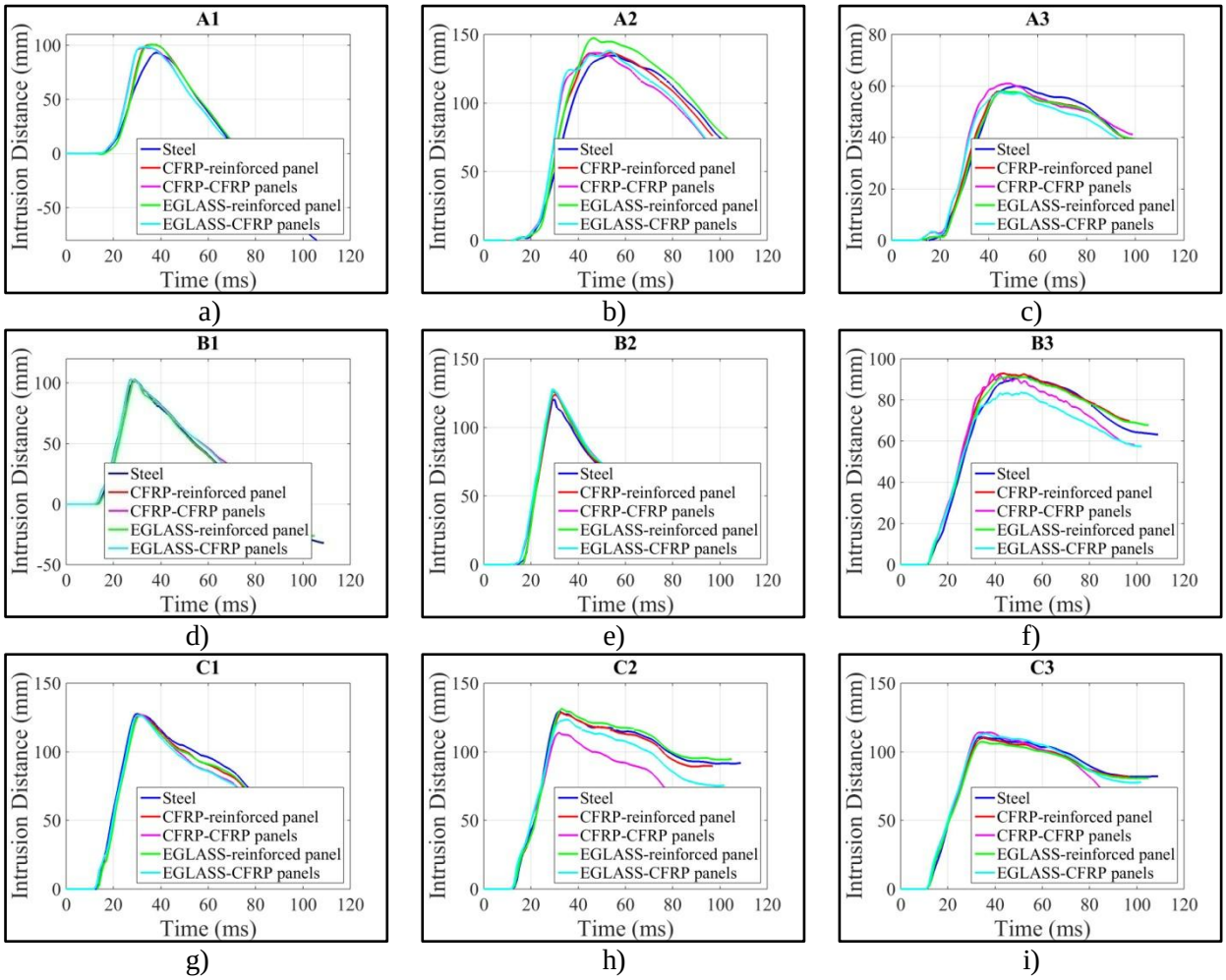

Figure 7.3-9 Intrusion displacement

7.3.4.2 Biomechanical response of dummy

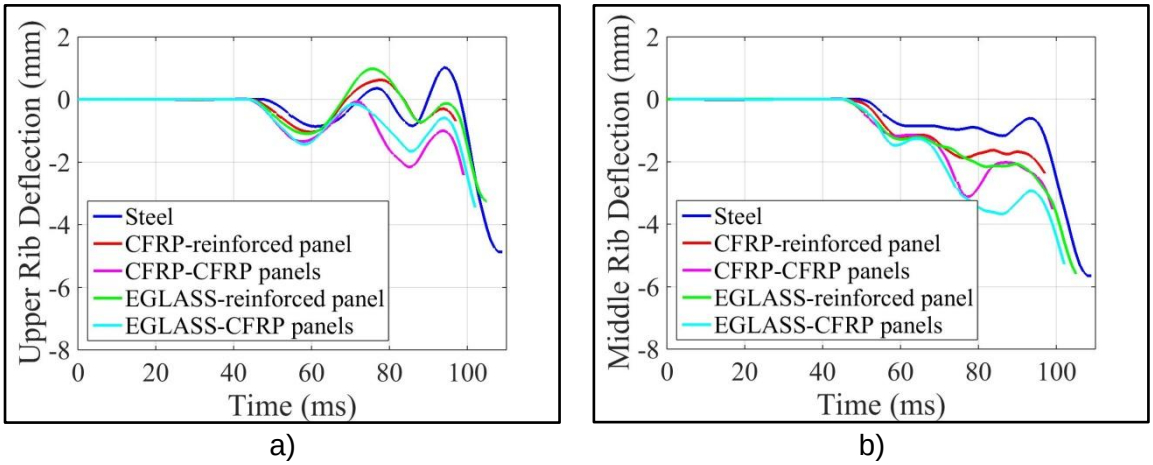

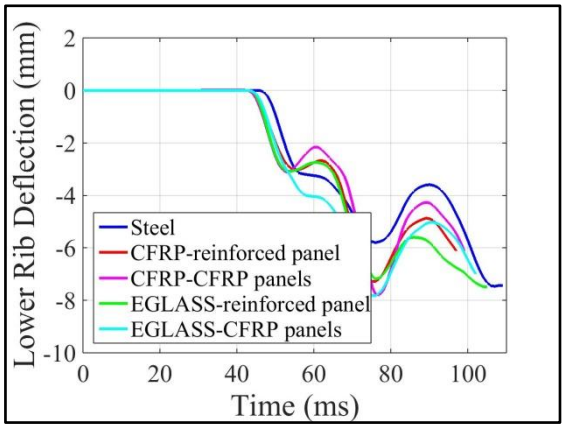

c)

Figure 7.3-10 Rib deflection a) Upper rib, b) Middle rib, c) Lower rib

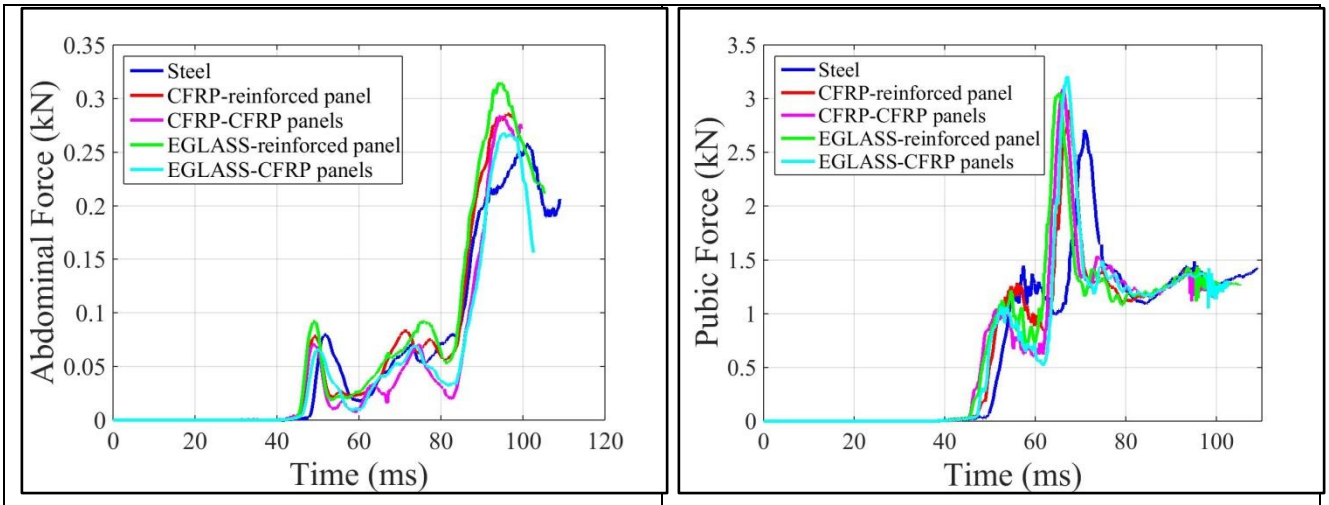

a) b)

Figure 7.3-11 a) Abdominal force, b) Pubic symphysis force

7.3.5 CSIMS and GSIMS

7.3.5.1 Intrusion displacement

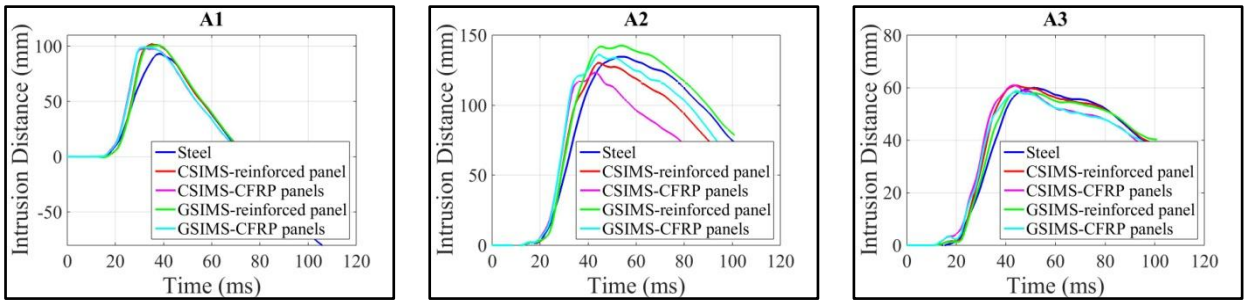

a) b) c)

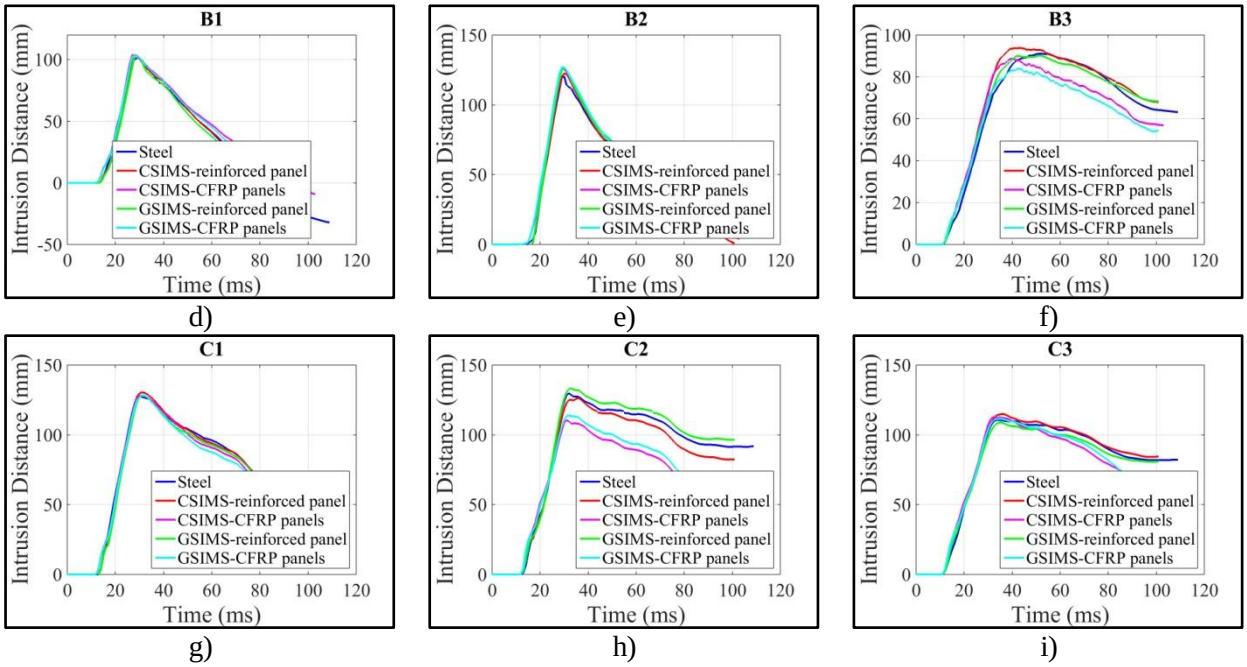

Figure 7.3-12 Intrusion displacement

7.3.5.2 Biomechanical response of dummy

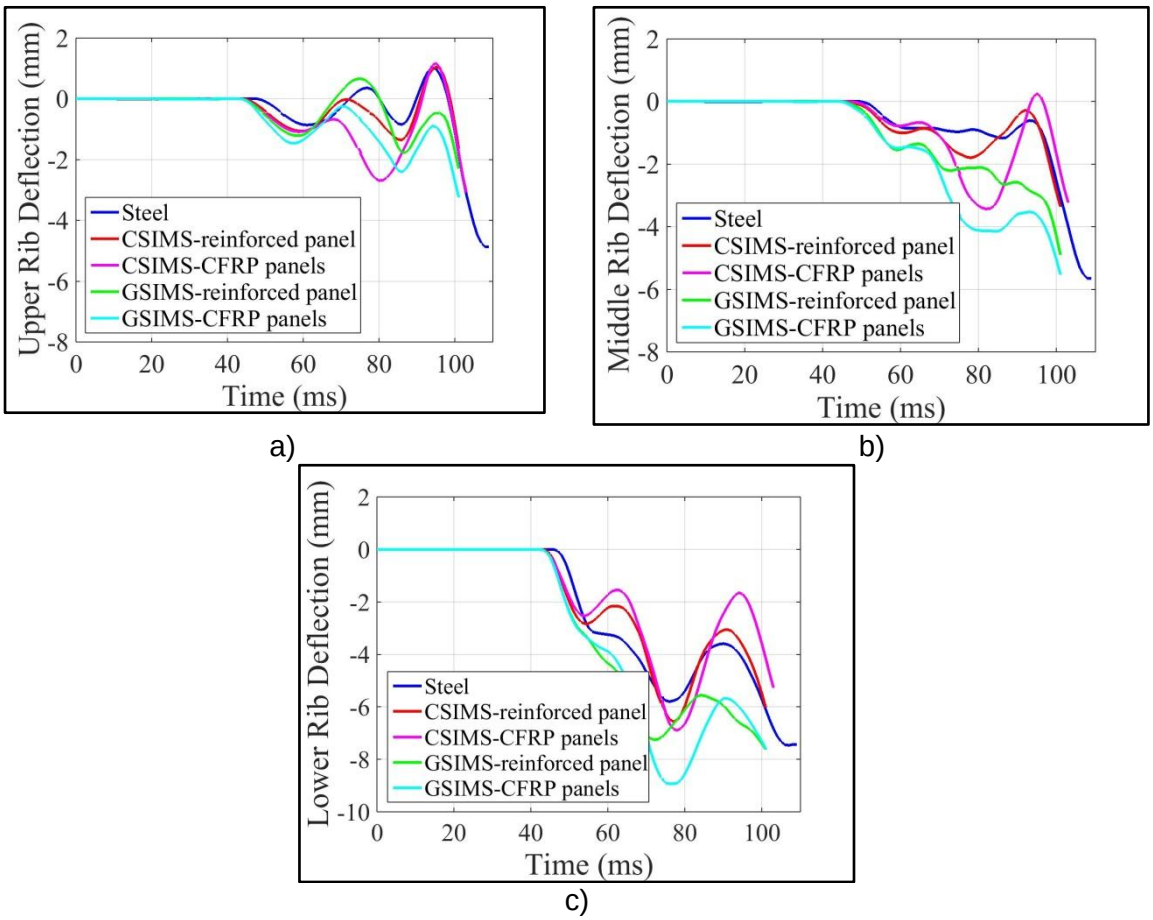

Figure 7.3-13 Rib deflection a) Upper rib, b) Middle rib, c) Lower rib

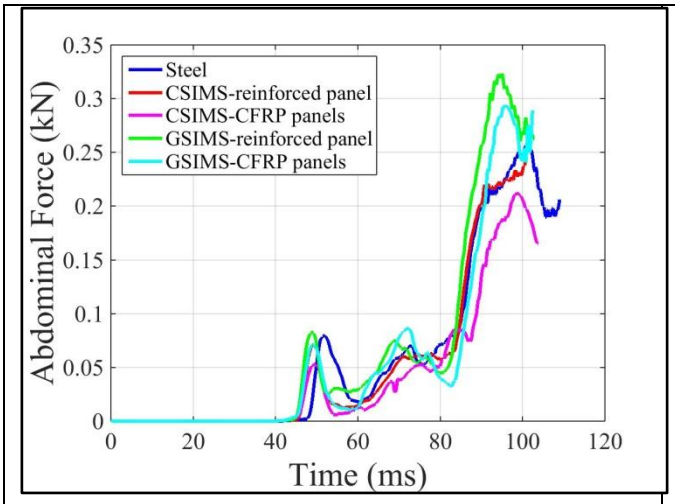

a)

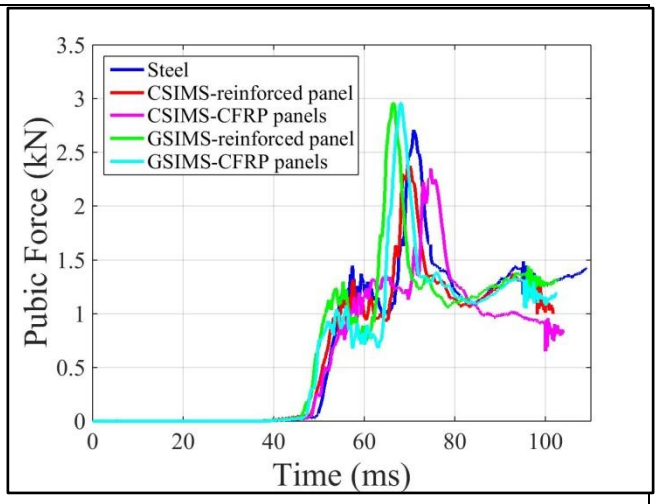

b)

Figure 7.3-14 a) Abdominal force, b) Pubic symphysis force

7.3.6 Mass reduction

Lightweight design is the starting point and also is the fundamental target of this research, all the composite solutions should be evaluated based on mass reduction. Mass reduction analysis between composite door solutions and the steel reference solution is summarized in the following Table 7.3-1. In this table, thickness is the thickness of composite innovative reinforcing panel, which are different for different materials; composite parts are those which are proposed to substitute some relative steel parts; relative mass reduction is mass difference between mass of composite parts and mass of original replaced steel parts; final mass reduction ratio is calculated on total mass reduction and total mass of original lateral door structure integrated in Yaris model, which is $19.2\ kg$.

Table 7.3-1 Mass reduction of composite side door models

Composite lateral door solutions		***Thickness*** (mm)	***Mass of Composite parts*** (kg)	***Mass of Steel parts*** (kg)	***Relative mass reduction*** (kg)	***Final mass reduction Ratio***
GMT	***GMT-reinforce panel***	2.3	2.26	2.93	0.66 (22%)	3.4%
	GMT-CFRP panels	2.3	8.85	15.06	6.21 (41%)	32%

TEX	***TEX-reinforce panel***	2.0	1.96	2.93	0.97 (33%)	5.1%
	TEX-CFRP panels	2.0	8.54	15.06	6.52 (43%)	34%
UD	***UD-reinforce panel***	2.0	2.01	2.93	0.92 (32%)	4.8%
	UD-CFRP panels	2.0	8.59	15.06	6.47 (43%)	34%
CFRP	***CFRP-reinforce panel***	1.0	1.18	2.93	1.75(60%)	9.1%
	CFRP-CFRP panels	1.0	7.76	15.06	7.30 (48%)	38%
GFRP	***GFRP-reinforce panel***	1.0	1.51	2.93	1.42(48%)	7.4%
	GFRP-CFRP panels	1.0	8.09	15.06	6.97 (46%)	36%
CSIMS	***CSIMS-reinforce panel***	2.0	1.99	2.93	0.94(32%)	4.9%
	CSIMS-CFRP panels	2.0	8.57	15.06	6.49 (43%)	34%
GSIMS	***GSIMS-reinforce panel***	2.0	2.20	2.93	0.73(25%)	3.8%
	GSIMS-CFRP panels	2.0	8.78	15.06	6.28 (42%)	33%

If we only consider innovative reinforcing panel without any material substitution of outer and inner panels, result is giving us that the smallest thickness of innovative panel is $1\ mm$ for CFRP solution and maximum value is $2.3\ mm$ for GMT one, consequently the mass reduction are $1.75\ kg$ and $0.66\ kg$ for these two solutions, related to relative mass reduction ratio 60% and 22% respectively. And the final mass reduction ratios are 9.1% and 3.4%, which are not considerable because the total mass of original Yaris lateral door is higher. Composite solutions of GMT-TEX and GMT-UD have mass reduction about $0.97\ kg$ and $0.92\ kg$, relative mass reduction ratio are 33% and 32%.

Semi-impregnated micro sandwich materials CSIMS and GSIMS also have a larger mass reduction $0.94\ kg$ and $0.73\ kg$ because of their physical structure with lower density, relative reduction ratios are 32% and 25% compared to the mass of steel replaced parts.

Materials of outer and inner panels could be replaced by CFRP at the further stage, which is also analyzed at the same time. From Table 7.3-1, mass of all replaced steel parts is $15.06\ kg$ and mass of substituting composite components are ranging from $7.76\ kg$ to $8.85\ kg$, this means that mass reduction value under this case is more than $6.2\ kg$ if composite solutions are adopted. The largest relative mass reduction solution is 48% coming from CFRP door structure and the smallest reduction is 41% if GMT material is considered. And the final mass reduction ratio is located between 32% and 38%, which are remarkable and consequently this will reduce fuel consumption considerably.

7.4 Reference

[1]. http:/www.iihs.org.

[2]. G.Belingardi, R.Duellaand and A.Caminiti, “Opitmal Choice of the Foam Design Parameters in Order to Meet the HIC Index Limit of the FMVSS201 Standard”, 2002 Society of Automotive Engineerings, Inc., 2002.

[3]. G.Belingardi, R.Duella and F.Capello, “Relative role of foam thickness and foam density in the design of a car-body pillar and dash-board in order to optimize the HIC index”.

8 Chapter 8 Conclusions

8.1 Conclusions

The main research activity in this thesis addressed the issues of vehicle lightweight design and vehicle passive safety through implementing potential composite materials for automotive applications. At the moment Green House Gas pollution and vehicle fuel consumption are two big issues around the world, as reported in chapter 1. As the number of cars on the road has grown, consequently, carbon dioxide (CO_2) emissions from road transport have increased by 21% between 1990 and 2011, also they account for about 23% of the EU's total CO_2 emissions, which is responsible for global temperature increasing and climate change at the moment. In order to ensure that the EU meets its greenhouse gas emission targets, a comprehensive strategy to reduce CO_2 emissions from new cars and vans sold in the European Union was adopted in 2007. The Regulation set a short-term target of $130\ g\ CO_2\ /km$ by 2015, to be phased in from 2012, and a long term target of $95 g\ CO_2\ /km$ by 2020. These limits are progressively modified (some increment is allowed) to take into account the mass of the vehicle itself.

Effective strategies have been adopted by car manufactures in order reach vehicle noxious gas emissions and fuel consumption reduction targets. One of the possible concurrent strategies is weight reduction. Every 10% of weight reduced from the average new car can decrease fuel consumption by around7%. Alternative materials, such as composites, can be used to substitute the traditional materials to reach the lightweight design targets, such as composites. Composite materials have many advantages comparing to traditional material and could easily satisfy structural requirement, such as high strength/weight ratio and high capacity to absorb energy during crash impact; however other problems must be considered before they are brought into automotive industry with a huge amount of produced parts, such as high cost of the raw material, joining problems and low production speed. But, on the other hand, in evaluating the cost of composite parts one has to consider that the new design of the part can include into one piece a number of sub-parts (thus simplifying the production and assembly process), the cost of the tooling

is generally lower with respect to that needed to manufacture traditional material parts. Therefore it is possible to calculate a breakeven point.

Lightweight design of vehicle could improve overall safety of transportation system, including the safety of other drivers, other passengers, pedestrian and other vulnerable road users.

In reality vehicle side door structure is not a simple panel but rather a substructure system which satisfies many different functions, especially the door structure would protect passengers during a side crash event. Traditionally, the car side door structure is built from steel material as, for example, is with the vehicle Toyota Yaris 2010. This vehicle is used reference in this research because its finite element model is available from NCAC research website. This study has developed several types composite door solutions, numerical simulation was used to analyze the structural performance of the innovative solutions that were also compared with Yaris steel reference solution.

At first composite vehicle side door was composed by thin-walled CFRP (T300/5208) beams that are connected by aluminum alloy joint (AW6016) through epoxy adhesives. As second step, the Yaris steel door model was isolated from the whole model and considered as the reference solution. Two composite door solutions have been considered: one composite solution has straight lateral profile and the other has curved profile as in the real door structure. These two composite door solutions were analyzed under vertical and horizontal load cases, structural results have been compared with steel reference solution. Results of load-displacement analysis showed that the stiffness of two composite solutions were higher than that of steel reference solution.

Further quasi static intrusion with rigid pole was simulated for three solutions. This study was based on the rigid pole test in vehicle side safety regulation; in this case rigid pole was pushed against door outside surface by one concentrated force applied at the center of pole. Numerical results gave us that intrusion displacements of two composite solutions were smaller than that of reference solution.

In order to evaluate the weight advantage that can be gained, since in the two composite models there were only the door frame while no inner or outer panels have been included, in order to consider to give more realistic values, the current weight values could be doubled, obtaining $7.2kg$

and $7.0kg$ while the reference solution mass is of $17.2kg$. As we can see, the weight is remarkably reduced in comparison with that of traditional steel door model, more than 50%.

The above mentioned composite solution could not be integrated into Yaris door structure directly because outer and inner panels were not considered in composite solutions, which could cause surface consistence problem. So the next step was to develop a composite door which fit with the available Yaris model. So material substitution of outer panel, inner panel and impact beam by composite material was considered. The thicknesses of composite parts were calculated approximately based on equal stiffness criteria. The material substitution was divided into two stages: only materials of panels were substituted; secondly not only panels but also impact beam were substituted. Static, modal and dynamic behavior were analyzed and compared between two composite solutions and reference solution. The results summarized with the following four points.

- Under static loading in the cases finalized to the evaluation of lateral stiffness and sagging strength, it came out the both performance are comparable with those of the steel reference solution. Moreover maximum stresses created in different parts were smaller than yield limit value of each material; consequently static design requirements were satisfied.
- The natural frequencies of composite door structures were higher than that of reference door as NVH design criteria required.
- Crashworthiness evaluation was also analyzed using a movable deformable bumper part as impacting structure. Side door structure and Yaris side frame were simulated as target model. The final numerical results told us that the intrusion displacements of two composite solutions were smaller than that of reference one while had larger capacity to absorb energy.
- Composite solutions with a huge mass reduction about$6.7\ kg$, that is around 35% mass of total original Yaris door structure.

In order to analyze the crashworthiness of composite side door more exactly and practically, side impact crash with movable deformable barrier (MDB) was simulated by LS-DYNA, according to safety regulation FMVSS214. Also EuroSID 2 dummy was placed at the driver's seat and the

biomechanical response of dummy was collected in order to evaluate injuries transferred to driver and results were compared with reference solution. The main results were following:

- Intrusion displacements of occupant compartment: the composite solutions had almost same structural response as reference solution, even better at some particular points.
- Acceleration of head: accelerations much higher than limit value required in safety regulation have been obtained presented because head of dummy was impacting roof rail directly during crash impact, but in the reality foam layer around rail and side air bags could prevent this intense impact to happen. And these two effective strategies were not considered in the numerical model.
- Deflection of three ribs, resultant abdominal force and pubic symphysis force were also calculated and compared between three solutions, small differences were found among them. The limit value in safety regulation FMVSS214 were much higher than peak value resulted in each body part for composite and steel solutions. This means that composite solutions could offer the same safety level to driver compared with reference solution. Also improvement toward the lightweight target was obtained.

The last solution of this research work was an innovative composite structure to reinforce the side door against lateral impact. Once again the Yaris door has been considered, in this propose, the traditional impact beam and some reinforcements were replaced by an innovative middle reinforcing panel, which has an irregular profile and was working together with surface panels of side door. This model was installed in Yaris physical structure and the crashworthiness of this new door structure was also investigated with LS-DYNA tool according to regulation FMVSS214. Different composite materials were characterized by other researchers and they were considered to make this new reinforcing panel, including GMT, GMT-TEX, GMT-UD, CFRP, GFRP, CSIMS and GSIMS. Numerical simulation results revealed that composite solutions had almost same intrusion displacements of passenger compartment with respect to reference solution. About the biomechanical response of dummy, except for the high head acceleration values (that have the already discussed explanation), indexes were all located within the safe range required by regulation of FMVSS214 with large margins. If these innovative solutions are adopted into Yaris

structure, a considerable mass reduction was obtained between $6.21\ kg$ and $7.30\ kg$, which are 32% and 38% of total mass of original Yaris side door structure.

From this thesis we can conclude that composite door solutions satisfy not only static design criteria but also crashworthiness requirement. At the same time composite solutions have a remarkable mass decrease, more than 32% of total mass of Yaris reference door structure. This will be a great contribution to the expected reduction in fuel consumption and vehicle emission.